General Disclaimer

One or more of the Following Statements may affect this Document

- This document has been reproduced from the best copy furnished by the organizational source. It is being released in the interest of making available as much information as possible.

- This document may contain data, which exceeds the sheet parameters. It was furnished in this condition by the organizational source and is the best copy available.

- This document may contain tone-on-tone or color graphs, charts and/or pictures, which have been reproduced in black and white.

- This document is paginated as submitted by the original source.

- Portions of this document are not fully legible due to the historical nature of some of the material. However, it is the best reproduction available from the original submission.

Produced by the NASA Center for Aerospace Information (CASI)

175210

SQT

(E84-10110) DETECTION OF HIDDEN MINERAL DEPOSITS BY AIRBORNE SPECTRAL ANALYSIS OF FOREST CANOPIES Final Report (Columbia Univ.) 79 p HC A05/MF A01 CSCL 02F

N84-21928

Unclas
G3/43 00110

MAR 1984
RECEIVED
NASA STI FACILITY
ACQ BRANCH

DETECTION OF HIDDEN MINERAL DEPOSITS BY AIRBORNE SPECTRAL ANALYSIS OF FOREST CANOPIES

MAR 1984
RECEIVED
NASA STI FACILITY
ACQ BRANCH

BY

WILLIAM COLLINS

SHENG-HUEI CHANG

JOHN T. KUO

Aldridge Laboratory of Applied Geophysics
Columbia University
New York, New York 10027

Final Report To NASA, Contract NSG-5222*

*Research also supported by NSF Grant DAR-78-16320

...inal photography may be purchased
... EROS Data Center
... Falls, SD 57198

TABLE OF CONTENTS

I. INTRODUCTION

Field surveys and data anlysis of several biogeochemical test sites have been completed under National Science Foundation Grant DAR-78-16320 to Columbia University. The research has been in cooperation with Dr. Frank Canney, Dr. Gary Raines, and Dr. Roger Ashley of the U.S. Geological Survey. The earlier phases of airborne data acquisition and preliminary analysis were conducted under NASA Grant NSG-5222 to Columbia University.

Very promising results have been obtained in the four major test sites of the study. These sites are:

1. Cotter Basin, Montana;
2. Spirit Lake, Washington;
3. Blacktail Mountain, Montanta;
4. Catheart Mountain, Maine.

Known or suspected sulfide zones were detected on each site. The Cotter Basin experiment, furthermore, was able to successfully repeat the results of a survey flight two years previous.

The present research was stimulated by the earlier successful results obtained in a Goddard Institute for Space Studies funded Columbia University experiment in Cotter Basin (Collins, et al., 1978). In that study, anomalous spectral properties of the forest canopy growing in a known copper, lead, zinc zone were discovered using the prototype airborne spectroradiometer system designed and developed at

Columbia University and Goddard Institute for Space Studies (Chiu and Collins, 1978).

Results of field data analysis under the present NSF grant strongly correlate with our past results indicating that sulfide mineralization can affect overlying vegetation, and hence induce anomalous spectral reflectivity properties. The spectral region most affected by mineral stress is between 550nm and 750nm. The spectral variations observed in the field occur on the wings of the red chloropyhll band centered at about 680nm. The metal-stress-induced variations on the absorption band wings are most successfully resolved in the high-spectral-resolution field data using a waveform analysis technique being developed at Columbia University.

Complimentary studies on laboratory grown plants have been conducted under the present NSF grant to Columbia University The same spectral effects that we observe in the field data have been reproduced in our laboratory studies (Chang and Collins, 1980). Doping of greenhouse plants with copper and zinc retards the development of the chlorophyll pigments. The lowered chlorophyll production in metal poisoned laboratory plants results in specificly identified changes on the wings of the chlorophyll bands of reflectance spectra from those plants. These spectral effects are now well documented and identical to those observed in the field.

The laboratory studies have also yielded convincing evidence that the present high resolution spectoradiometer insturmentation and waveform analysis techniques offer the most sensitive method of stress detection, especially under field conditions (Collins, et al., 1980). The major problem we encounter in field data analysis is

filtering of noise induced by vegetation canopy and other environmental effects. The noise is especially bothersome because it contains low-frequency components that are very similar in nature to the spectral waveforms related to stress but at much higher amplitudes. With the waveform technique, we establish a very sensitive narrow band-pass filter that passes the specific spectral curves indicating metal stress and rejects all other low and high frequency spectral features present in the airborne survey data. The prospects of developing a new mineral exploration technique based on these techniques looks very hopeful.

Preliminary analyses to determine the potential for using discrete spectral bands and imaging techniques for detection of mineral stressed vegetation have also been assessed in the present study. Our studies show that the LANDSAT broad bands will not work. Stress detection, however, may be possible using multiple narrow bands in the 550nm to 750nm region. Determination of specific bands will require further study of filtering techniques to remove the effects of canopy density, slope, texture, and irradiance angle. These effects produce broad-band radiance variations two orders of magnitude greater than the subtle variations caused by mineral rich soils.

II. COTTER BASIN TEST SITE

A spectral anomaly in the forest canopy growing over a sulfide vein system was detected in a Columbia University experimental survey flown in 1976 (Collins, Raines, and Canney, in press). The test site in the Cotter Basin area, Lewis and Clark County, Montana, was flown for the second time in 1978 to assure the repeatability of the earlier results and to allow further analyses of the vegetation stress phenomenon.

Mineralization in Cotter Basin occurred along westerly striking shear zones in Precambrian sedimentary rocks. Veins up to 3 feet thick are calcitic with copper and lead sulfide mineralization. Geochemical studies indicate anomalously high concentrations also of Ag, Zn, and Au in the soil. The soil concentrations are up to 10,000 ppm copper, up to 1,500 ppm lead, and up to 400 ppm zinc. The copper geochemical anomaly as mapped by Utah International, Inc. is shown in Figure 2. More complete geochemical and plant ash sampling are presently being conducted by the U.S. Geological Survey and Columbia University.

The high mineral content of the soil, are (A) in the aerial photo of the test site (Figure 1), has resulted in a natural clearing where the local tree species fail to grow. The cleared areas (B) and (C) are open cuts on the sulfide veins. The geologic data indicates westerly striking shear zones (D) through the northern open cut area (C) and through the southern clearing and open cut area (B and A). The clearings and mineralization are located on a northerly facing slope. The area is thickly forested with a mature (climax) growth of spruce and pine.

The airborne survey procedure acquires 500-channel spectra at the rate of 2.5 complete spectra per second along the flight path. The data comes out of the system in digital form and are stored on computer-compatible magnetic tape on board the aircraft. In the 1978 survey, the

ORIGINAL PAGE IS
OF POOR QUALITY

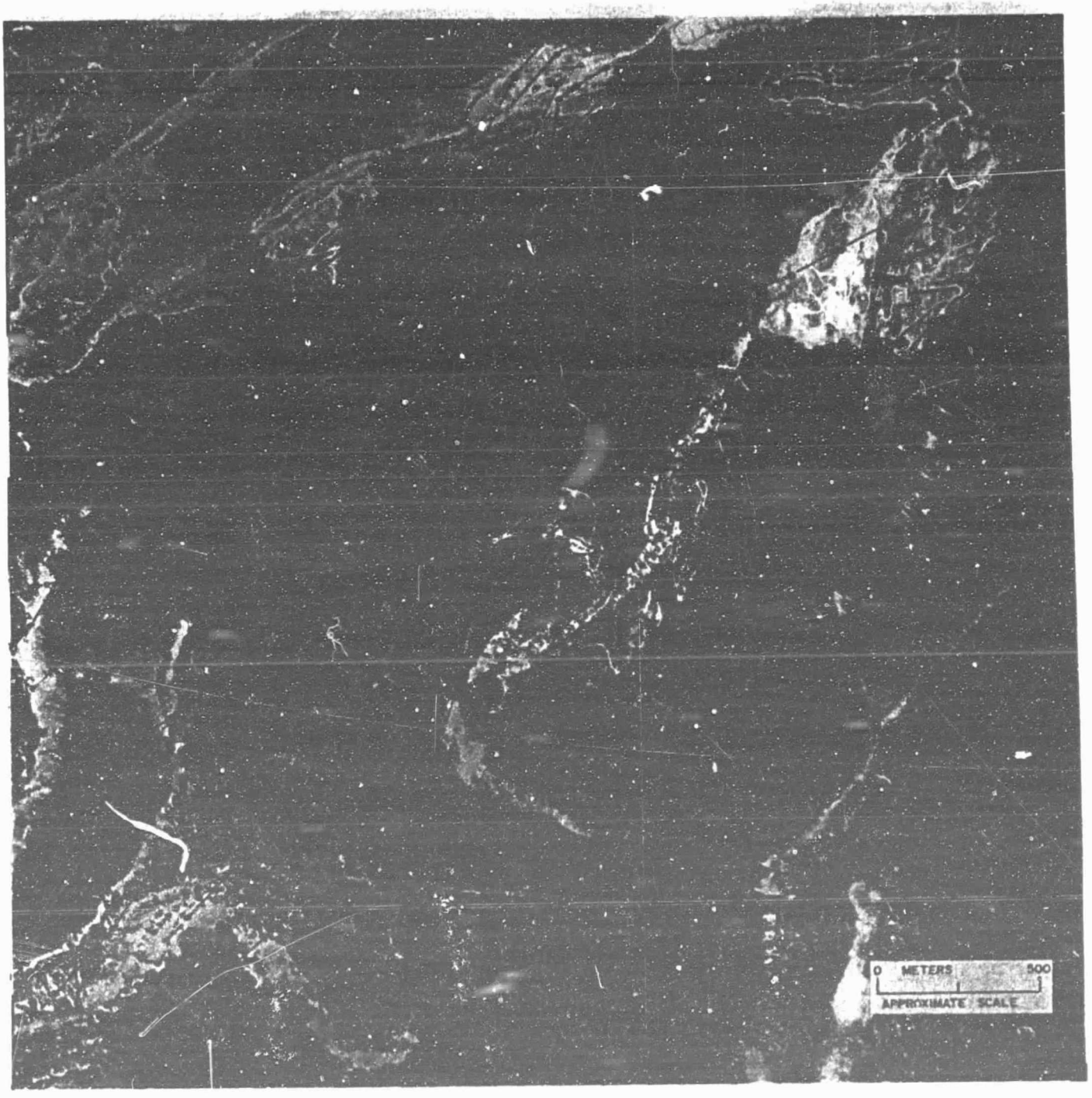

Figure 1. Photo of Cotter Basin site with 1978 survey traverses. Symbols mark the locations of every tenth spectral measurement, which are recorded on 35mm film taken simultaneously with the spectral measurements.

The spectroradiometer was flown at 610m above the ground surface and at 200km per hour ground speed. The target measurements were taken with an 18-meter square field-of-view and in a contiguous one-dimensional line sequence along the ground track. The survey site was covered in a pattern of south-north flight lines with about 200 feet of spacing between lines. The ground tracks of the flight lines, determined from aircraft 35mm film acquired simultaneously with the spectral data, are plotted in Figure 1. The survey lines are about 3 kilometers long and were planned to cover the areas of both background and anomalous vegetation. Each traverse contains 130 to 200 spectral measurements in 500 bands each. The symbols along each flight line in Figure 1 mark every tenth spectral measurement in the sequence, at which time the 35mm camera records an image of the ground track. All survey parameters were kept, as nearly as possible, the same as those of the 1976 survey.

The aircraft data are calibrated channel-by-channel for spectral radiance received at the entrance aperture. The data are processed first using our waveform analyses techniques. In the case of the Cotter Basin data, discrete band techniques were also applied to compare the two methods and to determine if discrete bands could be used in future sensor systems.

Waveform Analysis and Mapping of Spectral Anomalies

Our waveform analysis techniques for analysing the high density 500-channel spectrometer data have been used on all sites presented and have consistently produced the best results. The Chebyshev polynomial functions reduce the 500 point spectral curves to a small number of variables similar to the simulated spectral band ratio technique. In

ORIGINAL PAGE IS
OF POOR QUALITY

the Chebyshev functions, however, the relative values among many more points along the spectral curve are considered. We are, therefore, able to achieve much more reliable recognition of certain spectral patterns (Collins and Chiu, 1979).

With various polynomial functions we are able to recognize several spectral patterns which can, to varying degrees, be separated. The spectral variations caused by canopy density and irradiation level, however, remains by far the largest effect and the one that often limits recognition of other vegetation spectral features. For this reason, we have extended the mapping technique by allowing it to first identify and separate areas of thin canopy or low irradiance levels, where the data will tend to become unreliable. The computer pattern recognition technique can then be applied in a second step, and possible a third or more steps, using only data from areas with good vegetation cover and with good surface exposure to the solar irradiation. The multistage discrimination is useful mostly in areas where the vegetatation anomalies are very weak.

Thin Canopy Discrimination

The data from flight line 7 in Figure 1 were used for reference in developing a mapping technique for Cotter Basin and the other sites. This traverse crosses the main part of the geochemical anomaly. A polynomial function sensitive to canopy density along flight line 7 is plotted from south to north in Figure 2a.

To obtain a relative scale that will clearly resolve contrasts within the survey data set, each mapped polynomial function for the array of data points containing all spectra from all flight lines in the survey area are rescaled into the interval from 0 to 10. For each polynomial function, therefore, we have in the computer an array in which the x, y

ORIGINAL PAGE IS
OF POOR QUALITY

ORIGINAL PAGE IS
OF POOR QUALITY

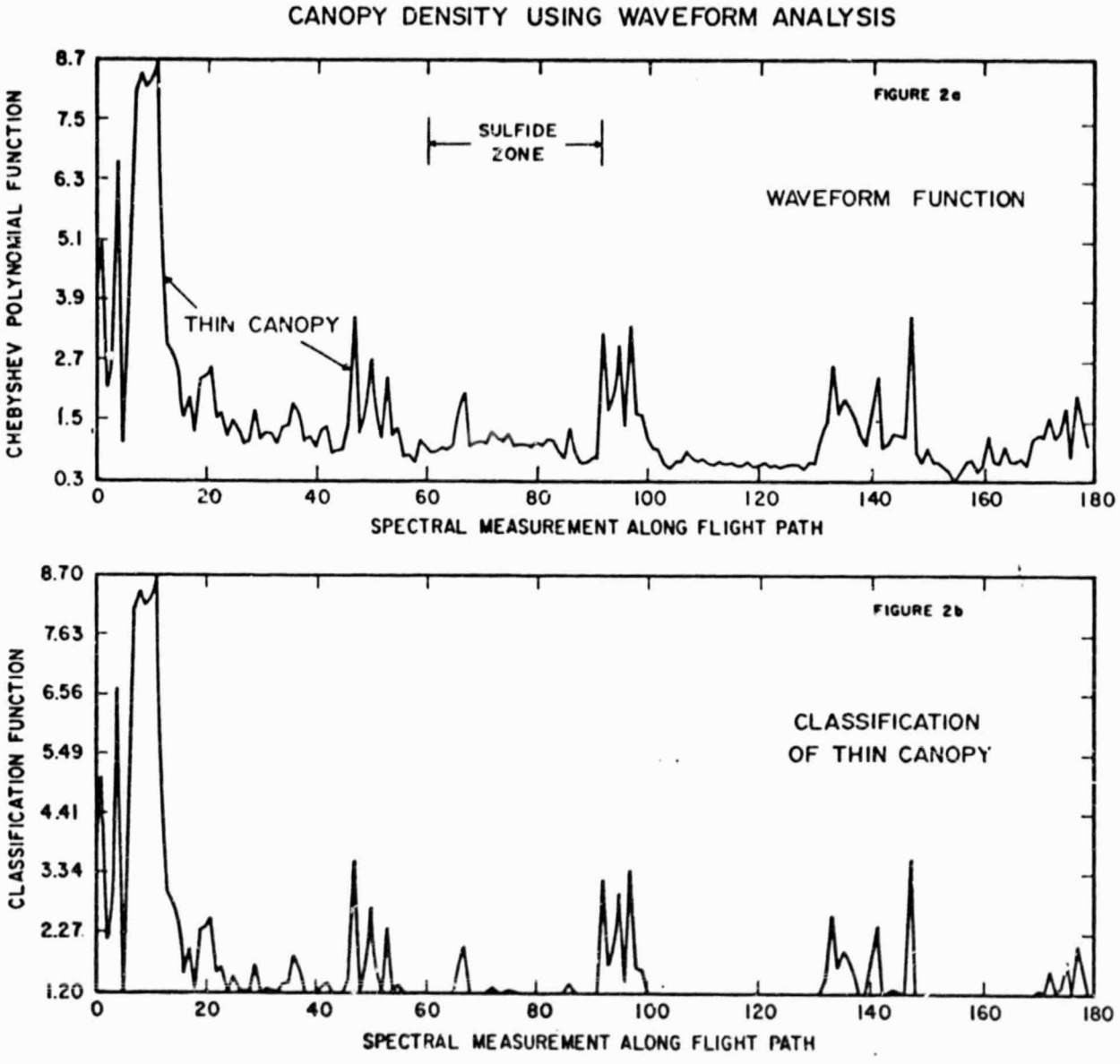

Figure 2. (a) Traverse 7 Chebyshev function sensitive to canopy density
(b) Classification of thin canopy along traverse 7.

ORIGINAL PAGE IS
OF POOR QUALITY

plane contains the coordinates of the survey grid shown in Figure 1. The z axis is the rescaled, from 0 to 10, magnitudes of a particular polynomial function. By this technique, the absolute values of the variations in polynomial functions are normalized, and the contrast is enhanced. For example, the variation in functions sensitive to cover density are two orders of magnitude greater than functions sensitive to the apparent stress variation (Figure 3a). The spectral variations reflected in Figure 3a would be imperceptible if plotted on the same absolute scale as the function in Figure 2a. Plots as shown of aircraft traverses are essentially a slice of the array. The variables plotted along aircraft traverses are on a maximum/minimum scale, also to enhance contrasting spectral qualities along the traverses. The y axis values are on the same 1 to 10 scale used in the survey grid array.

From the polynomial data in Figure 2a, a very precise separation of thin canopy areas can be made using a simple thresholding technique. Areas of thick canopy cover are well below 2 in magnitude on the relative scale, while areas of thin canopy are close to 10. The area of high values in the first 15 measurements along the traverse are mostly bare soil. Other areas of vegetation cover vary from a background value of approximately 1 or less in areas of thick cover to 2 and above for thinner forest canopy with soil showing through.

In the Cotter Basin survey, a good practical threshold for eliminating thin cover is 1.2 in the relative magnitude of this polynomial function. All points above 1.2 are eliminated from consideration in the next step of the analysis. The higher order polynomial terms used in calculating this and other functions are sensitive only to the relative wave shapes rather than absolute energy under the curve, or the amplitude. The 1.2 threshold limit, therefore, has proven to be transferable from this reference data to all other data in this survey site

ORIGINAL PAGE IS
OF POOR QUALITY

and in other survey sites with very good results. The results of the threshold discrimination are shown in Figure 2b. All points above 1.2 are considered thin canopy.

Anamalous Vegetation Mapping

The rescaled polynomial function sensitive to mineral-induced differences in the chlorophyll absorption region between 550nm and 750nm is shown in Figure 3a. Flight line traverse 7 crosses the sulfide zone between measurement 60 and 80. A very high contrast in the magnitude of the polynomial function sensitive to spectral waveforms of vegetation stress is very evident over the sulfide zone. The variation in the magnitude of this function is between 1 and 3 over background forest canopy areas. The signal in the anomalous region is greater than 200 percent above this background level using the polynomial technique. This signal to noise ratio is consistent in other sites where vegetation anomalies have been observed.

The spectrally anomalous vegetation in the Cotter Basin survey site has been mapped by threshold discrimination using the polynomial functions shown in Figure 3a. A threshold magnitude of 3 has been established for discriminating anomalous vegetation using the polynomial function in Figure 3a. This discrimination threshold has proved consistent in other sites. The discrimination results for traverse 7 or Cotter Basin are presented in Figure 3b.

The waveform analysis for the entire array of survey data points is presented in Figure 4. The fine cross hatching encompasses areas in which anomalous spectral properties were detected. The anomalous vegetation zone is centered over the known copper anomaly zone (white stippled area), and is elongated east/west similar to the mapped soil geo-

ORIGINAL PAGE IS
OF POOR QUALITY

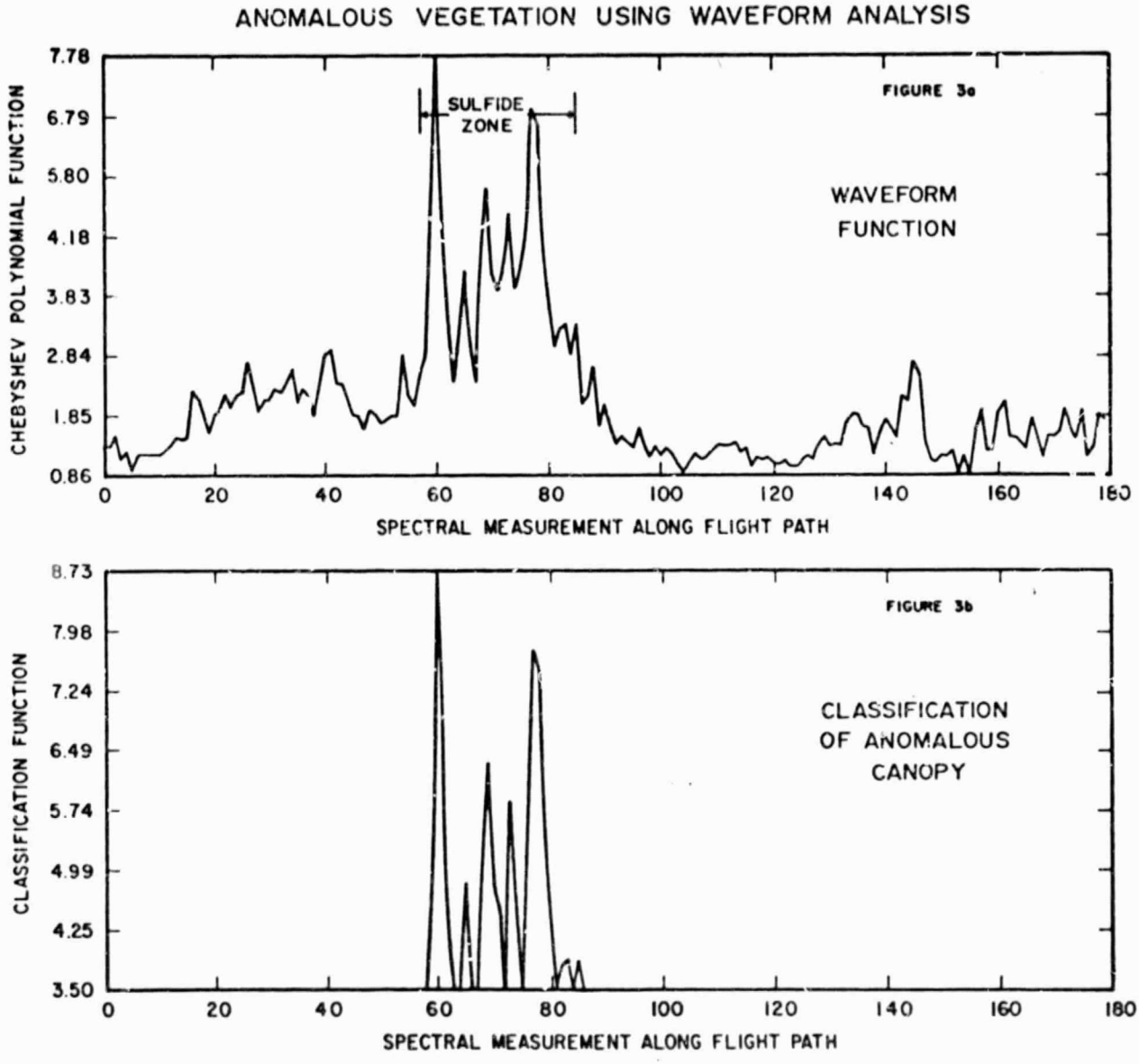

Figure 3. (a) Traverse 7 Chebyshev function sensitive to anomalous vegetaion.
(b) Classification of anomalous vegetation along traverse 7.

ORIGINAL PAGE IS
OF POOR QUALITY

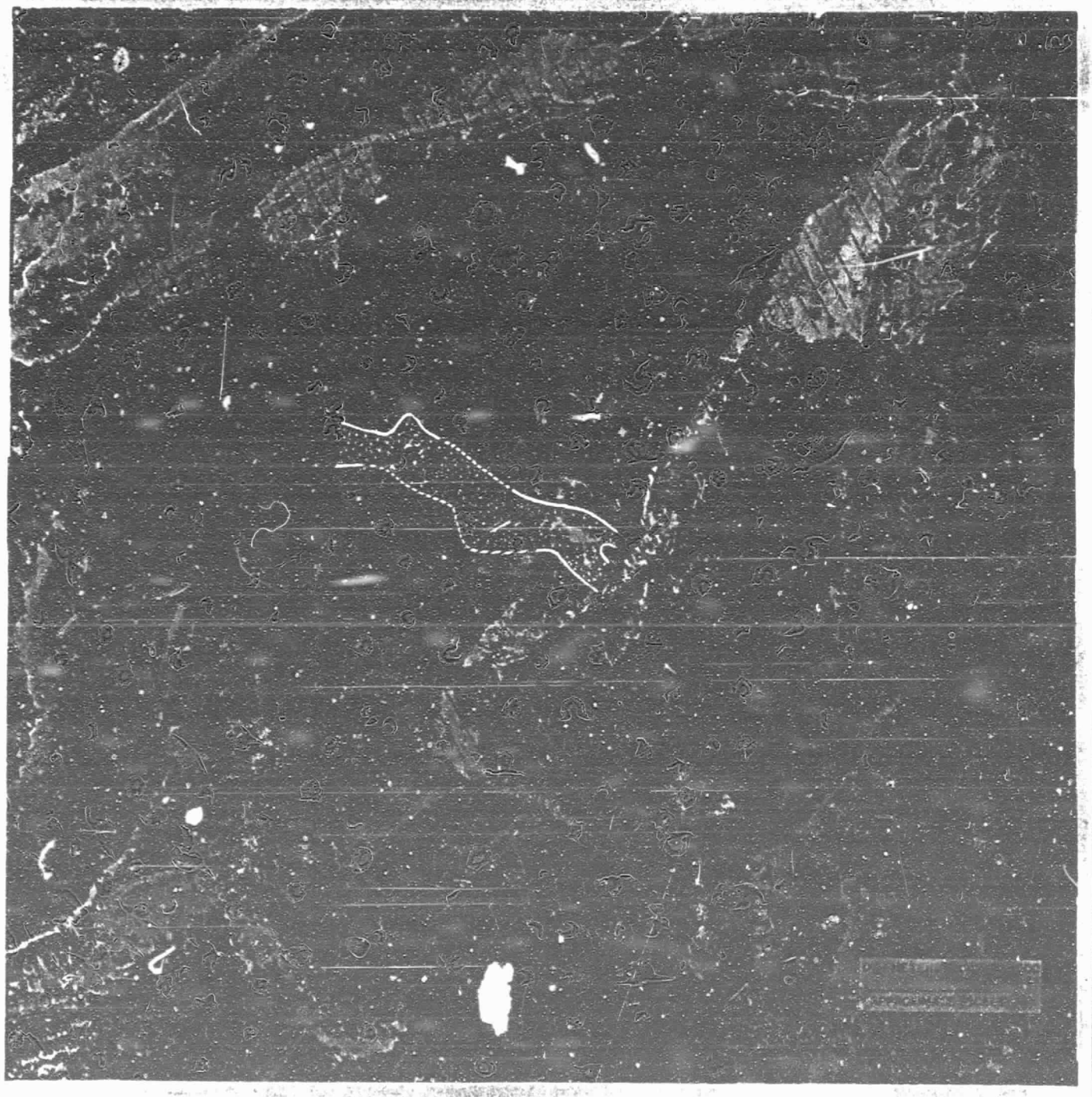

Figure 4. Photo of Cotter Basin with 1978 survey results. Anomalous vegetation mapped wi . the waveform analysis technique is indicated by fine cross hatching.

ORIGINAL PAGE IS
OF POOR QUALITY

chemical anomaly. Broader cross hatching (labeled no data) indicate areas where no geochemical data were available from the Utah International survey. Ground geochemical data from the area enclosed by the broad cross hatched pattern in Figure 4 indicates background metal content in soils.

The vegetation anomaly extends eastward to the rim of a large glacial cirque. Thin canopy conditions east of the rim may be masking vegetation anomalies in that area. The spectral survey indicates that the geochemical anomaly cuts off on the western edge about where the ground geochemical sampling stopped. Two geochemical sampling traverses were subsequently run along the western boundary by the U.S. Geological Survey and Columbia University. This data confirms that the geochemical anomaly does stop about where it is indicated by the spectral survey. The spectral anomaly extends to the south of the copper geochemical anomaly. Our ground reconnaissance reveals that previously unmapped porphyry outcrop extends to the south in the area of anomalous vegetation. The anomalous vegetation extends to the northeast. The reason for this distribution has not been determined.

should present ground data here

Correlation of Results from 1976 Survey with 1978 Survey Results

The two-fold aim of the 1978 survey flight over the Cotter Basin site was to determine both our experimental repeatability and the temporal persistance of the vegetation anomaly. The results were positive in both cases.

The results of the waveform analysis and mapping of anomalous vegetation are shown for both surveys in Figure 5. The cross hatching sloping down to the right indicates areas mapped with the 1978 survey data, as seen in Figures 4. Other areas with opposite cross hatching

were mapped from the 1976 survey data. The results are essentially the same. Differences in the shapes of the mapped areas can be attributed to the placing of flight lines and other experimental errors. The main anomaly areas, however, overlap very well.

From the results of the two Cotter Basin surveys and waveform analysis, we can conclude that vegetation anomalies over this sulfide zone can be detected with suitable remote sensors and data processing. It also appears that the vegetation anomalies are persistant over time. We still require further experimental surveys to determine the effects of season, sun angle, rainfall, and other environmental factors on the observed spectral properties of forest canopies.

Discrete Band Analysis

Several discrete band techniques have been employed in our analysis of the Cotter Basin data. The aim is to determine the effectiveness of discrete band measurements for detection of vegetation anomalies. Methods of detection using a limited number of fixed spectral bands are essential for future airborne and possibly satellite spatial scanner systems.

The spectral properties of the vegetation canopy observed in the Cotter Basin site are presented in the spectra of Figures 6. The long wavelength limit of photon absorption on the near IR absorption edge of spectra from the sulfide zone is shifted toward the shorter wavelengths. This change in the absorption properties of the chlorophyll pigments is often accompanied by a change in the spectral absorption properties of the 550nm and 650nm region on the short wavelength wing of the main chlorophyll a bank at 680nm. Further analysis of the chlorophyll spectral properties using laboratory grown plants

ORIGINAL PAGE IS
OF POOR QUALITY

ORIGINAL PAGE IS
OF POOR QUALITY

Basin plots comparing the results of the waveform
e 1976 and the 1978 surveys.

ORIGINAL PAGE IS
OF POOR QUALITY

have been obtained under the present National Science Foundation Grant. These results clearly substantiate the field observations presented here (Chang and Collins, 1980).

The spectrum of exposed white soil is included in Figure 6 to indicate the general shape of the normal solar spectrum in the absence of absorbing pigments. The slope of the reflected solar radiance curve changes from negative to positive in the 750nm to 770nm region on either side of the O_2 absorption band. The magnitude of the positive slope of the curve in this narrow region has been used successfully in analyzing the spectral properties of some types of agricultural vegetation (Collins, 1978). A negative slope in this region has also been used previously to detect the vegetation anomaly in Cotter Basin using the 1976 survey data (Collins, Raines, and Canney, in press). The slope in each case was determined using band ratio techniques. The discrete band methods, however, have high noise susceptibility in some cases, as we show in the following analysis.

Band Ratio

Bands of various widths, usually 10nm, have been computer simulated for the present study by integration of narrower (1.4nm wide) bands in the aircraft spectroradiometer data. The ratios of 10nm wide spectral bands placed at 745nm and 785nm are presented in Figure 7a. The data in Figure 7a is from reference traverse 7 of the 1978 survey as presented in Figures 2a and 3a. Other simulated band 745nm and 785nm ratios for a 1976 survey traverse, flown very close to the 1978 traverse in Figure 7a, are presented for comparison in Figure 7b. The ratios of these two bands tend toward unity as the

ORIGINAL PAGE IS
OF POOR QUALITY

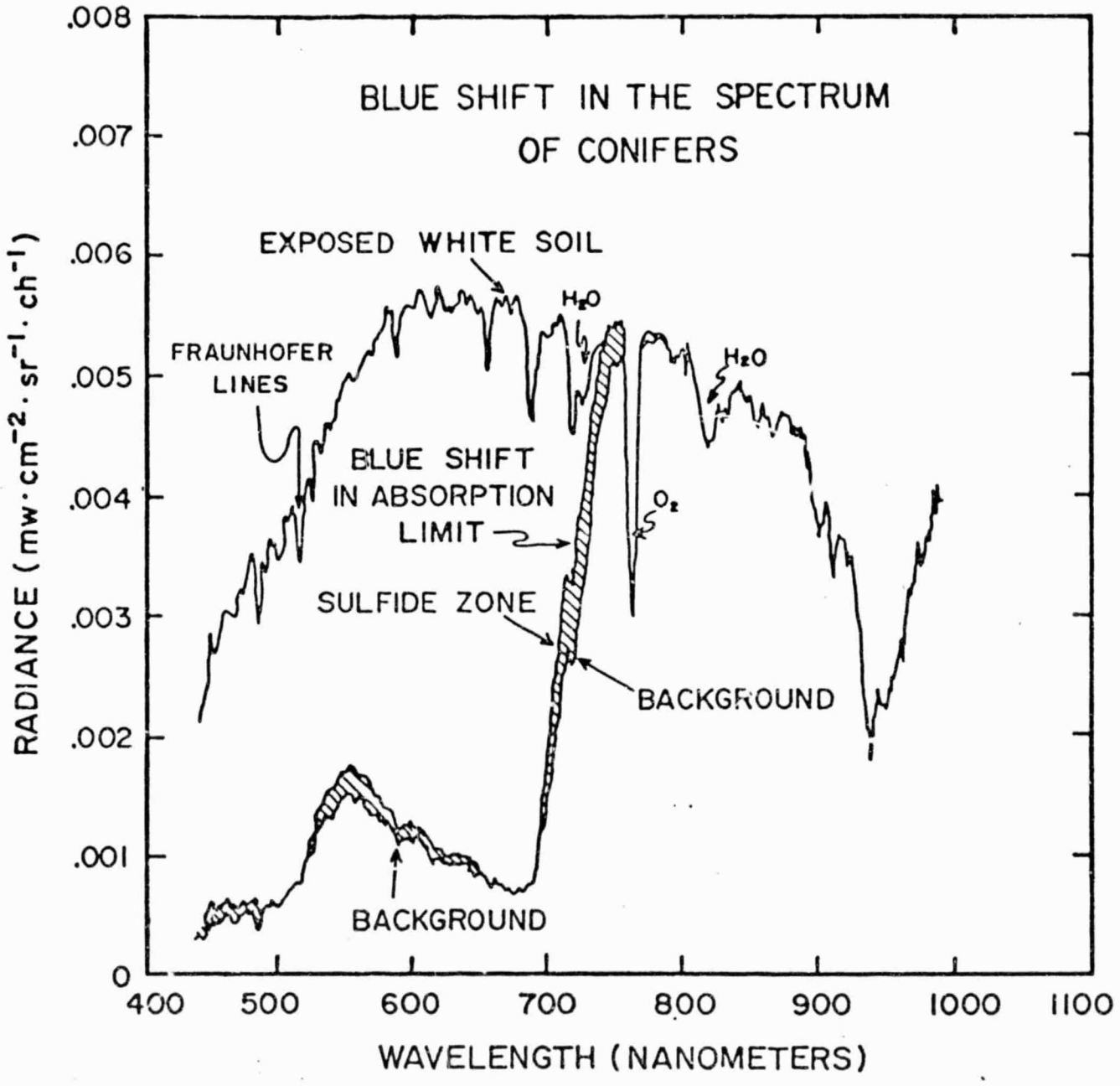

Figure 6. Spectra of background and anomalous vegetation and of white slope rubble taken from the 1978 Cotter Basin data.

ORIGINAL PAGE IS
OF POOR QUALITY

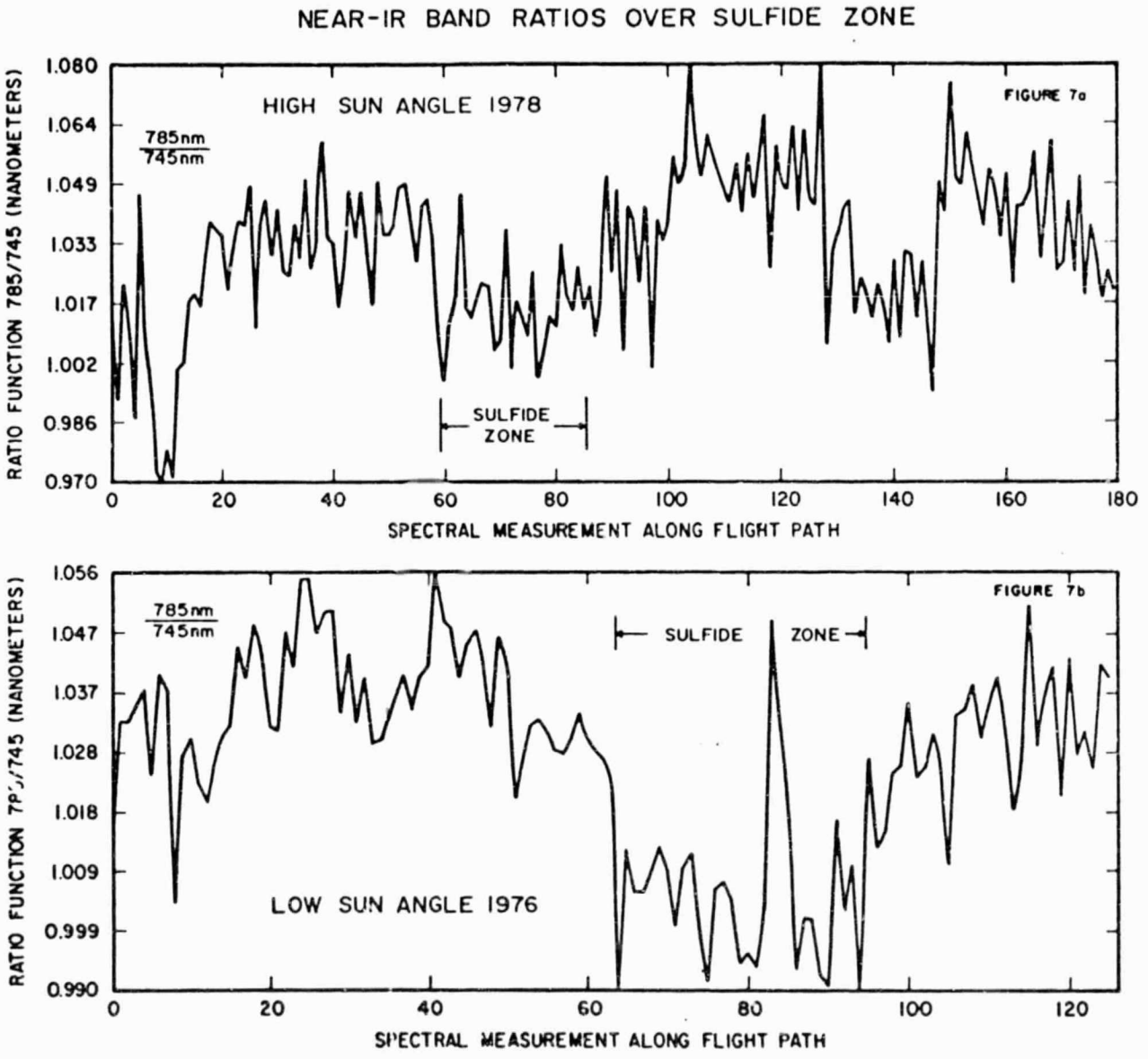

Figure 7. (a) Ratios of band 785nm over 745nm from the 1978 Cotter Basin survey, Traverse 7 (10nm wide bands)
(b) Ratios of same bands from a similar traverse in the 1976 survey (10nm wide bands)

ORIGINAL PAGE IS
OF POOR QUALITY

absorption edge shift to shorter wavelengths, and goes below one in the absence of a chlorophyll absorption feature in this wavelength region.

A decreasing trend is visible in the 785/745 band ratios in the area of sulfide zone, which falls between measurements 60 and 80. There is, however, a similar, and much larger, decreasing trend along the traverse caused by other canopy variations along the traverse in Figure 7a overwhelm the ratio changes over anomalous vegetation. This effect was not as serious in the earlier 1976 survey data because of the lower sun angle at that time. In the 1976 Cotter Basin survey, it was possible to map the vegetation anomaly using this ratio alone (Figure 7b). The 1976 traverse shown in Figure 7b crossed the geochemical zone between measurement 63 and 93 where the band ratio values are lowest. It becomes obvious in the 1978 survey data, then, that the combination of sun angle, ground slope, and canopy density are going to have a very serious negative effect on discrete band data analysis.

Other spectral band ratios were tested. Bands 10nm wide were simulated in parts of the spectrum selected for optimum sensitivity to the major wide band vegetation features. The bands were placed at 785nm on the near IR plateau, at 680nm in the red chlorophyll absorption band, at 550nm on the green peak, and at 480nm in the blue pigment absorption region. In each case the reference traverse 7 path from the 1978 survey are presented. The ratio of the 785nm near IR band over the 680nm chlorophyll absorption band in Figure 8a is very sensitive to canopy density variations. All the other spectral variations are submerged in the canopy density signal. The ratios of bands at 550nm

ORIGINAL PAGE IS
OF POOR QUALITY

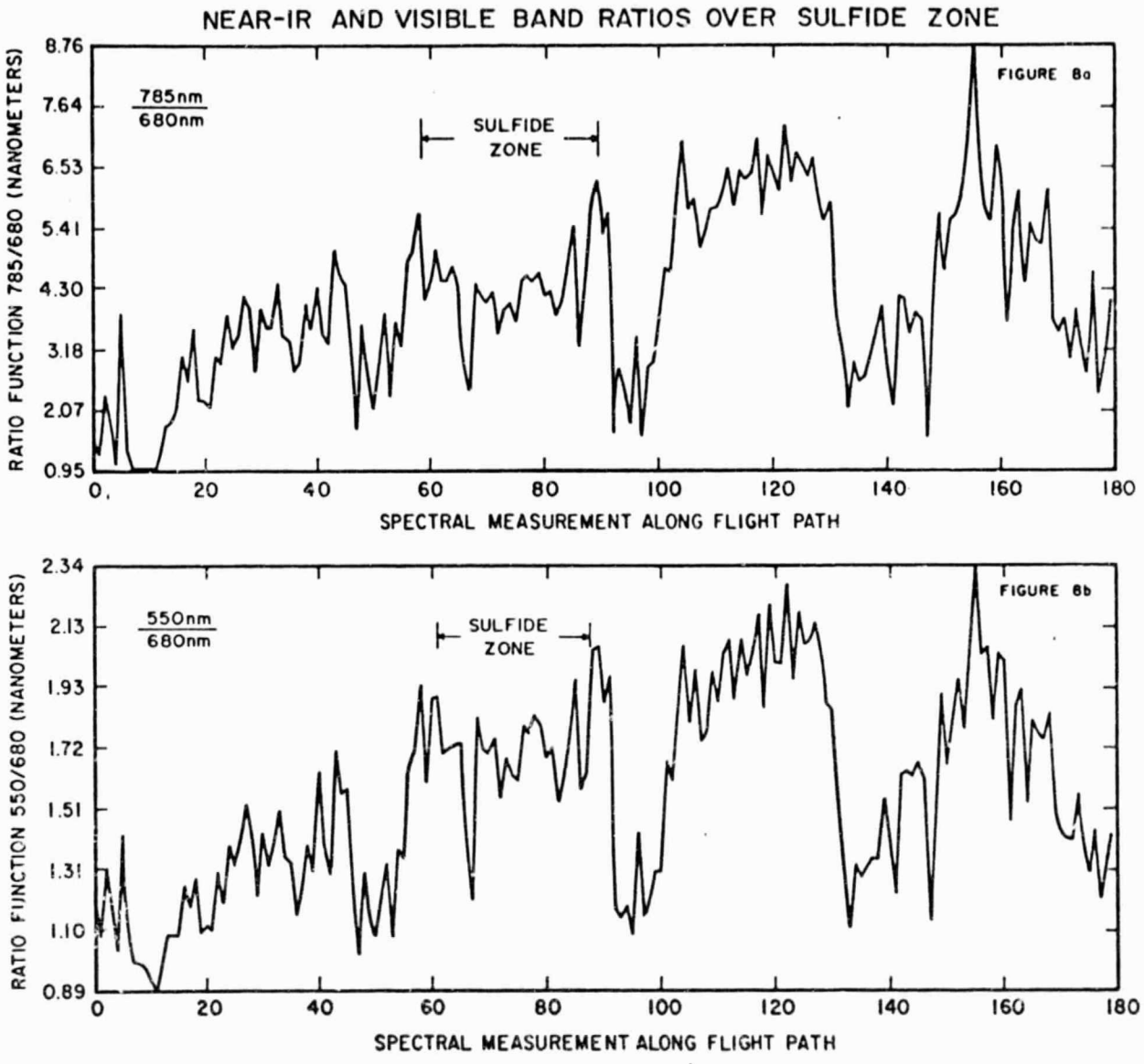

Figure 8. Band ratios of 1978 Cotter Basin data, Traverse 7 (10nm wide bands): (a) 785nm/680nm, (b) 550nm/680nm.

ORIGINAL PAGE IS
OF POOR QUALITY

over 680nm (figure 8b) are also dominated by the canopy density effect. The subtle changes in the green peak over the anomalous zone are submerged.

The ratios of bands in the blue and green region are dominated by two first order effects: canopy density, and irradiance level. The ratios of the 550nm band over the 480nm band, which are sensitive to canopy density, show an interesting artifact of the ratio technique. The Figure 6 spectral curves show that, in the first order approximation, there is essentially the same slope relationship between points at 480nm and 550nm on both the vegetation spectral curves and the curve for white soil. The radiance at 480nm, however, approaches a value close to zero in vegetation spectra at which point the ratios will rapidly approach a very large number not indicative of the true slope on the curve. The ratios of the same two points on the exposed soil curve, on the other hand, are the ratios of two large numbers, in which case the ratios will approach unity. This effect is demonstrated in the Figure 9a ratios where the traverse crosses exposed white soil and rock in the first 15 measurement points and several other areas along the flight path. The problem is that the simple band ratios are not a true $\Delta y/\Delta x$ function.

A more broadly varying slope or irradiance effect in the dense canopy areas is superimposed on the ratio cureves in Figure 9a and 9b. The ratios of the bands at 680nm and 480nm show the slope/irradiance effect very well in Figure 9b. The flight line 7 traverse crosses the south facing slope of the ridge above Cotter Basin at measurement 40 and traverses the north facing slope to the valley at measurement 120,

ORIGINAL PAGE IS
OF POOR QUALITY

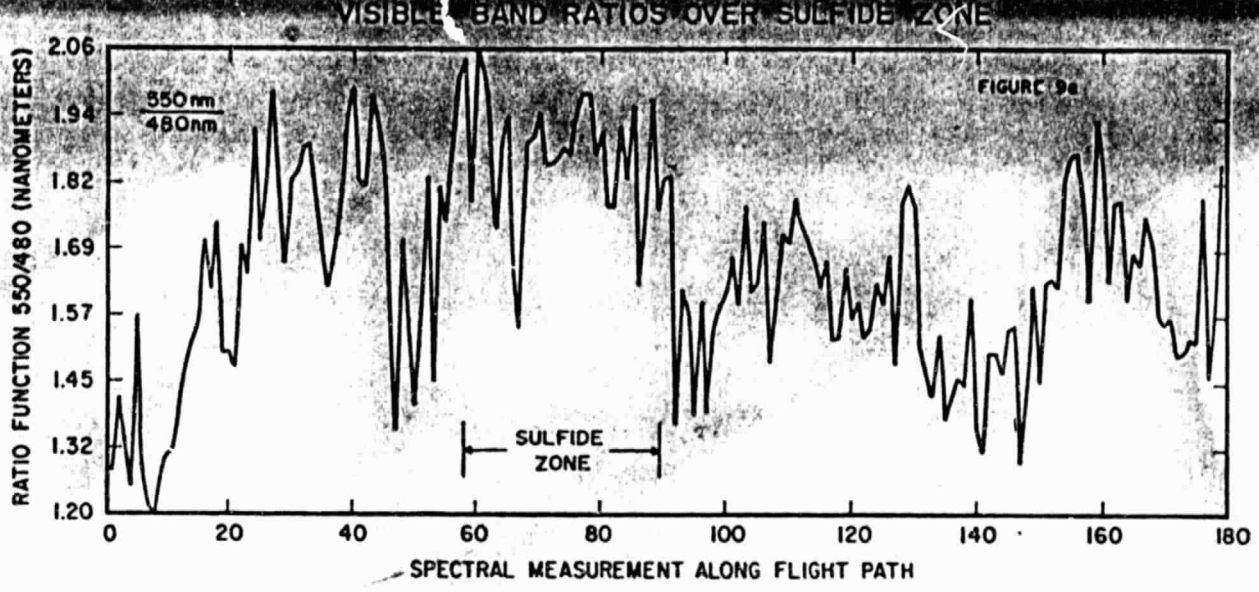

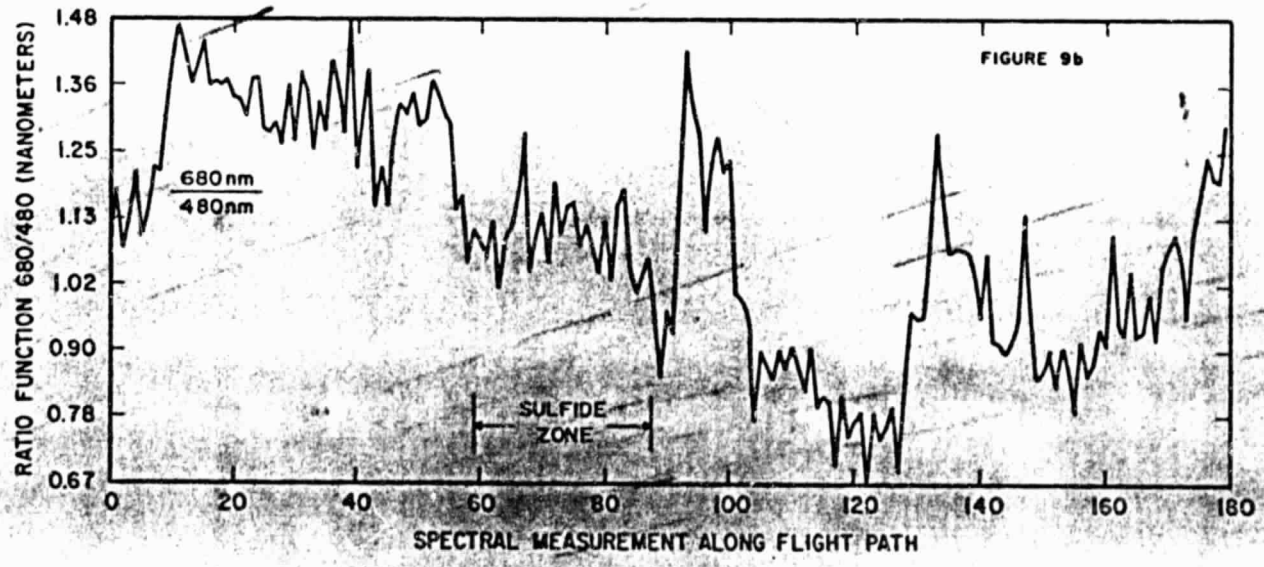

ORIGINAL PAGE IS
OF POOR QUALITY

Figure 9. Band ratios of 1978 Cotter Basin data, Traverse 7 (10nm wide bands): (a) 550nm/480nm, (b) 680nm/480nm.

where the terrain levels to become south facing again at measurement 160. The ratios in Figure 9b show a general high trend on south facing slopes and low on the north facing side with higher ratios in bare areas. This broad variation due to the slope effect is superimposed on the density effects in Figure 9a.

In conclusion, the simple band ratio technique will not detect second order effects in vegetated terrain. Narrow bands on the near IR shoulder or in other regions of the spectrum are dominated by the much larger first order effects of canopy density, irradiation level, and target slope and texture. This does not, however, preclude the use of multiple bands to filter the canopy-induced "noise" effects and extract the desired signal.

Multiband Analysis

The principal component technique of multiband analysis has been applied to the spectral data from reference traverse 7 in the Cotter Basin data. The multiband analysis using from 4 to 32 10nm wide bands in various regions of the spectrum yield promising results and indicate that filtering and analysis techniques using discrete bands are possible. The analysis was applied to the near-IR absorption edge between 710nm and 785nm, the chlorophyll absorption region between 560nm and 670nm, the blue chlorophyll region between 480nm to 680nm interval and the entire 480nm to 785nm pigment region, and to the 550nm to 780nm region used in the waveform analysis method.

The near-IR region was tested using 4 bands between 710nm and 785nm. The results plotted in Figure 10a indicate that a component exists in the 4 band relationships that can uniquely identify the vege-

ORIGINAL PAGE IS
OF POOR QUALITY

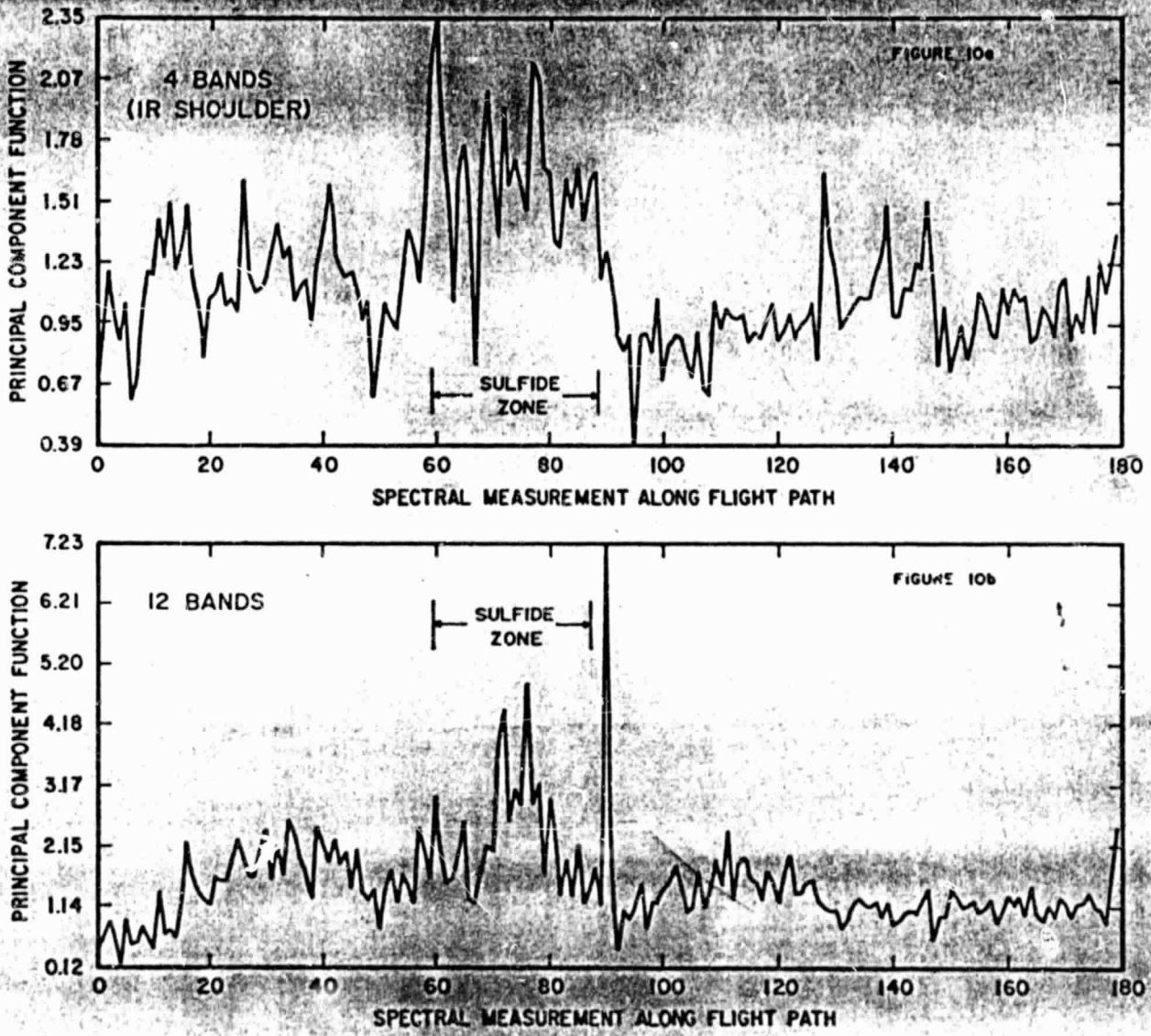

Figure 10. Principal component analysis of 10nm wide bands in 1978 Cotter Basin data, Traverse 7: (a) 710nm to 785nm region (4 bands), (b) 560nm to 670nm region (12 bands).

ORIGINAL PAGE IS
OF POOR QUALITY

tation anomaly in traverse 7. The spectral variation over the sulfide zone is less than 50% above the background noise; but this result using multiple bands is much improved over the two band ratio results in the near-IR bands of Figure 7a. The major noise factors are the thin canopy and slope/irradiance effects in the first part of the flight path and in the roads near the end. Through the use of additional bands we can establish that the canopy noise effects can be significantly reduced.

The short wavelength wing of the chlorophyll absorption band was tested using 12 contiguous narrow bands between 560nm and 670nm (Figure 10b). The response to the vegetation anomaly using this region alone is reduced and mostly submerged in the noise. The road effects seen in Figure 10a, however, can be filtered out using the principal component function in Figure 10b.

The blue pigment absorption region from 480nm to 550nm was tested using 8 bands in Figure 11a with essentially no improvement over the results using the 560nm to 670nm region. The response to the anomalous zone is only weakly above the noise level. Extension to 20 bands in the 490nm to 680nm interval in Figure 11b brings no improvement in the response to the sulfide zone. Instead, the sensitivity to background noise effects is increased.

With further extension of the principal component analysis to 32 bands, including the near-IR edge, the sensitivity to the anomalous zone increases significantly. The broad interval from 480nm to 785nm shown in Figure 12a, however, is still sensitive to background canopy-induced noise effects. These results are improved by narrowing the spectral region to 24 bands in the 550nm to the 780nm region (Figure 12b). The response to anomalous vegetation in Figure 12b comes closest

ORIGINAL PAGE IS
OF POOR QUALITY

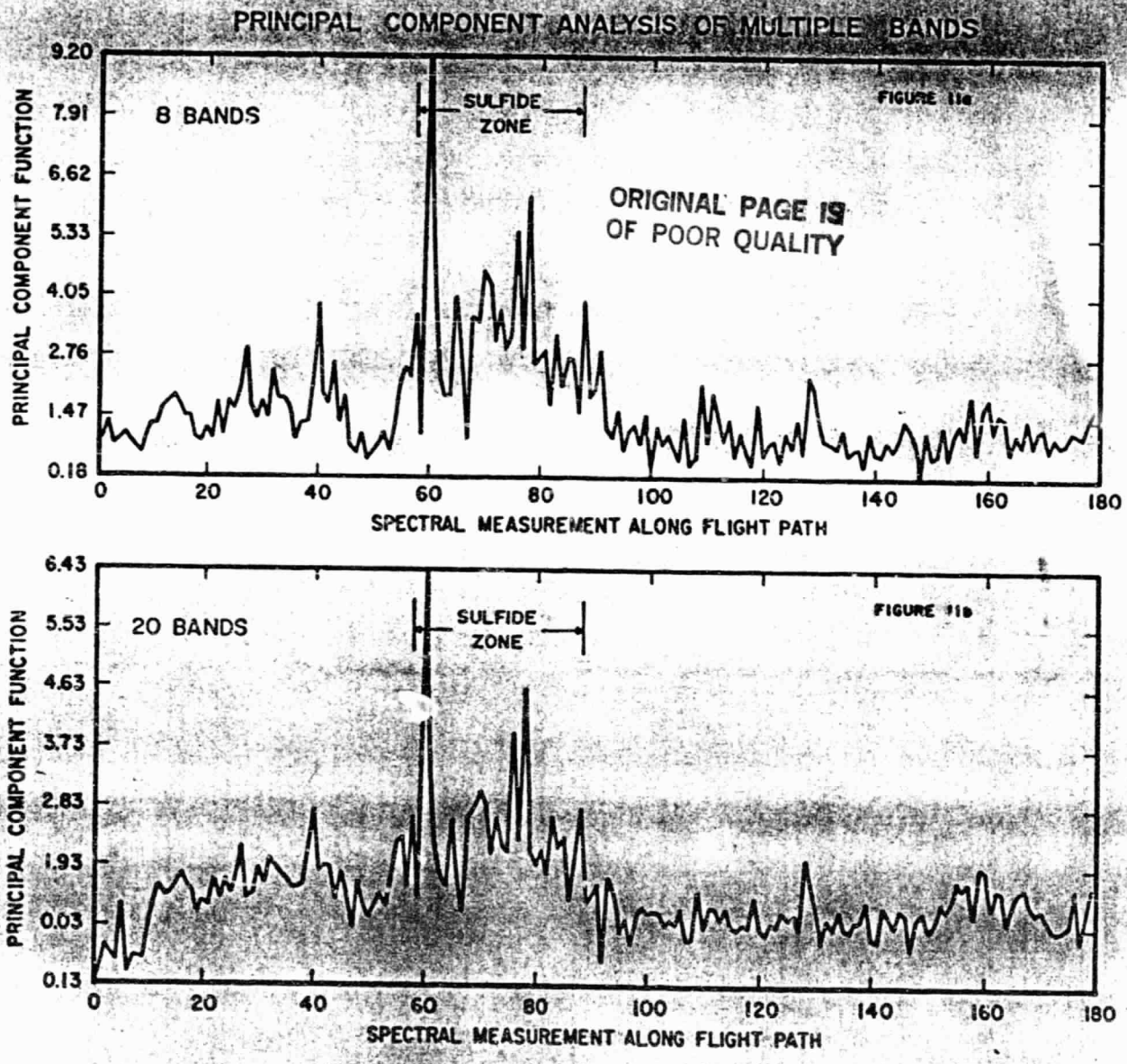

Figure 11. Principal component analysis of 10nm wide bands in 1978 Cotter Basin date, Traverse 7: (a) 480nm to 550nm region (8 bands), (b) 490nm to 680nm region (20 bands).

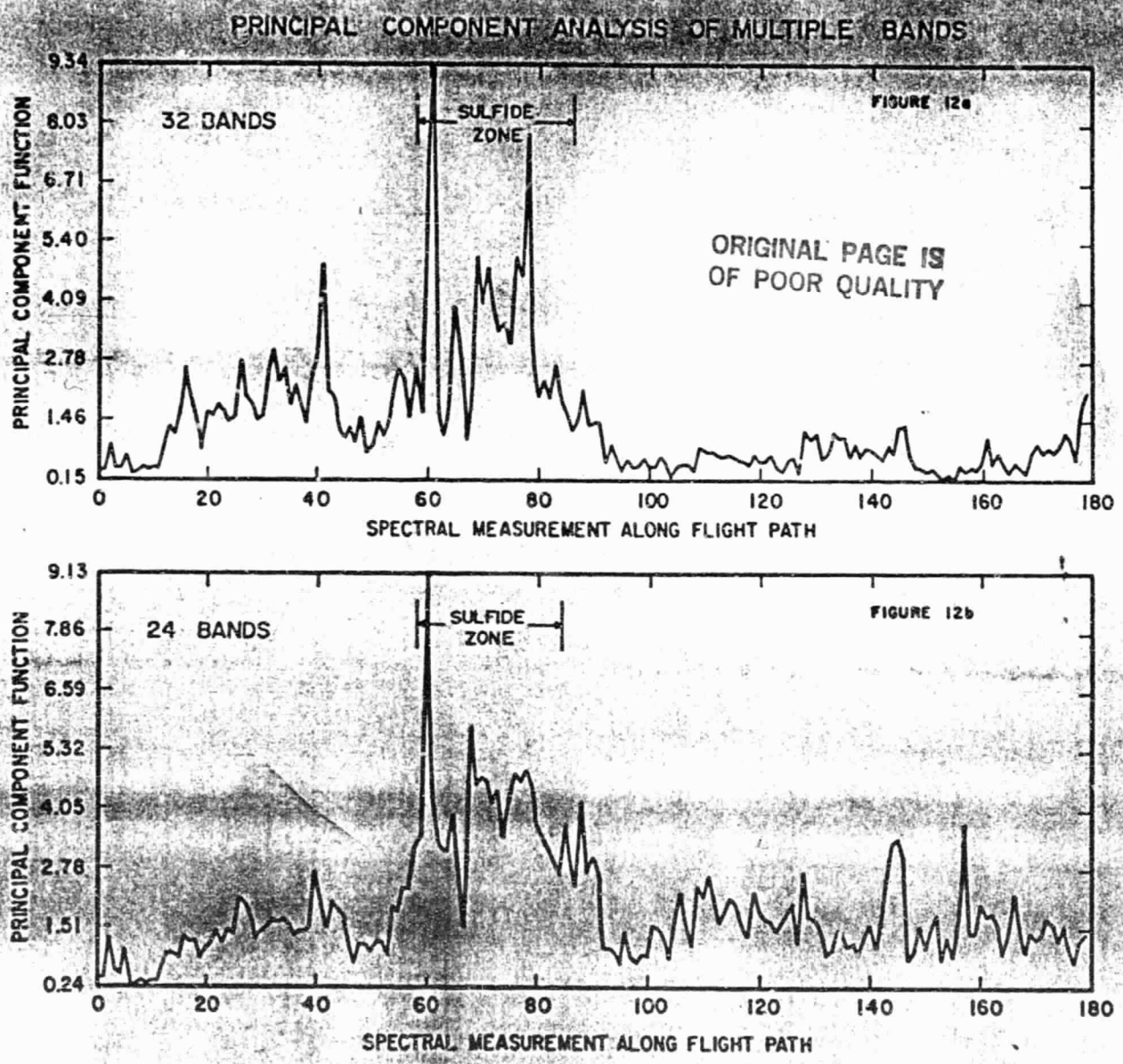

Figure 12. Principal component analysis of 10nm wide bands in 1978 Cotter Basin data, Traverse 7: (a) 480nm to 785nm region (32 bands), (b) 550nm to 785nm region (24 bands).

to the signal to noise ratio obtained with the waveform analysis technique in Figure 3a.

The multiband analysis indicates that the essential information lies in the 550nm to 785nm region of chlorophyll absorption, and that the near-IR edge region probably contains the most critical information. Bands in the pigment absorption region below 710nm are very sensitive to first order noise variations in the forest canopy. The key to discrete band analysis will be noise filtering.

Multiband Analysis Using LANDSAT Bands

The principal component method has been applied to the 1978 Cotter Basin reference traverse 7 to determine the possible LANDSAT system responsitivity to the vegetation anomaly. The four LANDSAT band responsitivities were simulated by integration of the radiance in the aircraft spectral curves over the spectral intervals of the LANDSAT bands. The principal component analysis results for the simulated LANDSAT bands along traverse 7 are plotted in Figure 13a-d.

The major component of the 4 band distribution is the canopy density effect shown in Figure 13a. The second component includes both the canopy density and the slope/irradiance effects (Figure 13b). The remaining components are esstially random noise.

The LANDSAT bands, it is concluded, are sensitive only to the gross first order variations in broad-band reflectance properties of vegetation canopies, and can not separate the subtle spectral variations seen in the vegetation anomaly of Cotter Basin.

Conclusions in Cotter Basin Experiment

The second Cotter Basin survey in 1978 successfully repeated the results obtained in the 1976 survey. In both cases the correlation of

ORIGINAL PAGE IS
OF POOR QUALITY

ORIGINAL PAGE IS
OF POOR QUALITY

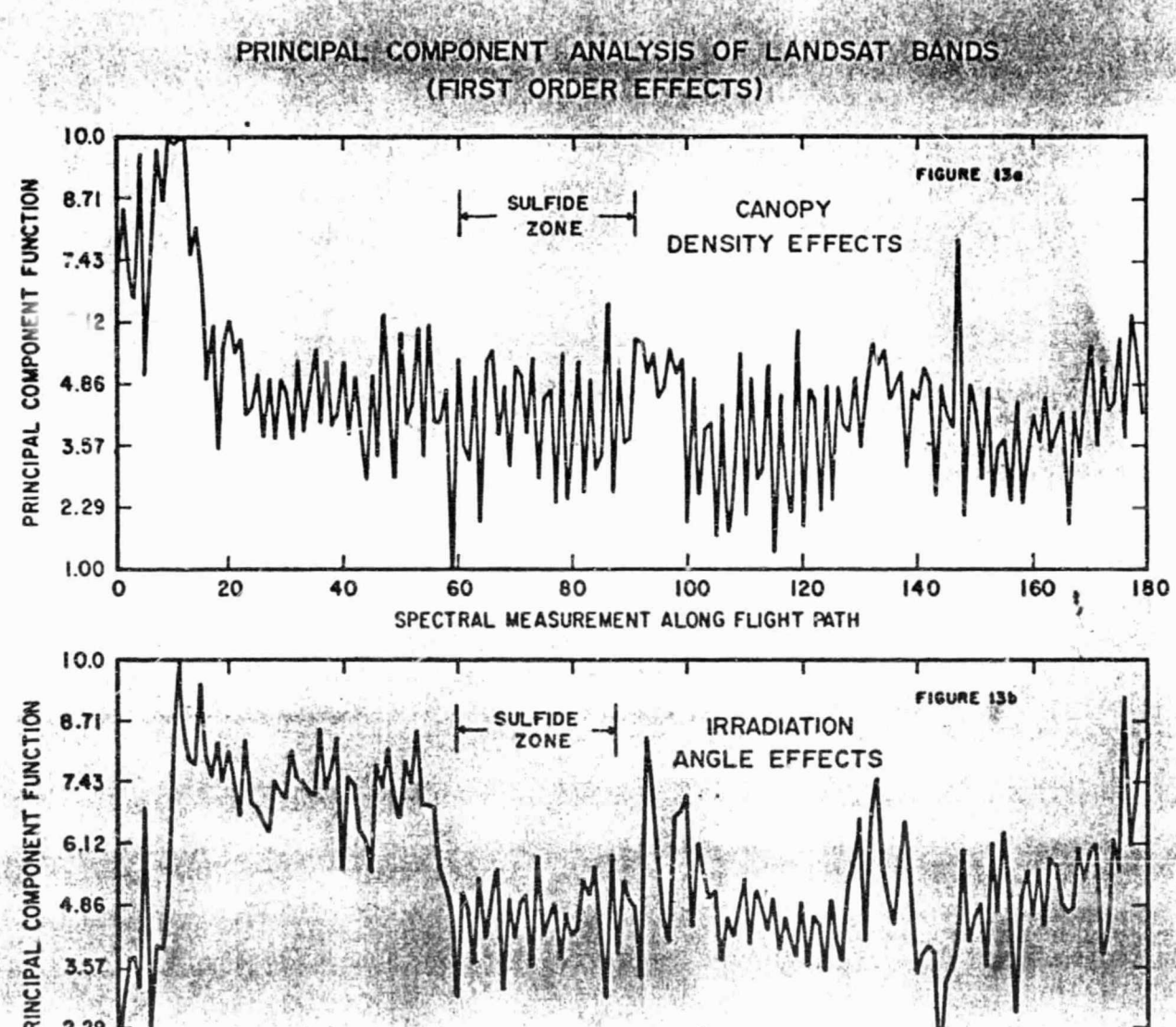

Figure 13a and b. Principal component analysis of simulated LANDSAT bands in the 1978 Cotter Basin data, Traverse 7. The LANDSAT bands are sensitive to canopy density (a), and irradiance level (b).

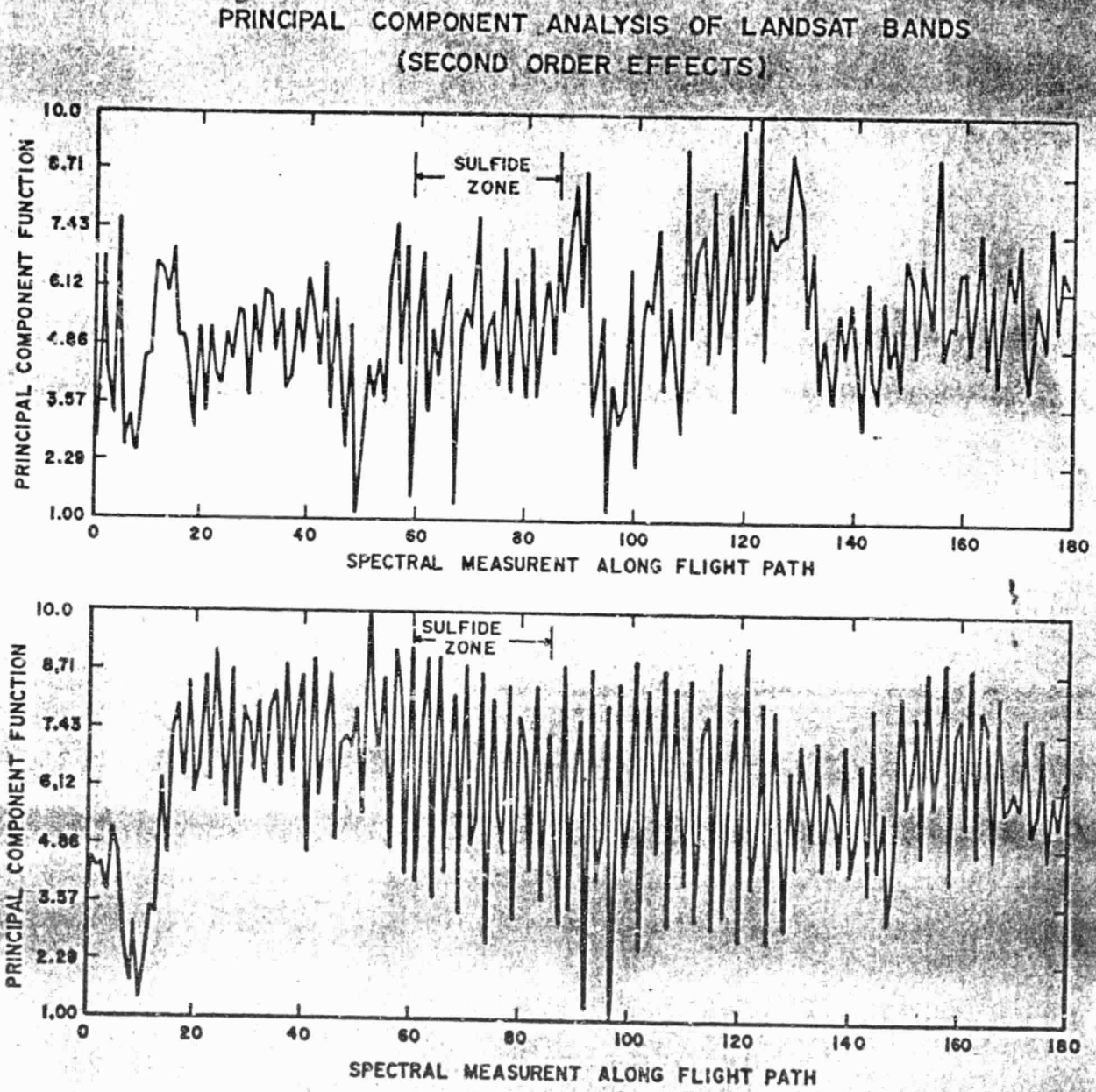

Figure 13 c and d. Principal component analysis of simulated LANDSAT bands in the 1978 Cotter Basin data. Other than the first order effects shown in 13 a and b, the LANDSAT bands show only random noise.

ORIGINAL PAGE IS
OF POOR QUALITY

the vegetation anomaly with the location and shape of the known copper geochemical anomaly is very good.

The vegetation anomaly extends farther from the sulfide veins than the soil geochemistry. But this is not surprising because it is expected that plant root systems will sample deeper and wider than conventional soil sampling techniques. In the case of the southward extension of the vegetation anomaly in Cotter Basin, the tree stress appears to be related to the altered porphyry bedrocks and clay rich soils. This correlation is interesting because our present laboratory studies indicate that plant stress may be related to low iron uptake. Low available iron in the leached porphyry zone could cause plant stress. We are further encouraged by our field reconnaissance revealing that the geochemical anomaly does cut off at the western edge as the spectral survey data indicates.

The important carry-on research includes continued analysis of the aircraft data to extend our knowledge about the spectral properties of natural targets, and noise filtering and signal extraction techniques for processing remote sensor data. These studies have been enhanced to a very large extent by our laboratory analysis of mineral stressed plants being conducted at the Aldridge Laboratory of Applied Geophysics (Chang and Collins, 1980).

Further research will include multiple flights over Cotter Basin to determine the effects of environmental factors on the vegetation anomaly. The contrast between background and anomalous vegetation apparently does change. The contrast in the anomalous zone was significantly greater in the 1978 data. This factor could be very sig-

ORIGINAL PAGE IS
OF POOR QUALITY

nificant in mapping applications aimed at detecting subtle second order spectral variations over sulfide mineral zones. The future research surveys will be conducted with the second generation Columbia University spectroradiometer system with improved data quality and extended spectral range to 2500nm. The laboratory studies have proven that the spectral features observed in the airborne surveys are indeed real phenomena related to copper and zinc in the soil. These studies have also shown that the present high resolution spectroradiometer instrumentation and waveform analysis techniques offer the most sensitive method of stress detection (Collins, et al., 1980).

ORIGINAL PAGE IS
OF POOR QUALITY

III. SPIRIT LAKE, WASHINGTON TEST AREA

The Spirit Lake test site in southwestern Washington was flown with a series of reconnaissance traverses to establish the area as a possible test site for the techniques developed from the Cotter Basin data. The survey covered two known sulfide occurrences in the central portion of the Spirit Lake quadrangle. Hydrothermal sulfide mineralization in the area is associated with Tertiary plutonic intrusions into earlier volcanic host rocks (Hollister, 1979).

The same waveform analysis and discrimination techniques developed in the Cotter Basin study detected strong vegetation anomalies associated with both the copper and the iron sulfide zones.

Goat Mountain Site

The Goat Mountain site in Figure 14 was traversed by five survey flight lines flown from west to east. Copper sulfide mineralization is associated with a circular porphyry intrusion on the south flank of Goat Mountain. The intrusion is surrounded by a pyritic hydrothermal halo. The porphyry and pyritic zones are shown on Figure 14.

The mineralized zones are covered by thin volcanic sediments and thin overburden on the upper slopes. The overburden on the lower slopes (roughly through the center of the mineralized zones shown on Figure 14) thickens rapidly to 110 feet and greater. The area is covered by very dense Douglas fir and pine forest. Spring water emerging near the middle and base of the slope is high in copper content. Samples of the Douglas fir taken by the Duval Corp. are high in copper, but this data is not yet available.

ORIGINAL PAGE IS
OF POOR QUALITY

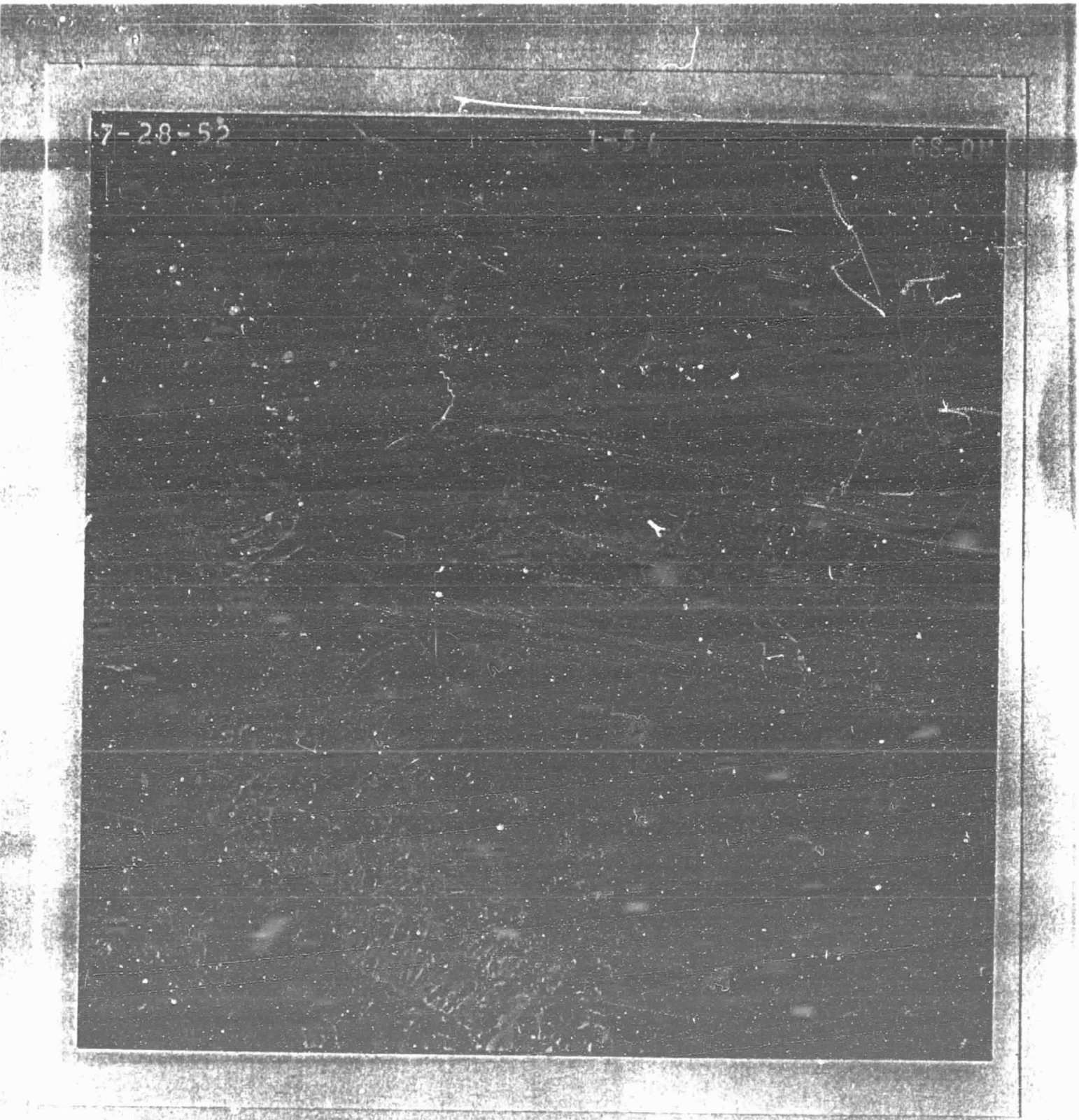

Figure 14. Photo, survey traverses, and analysis results of the Goat Mountain site.

ORIGINAL PAGE IS
OF POOR QUALITY

The survey lines were flown on the upper slope where tree roots would most likely reach soils and ground water rich in copper or where they would be affected by other weathering products of copper and iron sulfides. Strong vegetation anomalies were detected along these traverses. The anomalies fall within both the pyritic and copper porphyry zones. The strongest anomalies are near mid-slope where the interactive effects of down slope soil and ground water migration and thin overburden are most favorable for influencing the vegetation.

Another area of strong anomalies was detected to the west of the mapped pyritic zone. This area lies directly above the "Last Hope" mine. This and other anomalous areas are being examined further on the ground by Columbia University and the U.S. Geological Survey.

Red Springs Site

The Red Springs site five miles north of the Goat Mountain site is a pyritic alteration zone with very high levels of iron pyrite but little or no known copper mineralization. Three traverses shown in Figure 15 were flown over the pyritic zone and background forested areas.

The waveform analysis shows very strong anomalies in the Red Springs area in two apparently elongated zones. These vegetation anomalies occur over the zone of known pyrite mineralization and are elongated along the direction of known pyrite shear zones. The anomalous areas in Figure 15 are also shown in Figure 14.

The waveform analysis techniques have performed very well in analyzing the data from these test sites. The traverses in the Red Springs area crossed a wide variety of terrain and canopy conditions with no apparent false indications or noise problems. The detected

ORIGINAL PAGE IS
OF POOR QUALITY

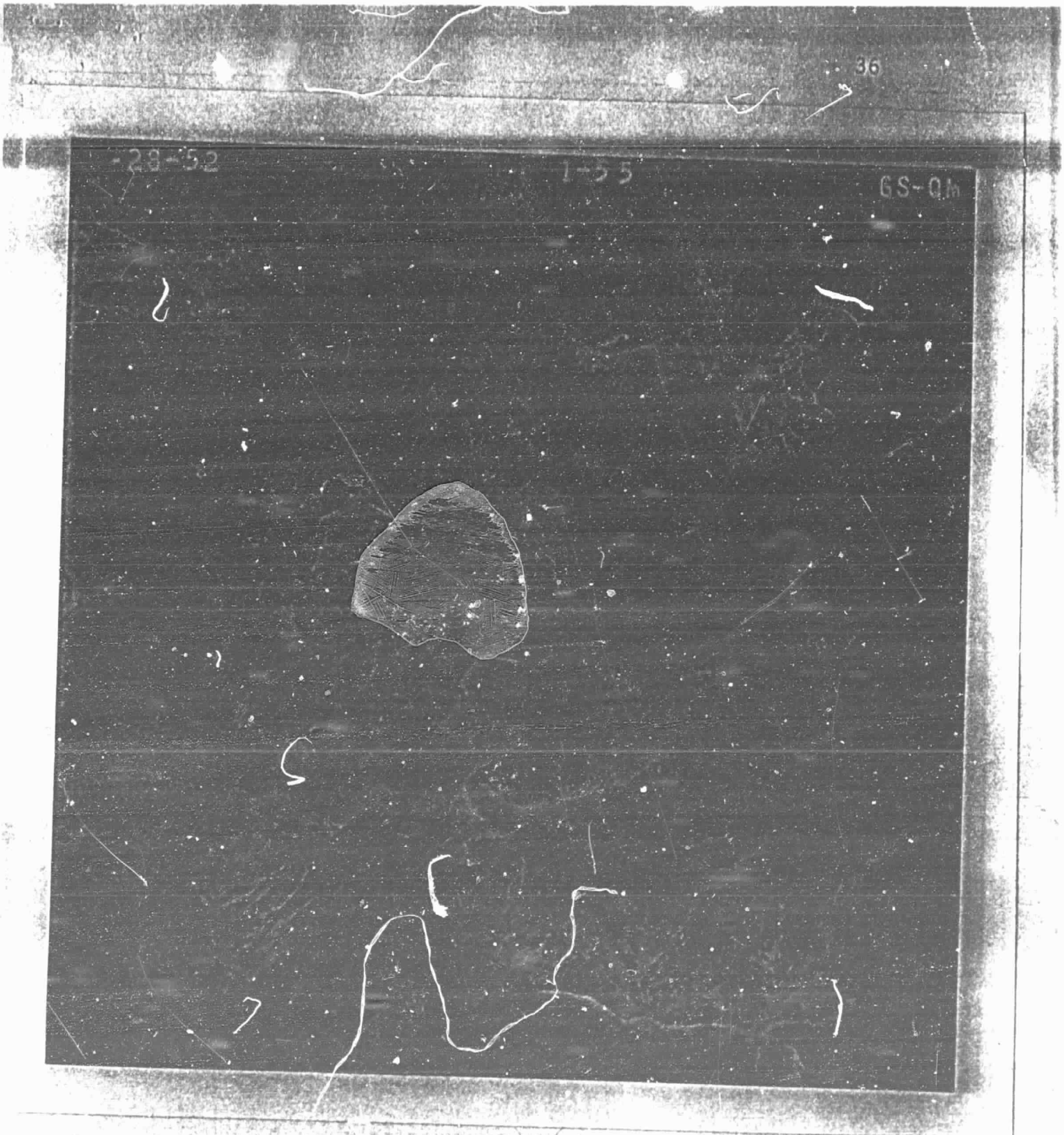

Figure 15. Photo survey traverses, and analysis results of the Red Spring site.

ORIGINAL PAGE IS
OF POOR QUALITY

anomalies, furthermore, lie on eastward, southward, and southwestward facing high slopes. The area to the southeast in Figure 15 lies in a valley and has higher and thicker valley forest cover. The waveform analysis is able to filter the widely varying terrain effects and uniquely classify the anomalous areas. The data analysis is reviewed in the following sections.

The anomalies detected in the Red Springs area are also being followed up with ground studies by Columbia University and the U.S. Geological Survey.

Spirit Lake Waveform Analysis

The waveform analysis from the Spirit Lake sites followed the same procedures as the Cotter Basin analysis with essentially the same results. The data from traverses E4 (Figure 14) and RS2 (Figure 15) were used for reference and are presented in the following figures. Traverse E4 was flown west to east and RS2 was flown east to west.

The waveform function sensitive to canopy density effects was used to threshold unreliable data from areas of thin canopy. The waveform function sensitive to the anomalous vegetation (Figure 16) is 100 percent to 300 percent above the background noise in the Spirit Lake data. The classification threshold was placed at magnitude of 3.0 for the waveform functions in Figure 16.

The results of this survey and data analysis very strongly correlate with the results of the Cotter Basin study. There is additional evidence in this area that the anomalous spectral properties of vegetation may not be restricted to the zone of heavy metal concentration. The strongest anomaly detected in the series of airborne surveys is the one in traverse RS2 (Figure 16b). This is an area with little reported heavy metal concentration but high iron pyrite mineralization and present

ORIGINAL PAGE IS
OF POOR QUALITY

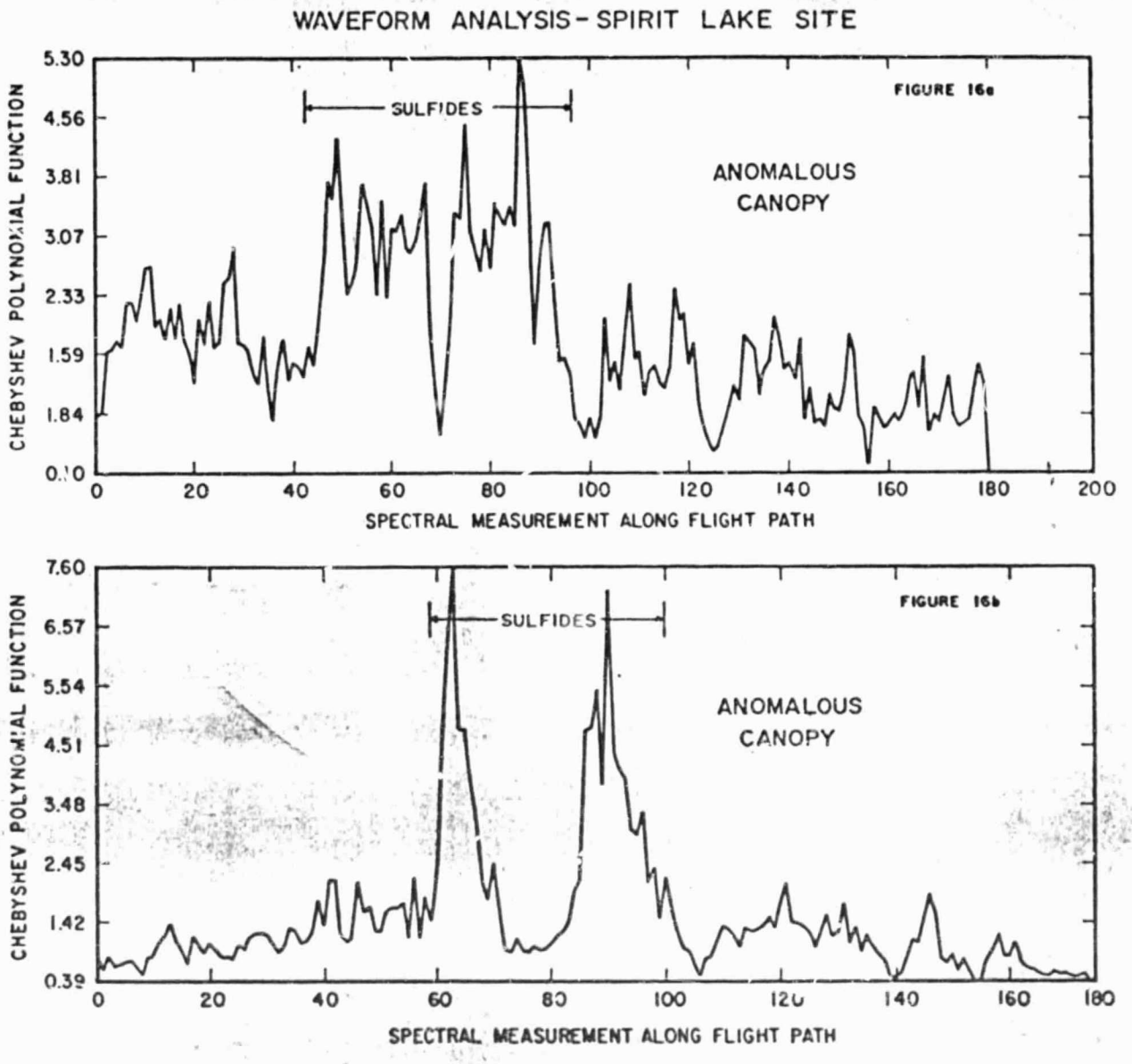

Figure 16. Waveform analysis of traverses from the Spirit Lake area: (a) Goat Mountain site, (b) Red Spring site.

ORIGINAL PAGE IS
OF POOR QUALITY

weathering. Ground water in the area carries very high concentrations of iron weathered from the pyrite zone. The effects of iron sulfides and acid soils on vegetation spectral properties are being studied in laboratory research at Columbia University.

Spectral "Signatures" from Spirit Lake Test Site

The spectral properties of the anomalous vegetation zones in Spirit Lake are the same as those observed in Cotter Basin. Spectral measurements from forest canopies in background and anomalous areas of Goat Mountain are presented in Figures 17a and b. The spectrum from background vegetation shows wider wings on both sides of the 680nm chlorophyll band.

The slope of the near-IR region on either side of the oxygen line at 760nm is positive for the background spectrum indicating pigment absorption in this region. The near-IR shoulder of the anomalous spectrum is sharper and shifted toward the shorter wavelengths. The near-IR change in the anomalous spectrum is accompanied by a steeper negative slope on the 550nm to 680nm wing, resulting in a more intense green peak.

These anomalous spectral curves in the 550nm to 780nm region pass through the filter function of the waveform analysis; and in this second test site, again are uniquely associated with the known mineralization.

Band Ratios in Spirit Lake Data

Several band ratios were tested again in the Spirit Lake data to test the results of the simple band ratio experiment with the Cotter

ORIGINAL PAGE IS
OF POOR QUALITY

GOAT MTN. TEST SITE

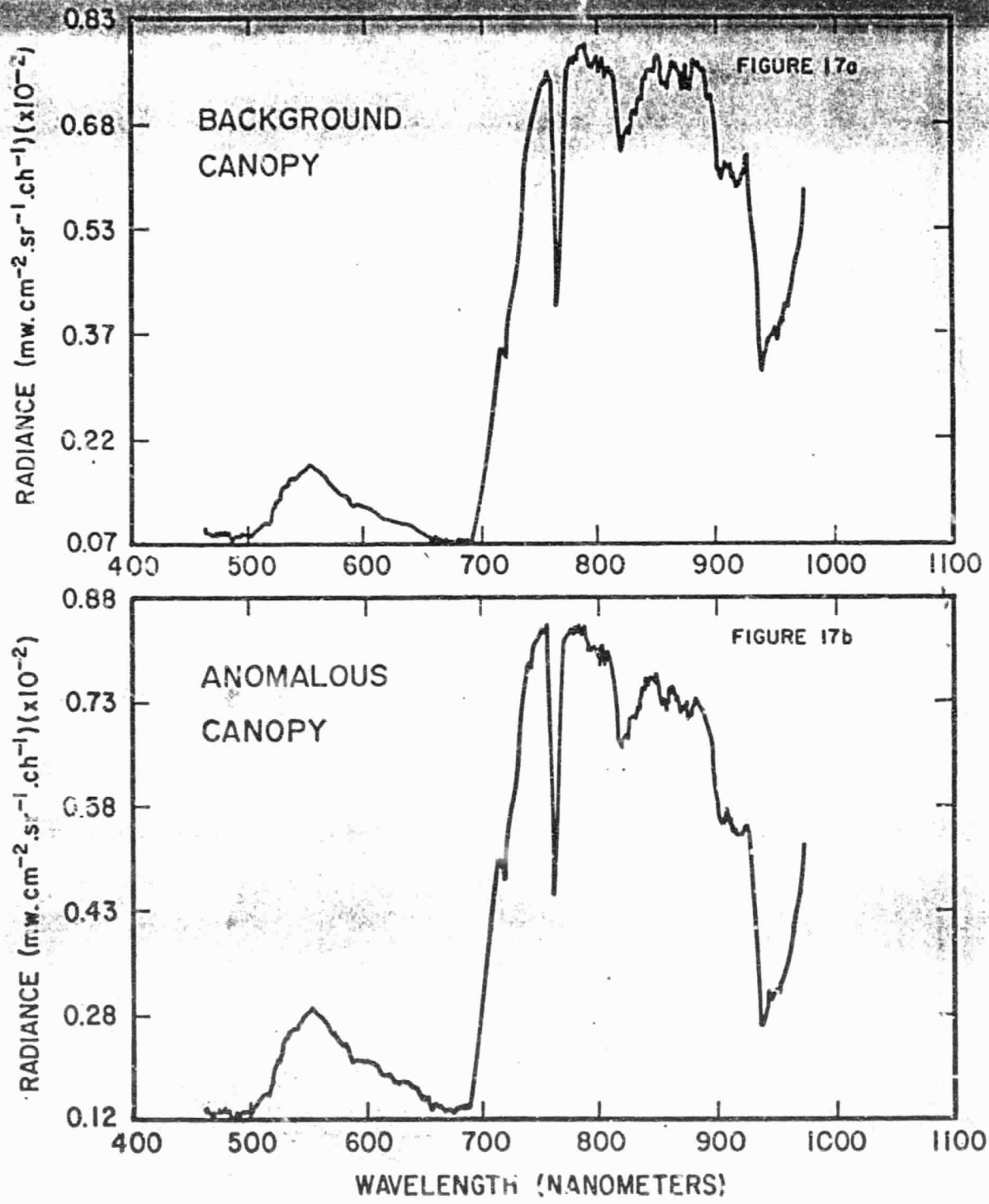

Figure 17. Spectral curves from the Spirit Lake area (Goat Mountain): (a) background vegetation, (b) spectrally anomalous vegetation.

ORIGINAL PAGE IS
OF POOR QUALITY

Basin data. The results substantiate the conclusions drawn for Cotter Basin: that noise filtering is the key to bringing out the second order effects of vegetation stress.

The ratios of simulated 10nm wide bands from the west to east traverse E4 of Figure 14 and 16a are plotted in Figures 18a through d. The anomalous zone occurs between measurement 45 and 85 of the traverse. There is a subtle decrease in the 785nm/745nm ratios in the anomalous zone, but these are obscured by larger variations caused by background canopy effects.

There is a general decrease also in the 785nm/680nm ratios in the anomalous zone, but there are much larger variations both within the anomalous zone and in the background areas caused by canopy thinning. The 680nm/550nm ratios are very sensitive to background canopy effects. There is also an apparent general increase in the 680nm/550nm ratios in the anomalous zone, but this is an artifact of the data. The higher ratios correlate with thin canopy patches. Careful comparison with the waveform analysis indicate that these points were filtered out as thin canopy, not anomalous vegetation.

The 550nm/480nm ratios again are sensitive to both canopy density and slope/irradiance effects. Traverse E4 started on a southwesterly facing slope with more direct sunlight (high ratio values) and followed around to a southeasterly facing slope with indirect sunlight (low ratio values).

Conclusion in Spirit Lake Experiment

The results of the Spirit Lake survey and data analysis very strongly enhance the conclusions drawn from the Cotter Basin site. We detect a unique spectral waveform that appears definitely associated with known sulfide mineralization. The analysis techniques developed

ORIGINAL PAGE IS
OF POOR QUALITY

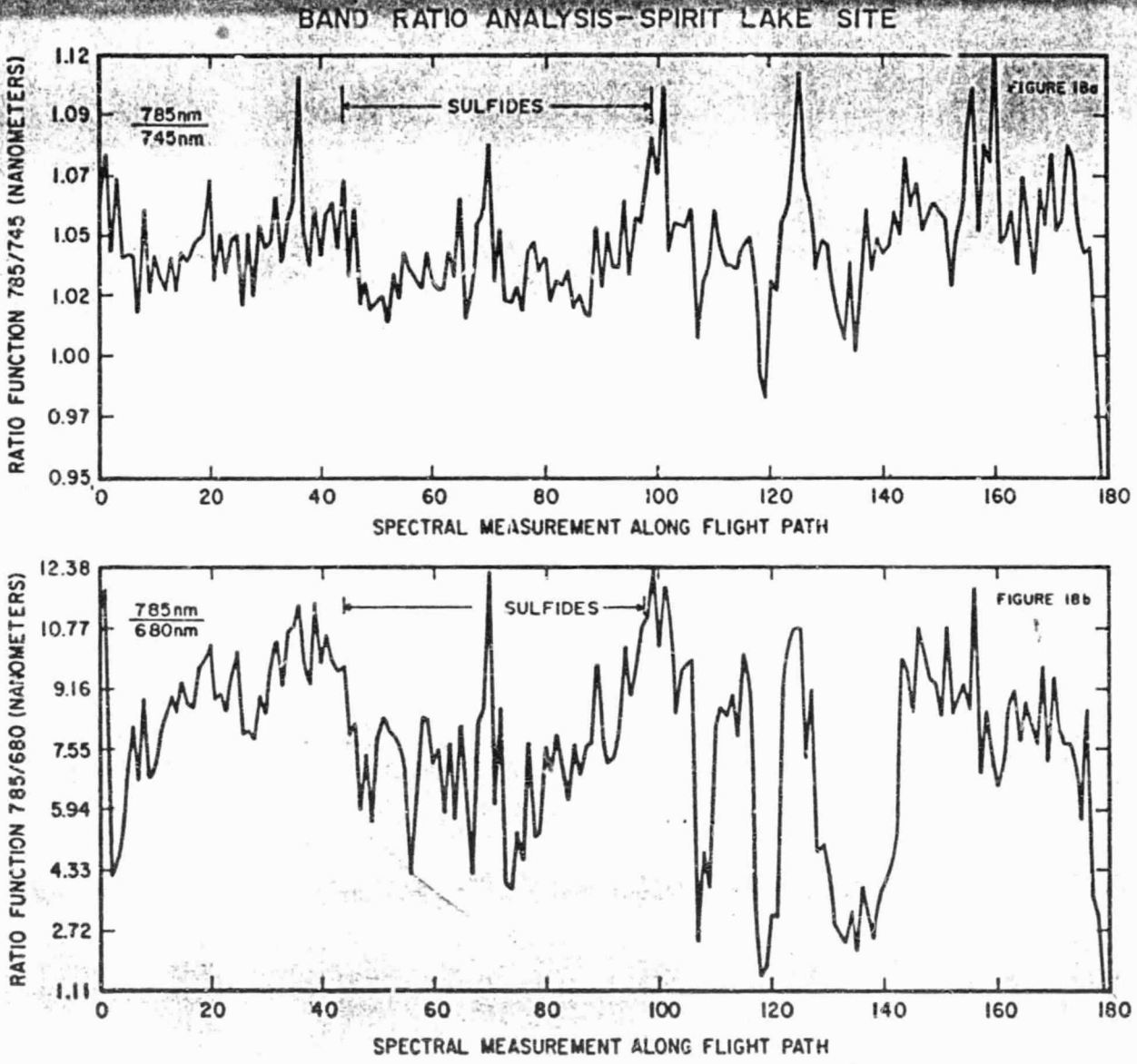

Figure 18 a and b. Ratios of simulated 10nm wide bands from traverse E4 over the Goat Mountain anomaly: (a) 785nm/745nm, (b) 785nm/680nm.

ORIGINAL PAGE IS
OF POOR QUALITY

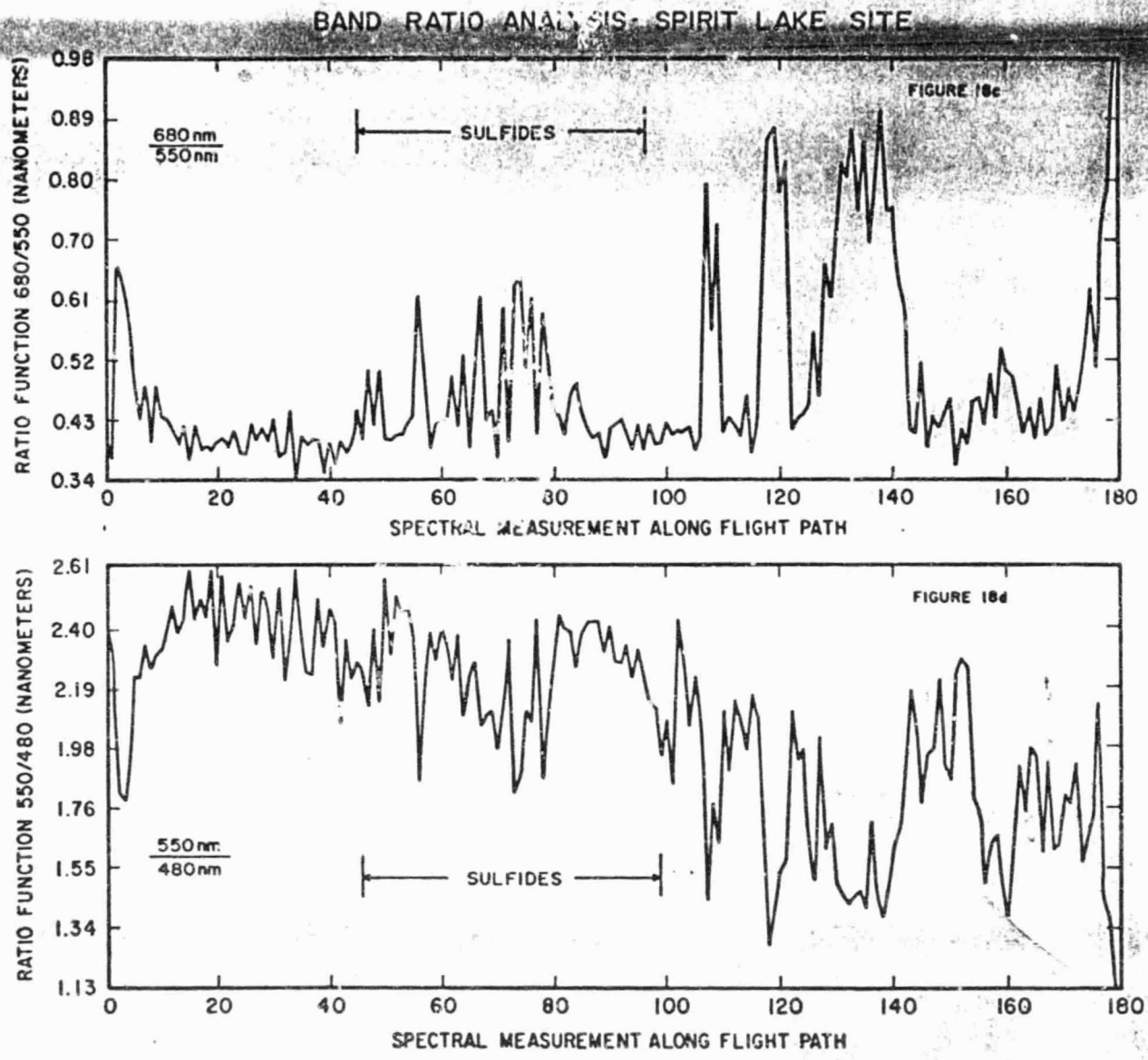

Figure 18 c and d. Ratios of simulated 10nm wide bands from traverse E4 over the Goat Mountain anomaly: (c) 680nm/550nm: (d) 550nm/480nm.

ORIGINAL PAGE IS
OF POOR QUALITY

at Cotter Basin applied to the new site with no modifications required. The terrain at Spirit Lake is much more varied than in Cotter Basin, but background canopy effects were successfully filtered in the analysis. We can draw a further conclusion from the Spirit Lake results that the vegetation stress may well be associated with iron pyrite geochemical effects rather than simple uptake of heavy metals.

ORIGINAL PAGE IS
OF POOR QUALITY

IV. BLACKTAIL MOUNTAIN, MONTANA, TEST AREA

The Blacktail Mountain, Montana site was flown with six reconnaissance lines to establish it as a possible test site. The results in this site are positive. This site will be flown in the future with a more specific flight line pattern.

The test site area contains a stratabound copper prospect. The mineralized geologic unit strikes northwest/southeast through Blacktail Mountain in the center of Figure 19. Drilling is now in progress on the site in the area of the dotted circle on Blacktail Mountain. This area was not covered by any aircraft traverses because the prospect was not well enough known at the time of the survey.

Flight lines were planned to cross the known copper-rich unit north and south of Blacktail Mountain. Using the same waveform analysis techniques applied in the two previous experiments, a strong anomaly was detected to the northeast of Blacktail Mountain along traverses 2 and 2a. The spectrally anomalous vegetation is within the solid circled area of these two traverses.

This anomaly correlates well with the known geology and suspected location of the stratabound copper minerals in the area. More specific data, however, are not yet available. The site will be studied on the ground and sampled by Columbia University and the U.S. Geological Survey.

ORIGINAL PAGE IS
OF POOR QUALITY

ORIGINAL PAGE IS
OF POOR QUALITY

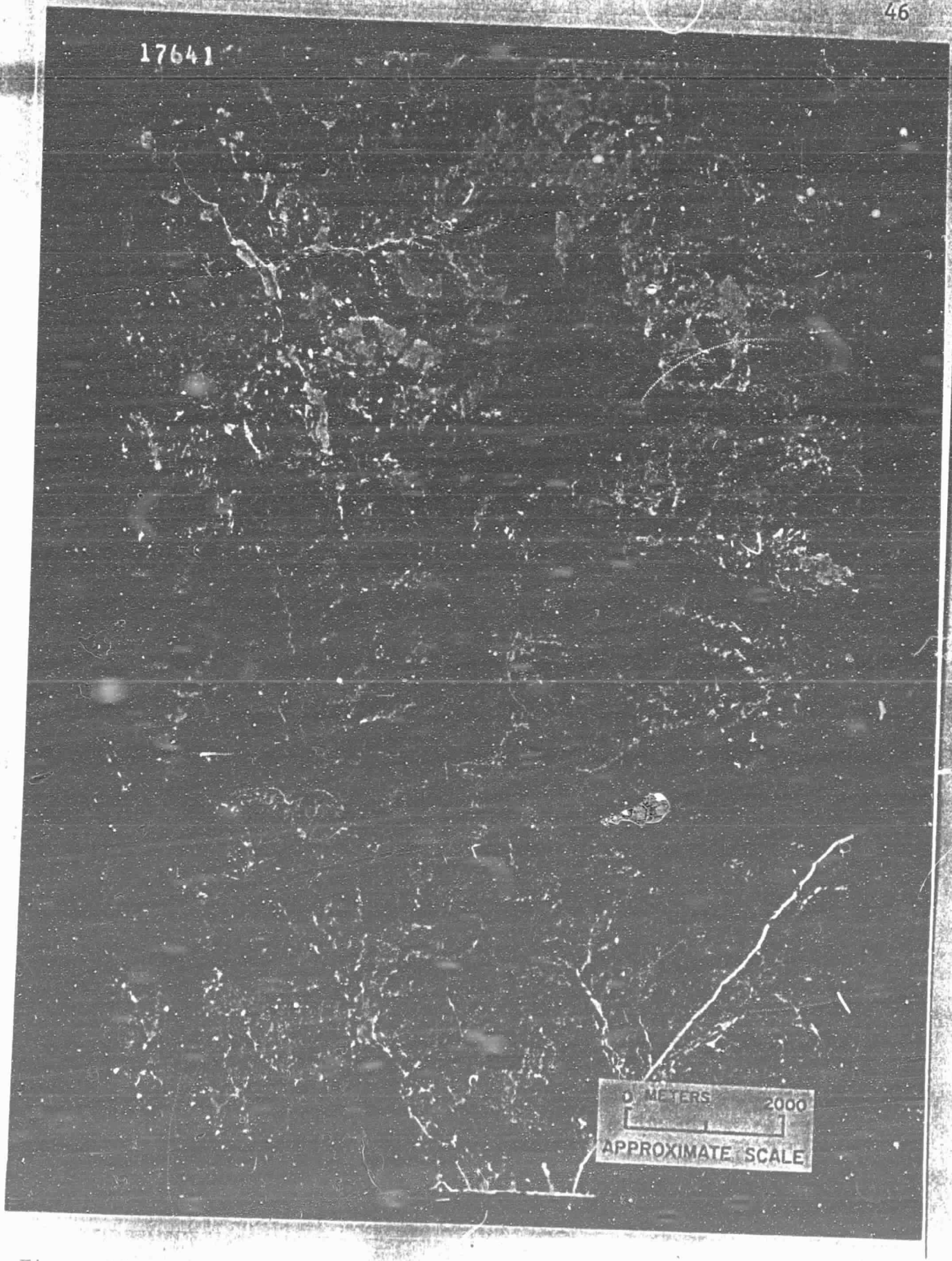

Figure 19. Photo, survey traverses, and analysis results of the Blacktail Mountain site.

V. CATHEART MOUNTAIN, MAINE, TEST SITE

ORIGINAL PAGE IS
OF POOR QUALITY

The Catheart Mountain site in north central Maine was flown in a closely spaced survey pattern with 15 traverses. The survey was flown to determine the spectral properties of the known porphyry copper prospect and the surrounding mixed forest terrain. The experimental results in this area are very promising. The Catheart test site has presented a special challenge to the techniques developed in the western states because of the background canopy variations and the weak anomalous vegetation features that were encountered. The experiment has been most useful in demonstrating the effectiveness of high spectral resolution data and the accompaning waveform analysis. Equally important, this site reveals some of the limitations imposed by general canopy variation effects.

The mineralization in the Catheart Mountain site is copper and molybdenum associated with a porphyry intrusive centered on the left flank of Catheart Mountain. The major mineralization is located by the dashed boundaries in Figures 25 and 26. Another area of strong mineralization, as indicated on the photo and map, occurs on the southwest flank. Total sulfides generally exceed two percent in these two areas (Schmidt, 1978). The two mineralized zones, within the dashed boundaries, have thin overburden and strong soil geochemical anomalies.

The test site is well forested with mixed conifer and deciduous trees. The distribution of species, however, is uneven, with spruce density increasing at higher elevations on mountain tops and also in wet bog areas. The spectral variety of the canopy over the survey area was further aggravated by the Autumn foliage change. The survey was flown September 2, 1978. An early Autumn change was just becoming apparent to the eye. The Autumn change was found to produce a red shift, toward the

long wavelength end of the spectrum, on the near - IR absorbtion edge. This spectral phenomenon is similar to the "red shift" seen in wheat (Collins, 1978) during heading, which is also the very early stage of senescence. The red shift would tend to cover up the type of spectral anomalies observed in the western test sites.

Spectral Signatures Observed in the Catheart Site

A variety of spectral properties of vegetation were observed in the Catheart survey. Spectral curves for spruce canopies from background areas and from Catheart Mountain (Figures 20a and b) show the typical spectral changes seen over sulfide zones. The near-IR edge moves toward the blue end of the spectrum and the shorter wavelength wing of the 680nm chlorophyll band increases in intensity. The same effect appears to develop in the deciduous trees (Figure 21a and b) but to a much weaker extent.

The normal spectral properties of the deciduous canopy in this area are confused because of the Autumn change effects. A background deciduous spectrum from an earlier Summer survey over Catheart in 1976 is compared with a background spectrum of deciduous trees taken from the 1978 survey in Figure 22a and b. The early effects of the Autumn change apparently cause the wings of the 680nm band to broaden considerably producing the red shift on the near-IR edge and the depressed green intensity seen in Figure 22a. This Autumn effect, then, would tend to obscure the opposite effect on the chlorophyll wings produced by stress or other related environmental or geological factors.

In addition to these spectral variations, we observe others in the spruce growing in bog areas. The dwarfed spruce growing in the wetter bog areas (Fig. 23a) have a sharp near-IR shoulder and an intense green peak

ORIGINAL PAGE IS
OF POOR QUALITY

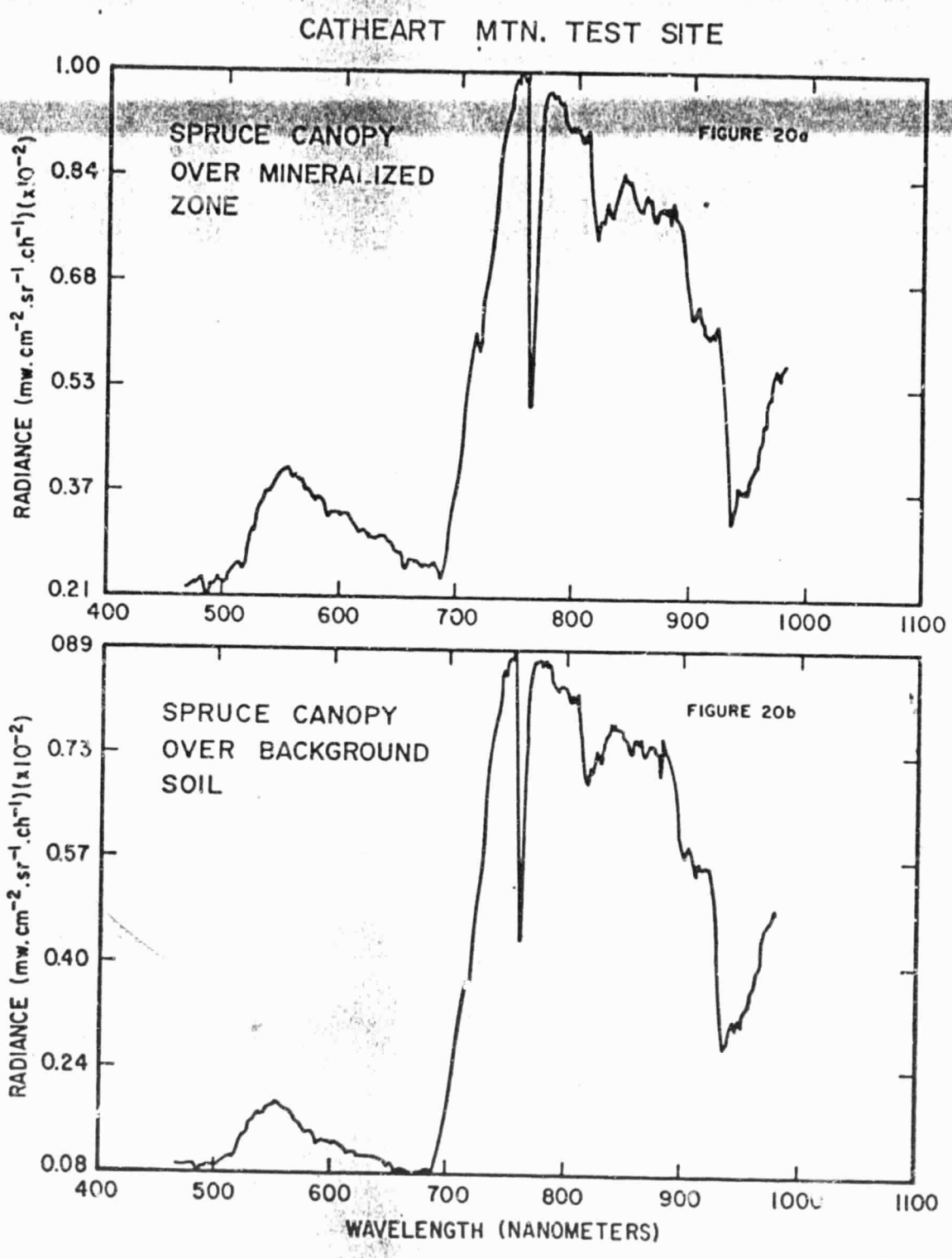

Figure 20. Aircraft spectral measurement of spruce stands in the Catheart test site: (a) spruce from Catheart Mountain with an anomalous near I-R shoulder, (b) spruce from an area in this site with no mineralization has less of a short wavelength shift on the near I-R edge and a lower green peak.

ORIGINAL PAGE IS
OF POOR QUALITY

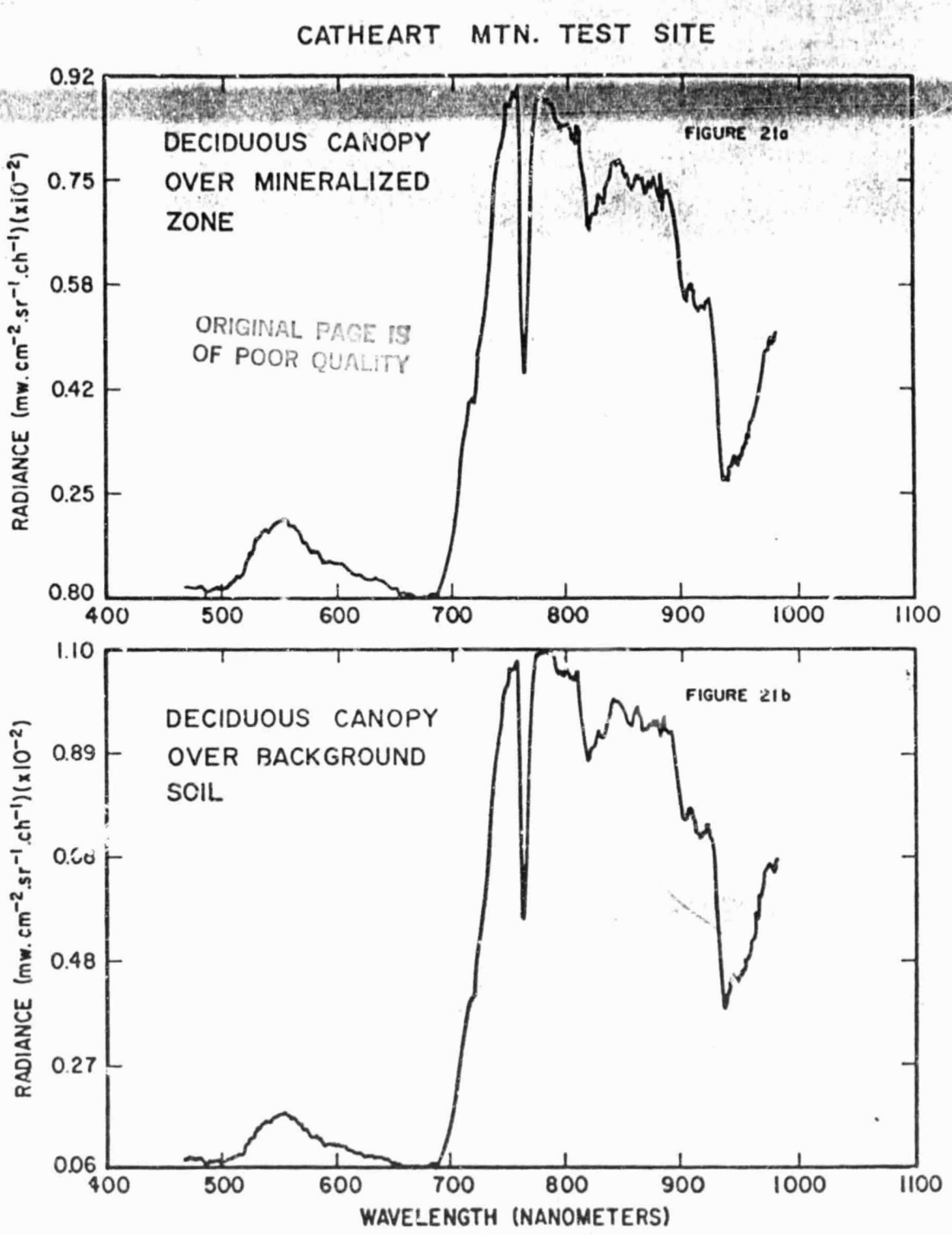

Figure 21. Aircraft spectral measurements of deciduous canopy in the Catheart test site: (a) deciduous trees from the mineralized flank of Catheart Mountain with a weak short wavelength shift on the near I-R shoulder, (b) deciduous trees from a background area with a normal near I-R edge and low green peak.

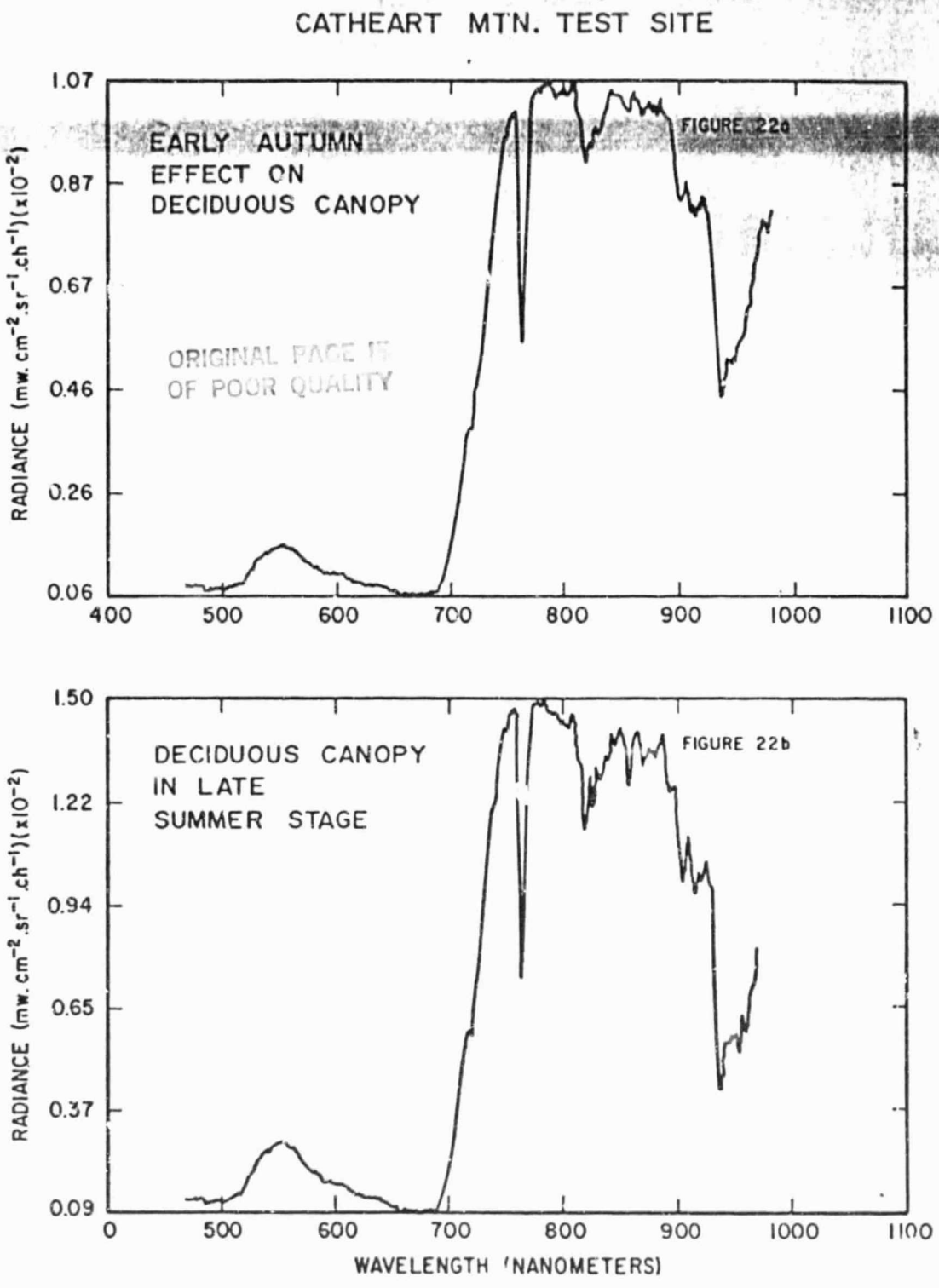

Figure 22. Aircraft spectral measurements of deciduous trees showing seasonal change: (a) spectrum from the 1978 survey during the Autumn color change, (b) spectrum from the 1976 survey before the Autumn effects.

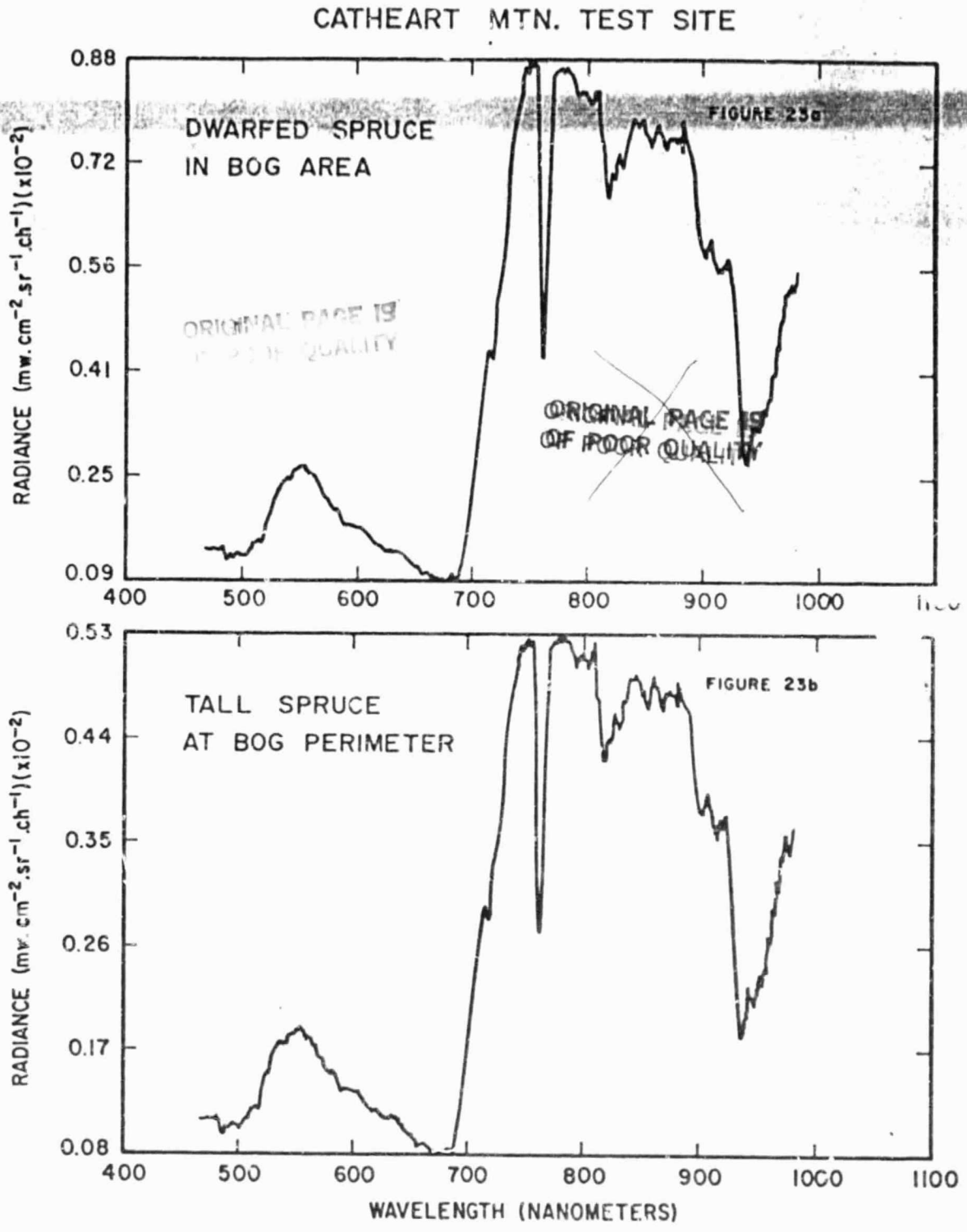

Figures 23. Aircraft spectra measurements of spruce stands in bog areas of the Catheart test site: (a) dwarfed spruce from very wet bog areas have sharp near I-R shoulder and high green peak, (b) taller spruce from bog perimeters generally have a less sharp near I-R shoulder but still intense green peak.

Taller background spruce (Figure 23b) growing on the bog perimeters have a more intense green peak than other background spruce (Figure 20b), but less of a shift toward the blue on the near-IR edge than the dwarfed spruce.

The spectral variety in this area, then, is considerable, and it complicates the data analysis.

Catheart Waveform Analysis

The waveform analysis technique developed in the western sites was used on the Catheart site, but with adjusted threshold limits to accomodate the data. The classification limits in this area were lowered to the degree that the second order effects of background spectral variations caused by species and bog conditions, as shown in the spectra of preceeding section, become a factor.

The Chebyshev functions along traverse 8 (Figure 25) are shown in Figure 24. The survey line, flown east to west, covers a large area of background mixed canopy then traverses Catheart mountain with dense spruce. The last portion traverses the porphyry zones to the west flank of Catheart. The west flank is mixed canopy.

The entire traverse covers very dense canopy, except for a few small, slightly thin, exploration cuts on Catheart mountain. These are indicated by the few peaks greater than 1.2 in Figure 24a. The waveform functions sensitive to canopy thinning in Figure 24a are generally very low and respond strongly, up to a magnitude of 9 (e.g. Figure 2a), over thin canopies. The variations below 1.2 are within the noise limit, and in this case reflect second order effects of spectral changes caused by species differences.

The species differences also appear as weaker second order variations in the waveform function (Figure 24b) sensitive to anomalous

ORIGINAL PAGE IS
OF POOR QUALITY

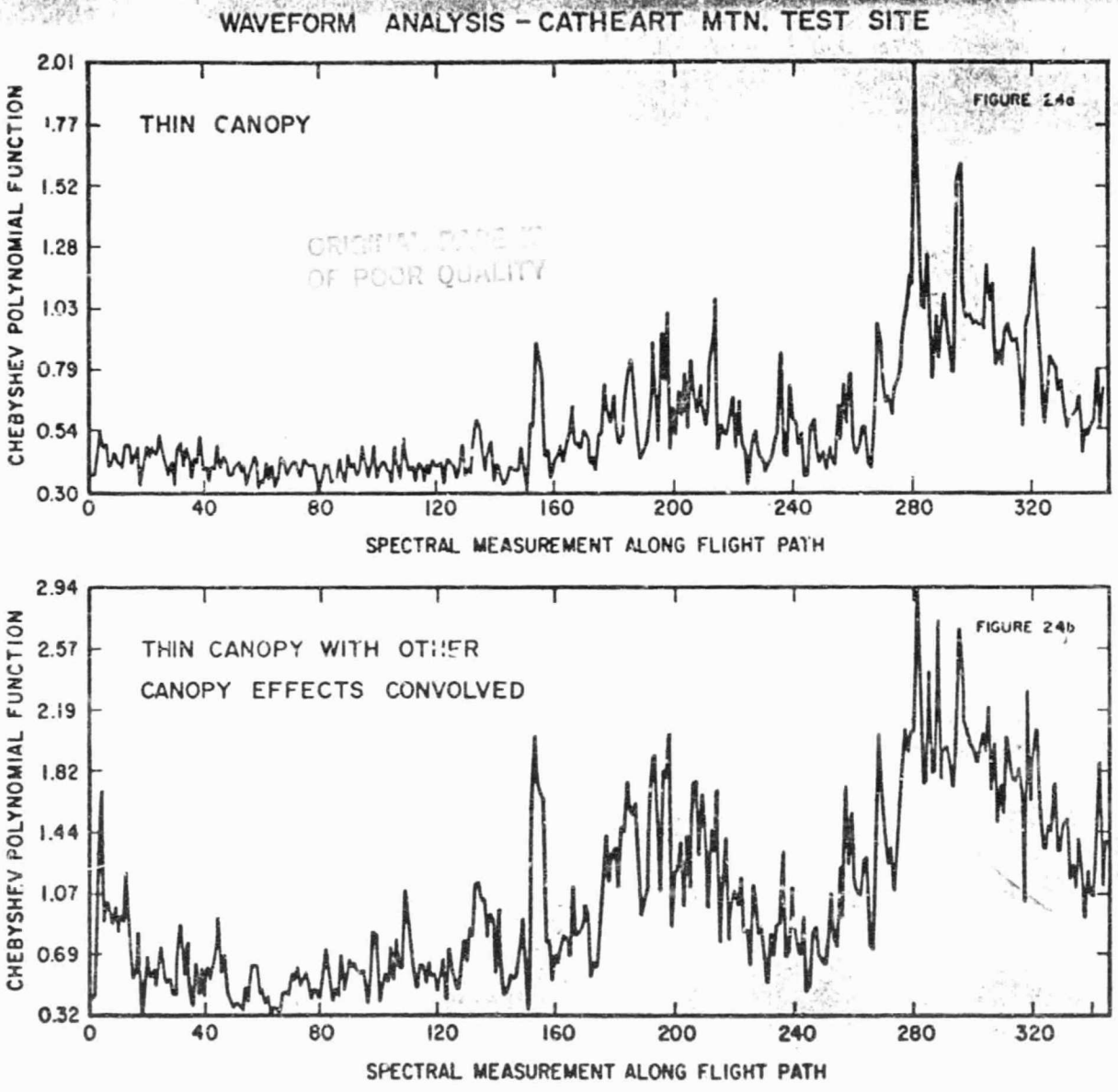

Figure 24. Waveform functions from traverse 8 in Catheart test site: (a) Chebyshev function generally sensitive to thin canopy, (b) Chebyshev function generally sensitive to anomalous vegetation.

chlorophyll features. The magnitude of this function is as high as 8 over sulfide zones, whereas they are generally below 2.2. in Figure 24b. The threshold of 2.5 used for classification of anomalous spectra in the western sites would see nothing in this area where all points are lower. The subtle variation of less than 2.5 in the Figure 24b functions reflect the spectral differences among deciduous, conifer, and bog areas, as well as possible weaker mineralization effects. Successful data analysis in this terrain, then, is especially dependent upon precise filtering of many background effects. This will require a multi-step discrimination procedure with additional discrimination functions to separate the various effects. The technique is under study. But for the present analysis, we used the two step procedure , with the function shown in Figure 24a and b. The threshold for the vegetation mapping function, in Figure 24b, was lowered to 1.4 and 1.8. Separation of the various canopy effects was then accomplished using photo and map interpretation.

The computer mapping results are transferred to the site photo in Figure 25. The cross hatched areas along survey traverse lines indicate the areas discriminated using the lowered threshold values. The solid boundaries in Figure 25 outline areas discriminated from background forest. The dashed boundaries are the known mineralization. These boundaries have been transcribed to the topographic map of the site in Figure 26. From the topographic map, it can be seen that the computer mapping has identified very reliably two distinct environmental areas: mountain tops with spruce stands, and bog areas. Spruce areas indclude Catheart Mountain, two peaks to the southeast, Bean Brook Mountain, a peak between Bean Brook Mountain and Catheart Mountain, and a ridge in

ORIGINAL PAGE IS
OF POOR QUALITY

Figure 25. Photo, survey traverses, and analysis results of the Catheart Mountain test site.

ORIGINAL PAGE IS
OF POOR QUALITY

TOPOGRAPHIC MAP OF CATHEART MTN. TEST SITE

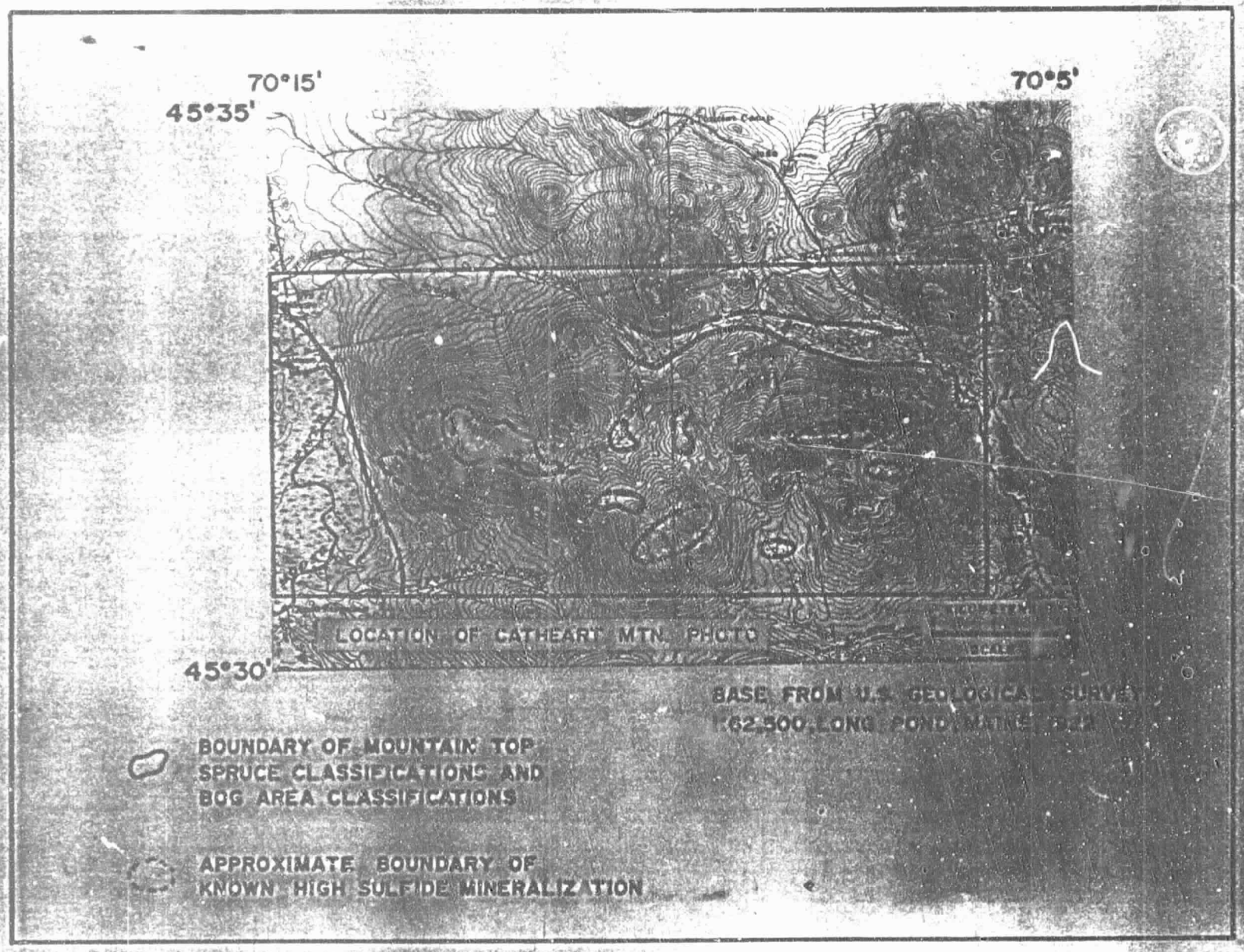

ORIGINAL PAGE IS
OF POOR QUALITY

the northeast corner. Bog areas include Moose River, Bean Brook, and small bogs east of Catheart Mountain and south of Bean Brook Mountain.

The only areas discriminated outside of the mountain spruce stands and the bogs fall within the dashed boundaries of the mineralized zones.

Conclusions in Catheart Mountain Experiment

The results of the Catheart Mountain survey study are especially encouraging because it demonstrates the capacity of the high-spectral-resolution system and data analysis techniques to opperate in complicated terrain. The mapping results, when accompanied by further map and photo interpretation are quite adequate for detecting anomolous spectral properties associated with mineralization in confined sites as in the Catheart survey. Regional reconnaissance will benefit from more sophisticated filtering techniques. However, these should be developed after more study has been made to determine the optimum seasonal periods for detection of mineral effects. The Autumn canopy changes appear to have a negative, or masking effect, in the deciduous canopy.

ORIGINAL PAGE IS
OF POOR QUALITY

VI SUMMARY AND RECOMMENDATIONS

The airborne system with high-spectral-resolution is able to detect an anomalous spectral waveform that appears definitely associated with sulfide mineralization. Along with the airborn instruments, background canopy-induced "noise" filtering and signal extraction techniques are essential for analysis and mapping of the more subtle vegetation features, such as those associated with mineralization. The computerized waveform filter and analysis technique under development is most sensitive to the second order vegetation signals, and it has proven applicable in several different sites with little or no modification. With more research, it will be possible to design discreet band systems for biogeochemical surveys; but the high resolution airborne spectroradiometer system and waveform analysis will remain the most versatile method for research and the most sensitive technique for survey applications.

Further research into biogeochemical techniques of exploration using airborne spectral sensors is recommended by three approaches: laboratory studies, airborne surveys extended to additional sites, and application of the developed techniques to mapping one or two extended areas.

Laboratory studies to explain the pigment absorption properties observed in the field, have proven of very great value in understanding these phenomena, and in guiding further field research. These studies are being conducted at Columbia University, under National Science Foundation funding. The laboratory studies are complicated, however, by the lack of capacity to reproduce the soil, plant and environmental factors present in the field. The laboratory studies, when correlated with field studies, promise the optimum return.

ORIGINAL PAGE IS
OF POOR QUALITY

Airborne research surveys are required over additional known sites to extend the techniques developed in the Columbia University research. These surveys offer an expeditious route to prove the airborne techniques and to develop them into survey methods. The additional surveys are essential for continued development of analysis methods to filter various unwanted canopy effects and for studying spectral "signatures" of various geologic features that will be encountered in extended terrain.

The very good experimental results obtained in Montana and Washington suggest that regional mapping in these areas is possible. Plans are being formulated to attempt larger scale mapping in the Spirit Lake region to coincide with present U.S. Geological Survey mineral mapping. This experiment will provide an excellent applications test for the techniques that appear so promising in the studies to date.

ORIGINAL PAGE IS
OF POOR QUALITY

REFERENCES

Chang, S.H., and Collins, W.E., 1980, Toxic effects of heavy metals on plants: Sixth Annual Pecora Symposium.

Chiu, Hong Yee, and Collins W. 1978, A spectroradiometer for airborne remote sensing; Photogrammetric Engineering and Remote Sensing. v. 44, no. 4, pp. 507-517.

Collins, W.E., 1978, Remote sensing of crop type and maturity: Photogrammetric Engineering and Remote Sensing, v. 44, no. 1, pp. 43-55.

Collins, W.E., Chang, S.H., Raines, G.L., Canney, F.C., and Ashley, R., 1980, Airborne Biogeochemical survey test case results: Sixth Annual Pecora Symposium.

Collins, W., and Chiu, H.Y., 1979, Signature evaluation of natural targets using high spectral resolution techniques: 13th ERIM Symposium Proceedings.

Collins, W., Raines, G.L., and Canney, F.C., 1978, Airborne spector-radiometer discrimination of vegetation anomalies over sulfide mineralization in the Cotter Basin area, Lewis and Clark County, Montana: U.S. Geological Survey Open File Report, (in press).

Grimes, D.J., and Earhart, R.L., 1975, Geochemical soil studies in the Cotter Basin area, Lewis and Clark County, Montana: U.S. Geological Survey Open File Report, pp. 72-75.

Hollister, V.F., 1978, Porphyry copper - type deposits of the cascade volcanic arc, Washington: Minerals Sci. Engng., vol. 11, No. 1.

Schmidt, R.G., 1978, The potential for Porfyry copper - molybdenum deposits in the Eastern United States: U.S. Geological Survey Prof. paper 907-E, 31 p.

ORIGINAL PAGE IS
OF POOR QUALITY

ACKNOWLEDGMENTS

This research was supported by NASA Grant NSG-5222 in the earlier phases that included field surveys and initial data processing. Field surveys were supported in part by U.S. Geological Survey funding which supported the field crews. We are especially grateful for the support and participation by Drs. Frank Canney, Gary Raines, Roger Ashley, and Larry Rowan of the U.S. Geological Survey.

The data analysis was completed under research Grant DAR-78-16320 from the Division of Applied Research of the National Science Foundation. The research presented in this report and continuing research is presently being funded under the NSF grant.

ORIGINAL PAGE IS
OF POOR QUALITY

APPENDIX I

The spectral analysis of data from the Columbia sensor systems depends heavily on the polynomial waveform analysis techniques developed at Columbia University. A standard polynomial function is used to fit the data. Differences in the frequency components of the spectral curves can be found by simply comparing the coefficients of polynomial terms. The particular function that we have found useful is the Chebyshev polynomial, which is defined:

$$T_0(x) = 1$$

$$T_n(x) = \cos(n\theta)$$

$$\cos\theta = x$$

A detailed presentation of the Chebyshev polynomials can be found in the standard texts, for example "Mathematical Analysis" by Lyvsternik and Yanpol'skii.

Enclosed are data for six aircraft spectra from Cotter Basin. Three are in background areas:

records 1458
1461
1474.

ORIGINAL PAGE IS
OF POOR QUALITY

and three are from the anomaly:

records 1414
1423
1426.

The data include:

1. radiance and wavelength of the 500 channels of data for each spectrum,
2. a plot of the above,
3. the corresponding polynomial coefficients derived from the six spectra.

The absolute values of the coefficients are dependent on the data, the coordinate space used, and the portion of the spectrum fitted. In interpreting the data, as in ratio techniques, etc., the relative values contain the useful information.

ORIGINAL PAGE IS
OF POOR QUALITY

RECORD NUMBER 1458

WAVELENGTH/RADIANCE

ORIGINAL PAGE IS
OF POOR QUALITY

ORIGINAL PAGE IS
OF POOR QUALITY

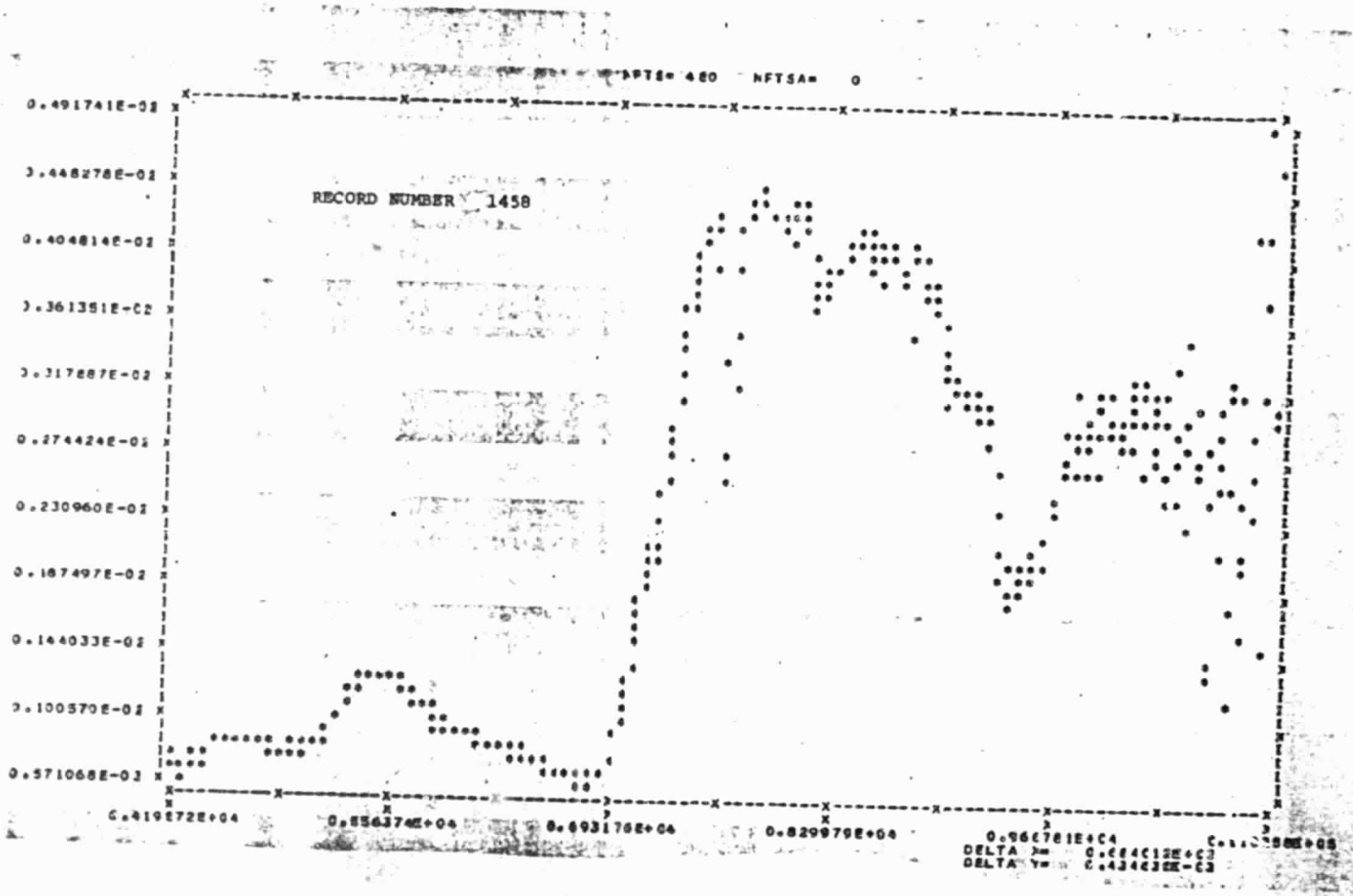

RECORD NUMBER 1461

WAVELENGTH/RADIANCE	WAVELENGTH/RADIANCE	WAVELENGTH/RADIANCE	WAVELENGTH/RADIANCE	WAVELENGTH/RADIANCE
4195.72= 0.773E-03	4210.00= 0.769E-03	4224.28= 0.780E-03	4238.56= 0.758E-03	4252.84= 0.754E-03
4267.12= 0.661E-03	4281.40= 0.681E-03	4295.68= 0.732E-03	4309.96= 0.744E-03	4324.24= 0.811E-03
4338.52= 0.810E-03	4352.80= 0.764E-03	4367.08= 0.790E-03	4381.36= 0.789E-03	4395.64= 0.855E-03
4409.92= 0.852E-03	4424.20= 0.830E-03	4438.48= 0.880E-03	4452.76= 0.857E-03	4467.04= 0.851E-03
4481.32= 0.904E-03	4495.60= 0.872E-03	4509.87= 0.874E-03	4524.16= 0.886E-03	4538.44= 0.886E-03
4552.71= 0.854E-03	4567.00= 0.894E-03	4581.28= 0.854E-03	4595.56= 0.907E-03	4609.84= 0.864E-03
4624.12= 0.931E-03	4638.40= 0.861E-03	4652.68= 0.862E-03	4666.96= 0.836E-03	4681.24= 0.851E-03
4695.52= 0.862E-03	4709.80= 0.806E-03	4724.08= 0.859E-03	4738.36= 0.864E-03	4752.64= 0.837E-03
4766.92= 0.884E-03	4781.20= 0.883E-03	4795.48= 0.874E-03	4809.76= 0.861E-03	4824.04= 0.811E-03
4838.32= 0.758E-03	4852.60= 0.781E-03	4866.87= 0.831E-03	4881.16= 0.823E-03	4895.44= 0.854E-03
4909.71= 0.819E-03	4924.00= 0.844E-03	4938.28= 0.841E-03	4952.56= 0.821E-03	4966.84= 0.834E-03
4981.12= 0.766E-03	4995.40= 0.814E-03	5009.68= 0.806E-03	5023.96= 0.839E-03	5038.24= 0.842E-03
5052.52= 0.845E-03	5066.80= 0.864E-03	5081.08= 0.868E-03	5095.36= 0.890E-03	5109.64= 0.878E-03
5123.92= 0.856E-03	5138.20= 0.856E-03	5152.48= 0.841E-03	5166.76= 0.905E-03	5181.04= 0.944E-03
5195.32= 0.989E-03	5209.60= 0.102E-02	5223.87= 0.105E-02	5238.16= 0.101E-02	5252.44= 0.105E-02
5266.71= 0.111E-02	5281.00= 0.113E-02	5295.28= 0.111E-02	5309.56= 0.114E-02	5323.84= 0.117E-02
5338.12= 0.119E-02	5352.40= 0.118E-02	5366.68= 0.119E-02	5380.96= 0.117E-02	5395.24= 0.115E-02
5409.52= 0.122E-02	5423.80= 0.120E-02	5438.08= 0.124E-02	5452.36= 0.122E-02	5466.64= 0.123E-02
5480.92= 0.125E-02	5495.20= 0.126E-02	5509.48= 0.127E-02	5523.76= 0.127E-02	5538.04= 0.124E-02
5552.32= 0.124E-02	5566.60= 0.121E-02	5580.87= 0.122E-02	5595.16= 0.123E-02	5609.44= 0.124E-02
5623.71= 0.119E-02	5637.99= 0.119E-02	5652.28= 0.120E-02	5666.56= 0.116E-02	5680.84= 0.111E-02
5695.12= 0.112E-02	5709.40= 0.115E-02	5723.68= 0.113E-02	5737.96= 0.109E-02	5752.24= 0.110E-02
5766.52= 0.108E-02	5780.80= 0.109E-02	5795.08= 0.108E-02	5809.36= 0.109E-02	5823.64= 0.110E-02
5837.92= 0.108E-02	5852.20= 0.110E-02	5866.48= 0.952E-03	5880.76= 0.971E-03	5895.04= 0.956E-03
5909.32= 0.101E-02	5923.60= 0.101E-02	5937.87= 0.101E-02	5952.16= 0.994E-03	5966.44= 0.966E-03
5980.71= 0.973E-03	5995.00= 0.996E-03	6009.28= 0.989E-03	6023.56= 0.101E-02	6037.84= 0.955E-03
6052.12= 0.957E-03	6066.40= 0.984E-03	6080.68= 0.938E-03	6094.96= 0.958E-03	6109.24= 0.924E-03
6123.52= 0.915E-03	6137.80= 0.905E-03	6152.08= 0.953E-03	6166.36= 0.923E-03	6180.64= 0.882E-03
6194.92= 0.911E-03	6209.20= 0.892E-03	6223.47= 0.871E-03	6237.76= 0.887E-03	6252.04= 0.847E-03
6266.32= 0.837E-03	6280.60= 0.865E-03	6294.8= 0.846E-03	6309.16= 0.884E-03	6323.44= 0.826E-03
6337.71= 0.887E-03	6352.00= 0.827E-03	6366.28= 0.868E-03	6380.56= 0.880E-03	6394.84= 0.838E-03
6409.12= 0.865E-03	6423.40= 0.833E-03	6437.68= 0.845E-03	6451.95= 0.816E-03	6466.24= 0.776E-03
6480.52= 0.756E-03	6494.80= 0.782E-03	6509.08= 0.779E-03	6523.36= 0.798E-03	6537.64= 0.745E-03
6551.92= 0.719E-03	6566.20= 0.743E-03	6580.48= 0.749E-03	6594.76= 0.757E-03	6609.04= 0.741E-03
6623.32= 0.766E-03	6637.60= 0.737E-03	6651.87= 0.732E-03	6666.16= 0.723E-03	6680.44= 0.750E-03
6694.71= 0.724E-03	6709.00= 0.717E-03	6723.28= 0.710E-03	6737.56= 0.696E-03	6751.84= 0.711E-03
6766.12= 0.720E-03	6780.40= 0.717E-03	6794.68= 0.734E-03	6808.96= 0.716E-03	6823.24= 0.702E-03
6837.52= 0.746E-03	6851.80= 0.724E-03	6866.08= 0.690E-03	6880.36= 0.721E-03	6894.64= 0.745E-03
6908.92= 0.683E-03	6923.20= 0.657E-03	6937.48= 0.672E-03	6951.76= 0.103E-02	6966.04= 0.105E-02
6980.32= 0.113E-02	6994.60= 0.114E-02	7008.87= 0.126E-02	7023.16= 0.132E-02	7037.44= 0.132E-02
7051.71= 0.150E-02	7066.00= 0.154E-02	7080.28= 0.162E-02	7094.56= 0.171E-02	7108.84= 0.135E-02
7123.12= 0.184E-02	7137.40= 0.186E-02	7151.68= 0.194E-02	7165.96= 0.185E-02	7180.24= 0.184E-02
7194.52= 0.195E-02	7208.80= 0.210E-02	7223.08= 0.219E-02	7237.36= 0.224E-02	7251.64= 0.232E-02
7265.92= 0.228E-02	7280.20= 0.250E-02	7294.48= 0.287E-02	7308.76= 0.268E-02	7323.04= 0.274E-02
7337.32= 0.269E-02	7351.60= 0.304E-02	7365.87= 0.313E-02	7380.16= 0.320E-02	7394.44= 0.314E-02
7408.72= 0.332E-02	7423.00= 0.331E-02	7437.28= 0.344E-02	7451.56= 0.348E-02	7465.84= 0.347E-02
7480.12= 0.351E-02	7494.40= 0.356E-02	7508.68= 0.355E-02	7522.96= 0.355E-02	7537.24= 0.342E-02
7551.52= 0.343E-02	7565.80= 0.349E-02	7580.08= 0.372E-02	7594.36= 0.364E-02	7608.64= 0.411E-02
7622.92= 0.419E-02	7637.20= 0.435E-02	7651.48= 0.423E-02	7665.76= 0.397E-02	7680.04= 0.388E-02
7694.32= 0.385E-02	7708.60= 0.358E-02	7722.87= 0.364E-02	7737.16= 0.363E-02	7751.44= 0.362E-02
7765.71= 0.365E-02	7780.00= 0.364E-02	7794.28= 0.362E-02	7808.56= 0.368E-02	7822.84= 0.365E-02
7837.12= 0.365E-02	7851.40= 0.369E-02	7865.68= 0.363E-02	7879.96= 0.359E-02	7894.24= 0.355E-02
7908.52= 0.353E-02	7922.80= 0.355E-02	7937.08= 0.354E-02	7951.36= 0.356E-02	7965.64= 0.351E-02
7979.92= 0.358E-02	7994.20= 0.365E-02	8008.48= 0.369E-02	8022.76= 0.349E-02	8037.04= 0.354E-02
8051.32= 0.354E-02	8065.60= 0.357E-02	8079.87= 0.346E-02	8094.16= 0.346E-02	8108.44= 0.351E-02
8122.71= 0.329E-02	8137.00= 0.333E-02	8151.28= 0.323E-02	8165.56= 0.316E-02	8179.84= 0.345E-02
8194.12= 0.304E-02	8208.40= 0.314E-02	8222.68= 0.316E-02	8236.96= 0.314E-02	8251.24= 0.345E-02
8265.52= 0.333E-02	8279.80= 0.330E-02	8294.08= 0.319E-02	8308.36= 0.348E-02	8322.64= 0.324E-02
8336.92= 0.328E-02	8351.20= 0.333E-02	8365.48= 0.338E-02	8379.76= 0.338E-02	8394.04= 0.335E-02
8408.32= 0.341E-02	8422.60= 0.344E-02	8436.87= 0.337E-02	8451.16= 0.342E-02	8465.44= 0.335E-02
8479.71= 0.344E-02	8494.00= 0.342E-02	8508.28= 0.333E-02	8522.56= 0.332E-02	8536.84= 0.326E-02
8551.12= 0.323E-02	8565.40= 0.322E-02	8579.68= 0.335E-02	8593.96= 0.333E-02	8608.24= 0.329E-02
8622.52= 0.327E-02	8636.80= 0.328E-02	8651.08= 0.321E-02	8665.36= 0.319E-02	8679.64= 0.311E-02
8693.92= 0.314E-02	8708.20= 0.316E-02	8722.48= 0.323E-02	8736.76= 0.322E-02	8751.04= 0.322E-02
8765.32= 0.345E-02	8779.60= 0.340E-02	8793.87= 0.320E-02	8808.16= 0.324E-02	8822.44= 0.321E-02
8836.71= 0.314E-02	8851.00= 0.309E-02	8865.28= 0.316E-02	8879.56= 0.305E-02	8893.84= 0.312E-02
8908.12= 0.324E-02	8922.40= 0.305E-02	8936.68= 0.257E-02	8950.96= 0.282E-02	8965.24= 0.281E-02
8979.52= 0.264E-02	8993.80= 0.266E-02	9008.08= 0.253E-02	9022.36= 0.256E-02	9036.64= 0.255E-02
9050.92= 0.260E-02	9065.20= 0.263E-02	9079.48= 0.263E-02	9093.76= 0.258E-02	9108.04= 0.253E-02
9122.32= 0.253E-02	9136.60= 0.237E-02	9150.87= 0.252E-02	9165.16= 0.247E-02	9179.44= 0.255E-02
9193.71= 0.243E-02	9208.00= 0.254E-02	9222.28= 0.258E-02	9236.56= 0.253E-02	9250.84= 0.244E-02
9265.12= 0.236E-02	9279.40= 0.232E-02	9293.68= 0.247E-02	9307.96= 0.182E-02	9322.24= 0.176E-02
9336.52= 0.197E-02	9350.80= 0.150E-02	9365.08= 0.135E-02	9379.36= 0.160E-02	9393.64= 0.182E-02
9407.92= 0.152E-02	9422.20= 0.164E-02	9436.48= 0.158E-02	9450.76= 0.164E-02	9465.04= 0.161E-02
9479.32= 0.158E-02	9493.60= 0.159E-02	9507.87= 0.165E-02	9522.16= 0.170E-02	9536.44= 0.161E-02
9550.71= 0.156E-02	9565.00= 0.172E-02	9579.28= 0.176E-02	9593.56= 0.179E-02	9607.84= 0.181E-02
9622.12= 0.186E-02	9636.40= 0.204E-02	9650.68= 0.192E-02	9664.96= 0.207E-02	9679.24= 0.205E-02
9693.52= 0.213E-02	9707.80= 0.216E-02	9722.08= 0.228E-02	9736.36= 0.225E-02	9750.64= 0.214E-02
9764.92= 0.228E-02	9779.20= 0.227E-02	9793.48= 0.227E-02	9807.76= 0.239E-02	9822.04= 0.234E-02
9836.32= 0.249E-02	9850.60= 0.247E-02	9864.87= 0.251E-02	9879.16= 0.237E-02	9893.44= 0.234E-02
9907.71= 0.243E-02	9922.00= 0.215E-02	9936.28= 0.211E-02	9950.56= 0.211E-02	9964.84= 0.195E-02
9979.12= 0.207E-02	9993.40= 0.240E-02	10007.68= 0.243E-02	10021.96= 0.247E-02	10036.24= 0.243E-02
10050.52= 0.229E-02	10064.80= 0.229E-02	10079.08= 0.220E-02	10093.36= 0.239E-02	10107.64= 0.241E-02
10121.92= 0.265E-02	10136.20= 0.258E-02	10150.48= 0.264E-02	10164.76= 0.265E-02	10179.04= 0.265E-02
10193.32= 0.257E-02	10207.60= 0.277E-02	10221.87= 0.253E-02	10236.16= 0.259E-02	10250.44= 0.271E-02
10264.71= 0.302E-02	10279.00= 0.273E-02	10293.28= 0.283E-02	10307.56= 0.258E-02	10321.84= 0.281E-02
10335.12= 0.283E-02	10350.40= 0.315E-02	10364.68= 0.332E-02	10378.96= 0.280E-02	10393.24= 0.326E-02
10407.52= 0.294E-02	10421.80= 0.303E-02	10436.08= 0.329E-02	10450.36= 0.325E-02	10464.64= 0.285E-02
10478.92= 0.245E-02	10493.20= 0.324E-02	10507.48= 0.324E-02	10521.76= 0.362E-02	10536.04= 0.304E-02
10550.32= 0.322E-02	10564.60= 0.351E-02	10578.87= 0.340E-02	10593.16= 0.321E-02	10607.44= 0.342E-02
10621.71= 0.341E-02	10636.00= 0.434E-02	10650.28= 0.336E-02	10664.56= 0.367E-02	10678.84= 0.341E-02
10693.12= 0.348E-02	10707.40= 0.446E-02	10721.68= 0.330E-02	10735.96= 0.524E-02	10750.24= 0.327E-02
10764.52= 0.532E-02	10778.80= 0.354E-02	10793.08= 0.451E-02	10807.36= 0.360E-02	10821.64= 0.342E-02
10835.92= 0.616E-02	10850.20= 0.419E-02	10864.48= 0.415E-02	10878.76= 0.476E-02	10893.04= 0.534E-02
10907.32= 0.512E-02	10921.60= 0.404E-02	10935.87= 0.769E-02	10950.16= 0.542E-02	10964.44= 0.774E-02
10978.71= 0.576E-02	10993.00= 0.792E-02	11007.28= 0.765E-02	11021.56= 0.742E-02	11035.84= 0.761E-02

ORIGINAL PAGE IS
OF POOR QUALITY

ORIGINAL PAGE IS
OF POOR QUALITY

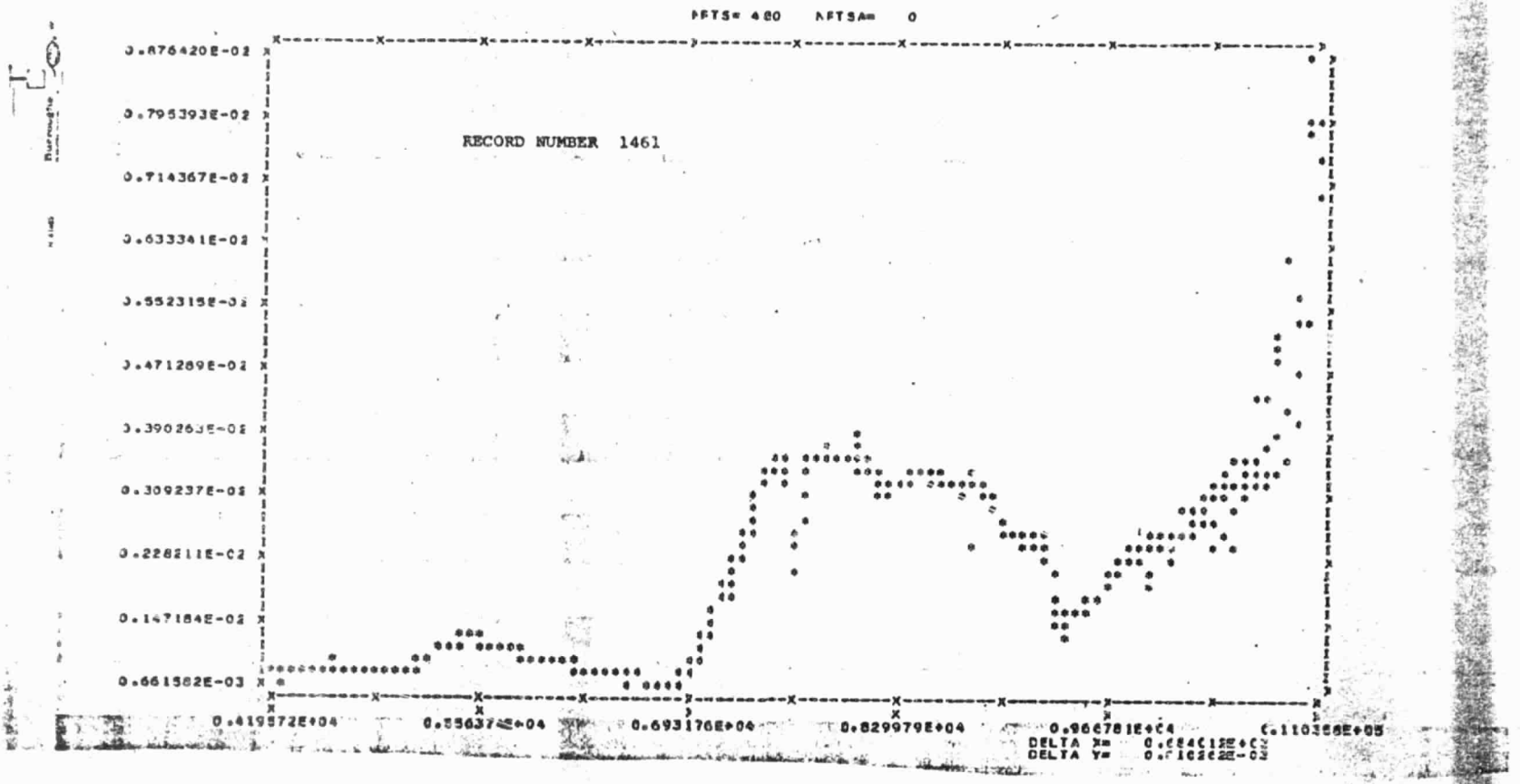

RECORD NUMBER 1474

WAVELENGTH/RADIANCE	WAVELENGTH/RADIANCE	WAVELENGTH/RADIANCE	WAVELENGTH/RADIANCE	WAVELENGTH/RADIANCE
4195.72= 0.819E-03	4210.00= C.790E-03	4224.28= 0.812E-03	4238.56= C.746E-03	4252.84= C.756E-03
4267.12= 0.665E-03	4281.40= C.676E-03	4295.68= 0.715E-03	4309.96= 0.758E-03	4324.24= C.800E-03
4338.52= 0.812E-03	4352.80= C.776E-03	4367.08= C.770E-03	4381.36= 0.809E-03	4395.64= C.822E-03
4409.92= 0.871E-03	4424.20= C.836E-03	4438.48= C.877E-03	4452.76= 0.854E-03	4467.04= C.903E-03
4481.32= 0.911E-03	4495.60= C.901E-03	4509.87= C.867E-03	4524.16= 0.886E-03	4538.44= C.881E-03
4552.71= 0.873E-03	4567.00= C.897E-03	4581.28= C.906E-03	4595.56= C.903E-03	4609.84= C.893E-03
4624.12= 0.897E-03	4638.40= C.863E-03	4652.68= C.870E-03	4666.96= 0.832E-03	4681.24= C.845E-03
4695.52= 0.877E-03	4709.80= C.859E-03	4724.08= C.856E-03	4738.36= 0.868E-03	4752.64= C.881E-03
4766.92= 0.872E-03	4781.20= C.876E-03	4795.48= C.885E-03	4809.76= 0.857E-03	4824.04= C.837E-03
4839.32= 0.723E-03	4852.60= C.771E-03	4866.87= 0.802E-03	4881.16= 0.822E-03	4895.44= C.800E-03
4909.71= 0.799E-03	4924.00= C.844E-03	4938.28= 0.818E-03	4952.56= 0.822E-03	4966.84= C.811E-03
4981.12= 0.788E-03	4995.40= C.767E-03	5009.68= 0.787E-03	5023.96= 0.831E-03	5038.24= C.852E-03
5052.52= 0.859E-03	5066.80= C.851E-03	5081.08= 0.859E-03	5095.36= 0.877E-03	5109.64= C.885E-03
5123.92= 0.921E-03	5138.20= C.870E-03	5152.40= 0.852E-03	5166.76= 0.910E-03	5181.04= C.954E-03
5195.32= 0.104E-02	5209.60= C.102E-02	5223.87= C.108E-02	5238.16= 0.106E-02	5252.44= C.101E-02
5266.71= 0.115E-02	5281.00= C.118E-02	5295.28= 0.121E-02	5309.56= 0.117E-02	5323.84= C.113E-02
5338.12= 0.126E-02	5352.40= C.125E-02	5366.68= C.128E-02	5380.96= 0.124E-02	5395.24= C.122E-02
5409.52= 0.127E-02	5423.80= C.126E-02	5438.08= 0.132E-02	5452.36= 0.128E-02	5466.64= C.131E-02
5480.92= 0.131E-02	5495.22= C.133E-02	5509.48= 0.132E-02	5523.76= 0.132E-02	5538.04= C.134E-02
5552.32= 0.130E-02	5566.60= C.126E-02	5580.87= 0.126E-02	5595.16= 0.128E-02	5609.44= C.126E-02
5623.71= 0.127E-02	5638.00= C.124E-02	5652.28= 0.124E-02	5666.56= 0.122E-02	5680.84= C.119E-02
5695.12= 0.113E-02	5709.40= C.116E-02	5723.68= 0.114E-02	5737.96= 0.113E-02	5752.24= C.112E-02
5766.52= 0.109E-02	5780.80= C.109E-02	5795.08= C.108E-02	5809.36= 0.109E-02	5823.64= C.105E-02
5837.92= 0.104E-02	5852.20= C.104E-02	5866.48= 0.990E-03	5880.75= 0.959E-03	5895.04= C.944E-03
5909.32= 0.969E-03	5923.60= C.990E-03	5937.87= 0.978E-03	5952.16= 0.975E-03	5966.44= C.995E-03
5980.71= 0.947E-03	5995.00= C.951E-03	6009.20= 0.956E-03	6023.56= 0.984E-03	6037.84= C.991E-03
6052.12= 0.973E-03	6066.40= C.946E-03	6080.68= 0.919E-03	6094.96= 0.917E-03	6109.24= C.894E-03
6123.52= 0.904E-03	6137.80= C.873E-03	6152.08= 0.860E-03	6166.36= 0.875E-03	6180.64= C.845E-03
6194.92= 0.866E-03	6209.20= C.851E-03	6223.48= 0.833E-03	6237.76= 0.840E-03	6252.04= C.851E-03
6266.32= 0.934E-03	6280.60= C.821E-03	6294.87= 0.818E-03	6309.16= 0.821E-03	6323.44= C.815E-03
6337.71= 0.823E-03	6351.00= C.800E-03	6366.28= 0.811E-03	6380.56= 0.822E-03	6394.84= C.783E-03
6409.12= 0.804E-03	6423.40= C.771E-03	6437.68= 0.772E-03	6451.96= 0.770E-03	6466.24= C.742E-03
6480.52= 0.737E-03	6494.80= C.728E-03	6509.08= 0.742E-03	6523.36= 0.720E-03	6537.64= C.765E-03
6551.92= 0.664E-03	6566.20= C.668E-03	6580.48= 0.707E-03	6594.76= 0.686E-03	6609.04= C.665E-03
6623.32= 0.639E-03	6637.60= C.671E-03	6651.87= 0.666E-03	6666.16= 0.631E-03	6680.44= C.643E-03
6694.71= 0.644E-03	6709.00= C.649E-03	6723.28= 0.632E-03	6737.56= 0.634E-03	6751.84= C.632E-03
6766.12= 0.661E-03	6780.40= C.651E-03	6794.68= C.636E-03	6808.96= 0.663E-03	6823.24= C.636E-03
6837.52= 0.665E-03	6851.80= C.657E-03	6866.08= C.634E-03	6880.36= 0.665E-03	6894.64= C.752E-03
6909.02= 0.783E-03	6923.30= C.832E-03	6937.48= 0.830E-03	6951.76= 0.967E-03	6966.04= C.101E-02
6980.32= 0.113E-02	6994.60= C.118E-02	7008.87= 0.130E-02	7023.16= 0.135E-02	7037.44= C.141E-02
7051.71= 0.157E-02	7066.00= C.156E-02	7080.28= 0.172E-02	7094.56= 0.181E-02	7108.84= C.185E-02
7123.12= 0.203E-02	7137.40= C.207E-02	7151.68= 0.215E-02	7165.96= 0.210E-02	7180.24= C.201E-02
7194.52= 0.211E-02	7208.80= C.234E-02	7223.08= 0.249E-02	7237.36= 0.251E-02	7251.64= C.226E-02
7265.92= 0.270E-02	7280.20= C.282E-02	7294.48= 0.291E-02	7308.76= 0.306E-02	7323.04= C.322E-02
7337.32= 0.329E-02	7351.60= C.357E-02	7365.87= 0.362E-02	7380.16= 0.368E-02	7394.44= C.375E-02
7408.71= 0.393E-02	7423.00= C.385E-02	7437.28= C.358E-02	7451.56= 0.405E-02	7465.84= C.401E-02
7480.12= 0.413E-02	7494.40= C.419E-02	7508.68= 0.414E-02	7522.96= 0.421E-02	7537.24= C.421E-02
7551.52= 0.425E-02	7565.80= C.412E-02	7580.08= 0.384E-02	7594.36= 0.327E-02	7608.64= C.291E-02
7622.92= 0.246E-02	7637.20= C.271E-02	7651.48= 0.302E-02	7665.76= 0.349E-02	7680.04= C.375E-02
7694.32= 0.407E-02	7708.60= C.410E-02	7722.87= 0.415E-02	7737.16= 0.423E-02	7751.44= C.422E-02
7765.71= 0.425E-02	7780.00= C.430E-02	7794.28= 0.423E-02	7808.56= 0.430E-02	7822.84= C.415E-02
7837.12= 0.421E-02	7851.40= C.425E-02	7865.68= 0.417E-02	7879.96= 0.410E-02	7894.24= C.414E-02
7908.52= 0.412E-02	7922.80= C.412E-02	7937.08= 0.408E-02	7951.36= 0.408E-02	7965.64= C.401E-02
7979.92= 0.407E-02	7994.20= C.408E-02	8008.48= 0.411E-02	8022.76= 0.396E-02	8037.04= C.417E-02
8051.32= 0.407E-02	8065.60= C.405E-02	8079.87= 0.401E-02	8094.16= 0.358E-02	8108.44= C.355E-02
8122.71= 0.394E-02	8137.00= C.379E-02	8151.28= C.360E-02	8165.56= 0.351E-02	8179.84= C.342E-02
8194.12= 0.343E-02	8208.40= C.354E-02	8222.68= 0.353E-02	8236.96= 0.347E-02	8251.24= C.352E-02
8265.52= 0.357E-02	8279.80= C.367E-02	8294.08= C.358E-02	8308.36= 0.359E-02	8322.64= C.365E-02
8336.92= 0.379E-02	8351.20= C.379E-02	8365.48= C.360E-02	8379.76= 0.381E-02	8394.04= C.385E-02
8408.32= 0.389E-02	8422.60= C.378E-02	8436.87= 0.377E-02	8451.16= 0.385E-02	8465.44= C.386E-02
8479.71= 0.379E-02	8494.00= C.385E-02	8508.28= 0.377E-02	8522.56= 0.367E-02	8536.84= C.362E-02
8551.12= 0.358E-02	8565.40= C.362E-02	8579.68= 0.373E-02	8593.96= 0.376E-02	8608.24= C.377E-02
8622.52= 0.367E-02	8636.80= C.380E-02	8651.08= 0.365E-02	8665.36= 0.362E-02	8679.64= C.385E-02
8693.92= 0.348E-02	8708.20= C.358E-02	8722.40= 0.364E-02	8736.76= 0.373E-02	8751.04= C.378E-02
8765.32= 0.316E-02	8779.60= C.374E-02	8793.87= 0.361E-02	8808.16= 0.354E-02	8822.44= C.360E-02
8836.71= 0.362E-02	8851.00= C.357E-02	8865.28= 0.363E-02	8879.56= 0.351E-02	8893.84= C.356E-02
8908.12= 0.328E-02	8922.40= C.384E-02	8936.68= 0.388E-02	8950.96= 0.325E-02	8965.24= C.311E-02
8979.52= 0.269E-02	8993.80= C.296E-02	9008.08= C.270E-02	9022.36= 0.282E-02	9036.64= C.282E-02
9050.92= 0.284E-02	9065.20= C.262E-02	9079.48= 0.287E-02	9093.76= 0.287E-02	9108.04= C.281E-02
9122.32= 0.275E-02	9136.60= C.275E-02	9150.87= 0.274E-02	9165.16= 0.275E-02	9179.44= C.271C-02
9193.71= 0.263E-02	9208.00= C.266E-02	9222.28= 0.279E-02	9236.56= C.277E-02	9250.84= C.270E-02
9265.12= 0.258E-02	9279.40= C.238E-02	9293.68= C.230E-02	9307.96= 0.209E-02	9322.24= C.181E-02
9336.52= 0.166E-02	9350.80= C.174E-02	9365.08= 0.188E-02	9379.36= 0.180E-02	9393.64= C.174E-02
9407.92= 0.157E-02	9422.20= C.164E-02	9436.48= C.157E-02	9450.76= 0.165E-02	9465.04= C.162E-02
9479.32= 0.161E-02	9493.60= C.154E-02	9507.87= 0.166E-02	9522.16= 0.165E-02	9536.44= C.158E-02
9550.71= 0.178E-02	9565.00= C.158E-02	9579.28= 0.136E-02	9593.56= C.176E-02	9607.84= C.161E-02
9622.12= 0.203E-02	9636.40= C.207E-02	9650.68= 0.219E-02	9664.96= 0.224E-02	9679.24= C.201E-02
9693.52= 0.209E-02	9707.80= C.212E-02	9722.08= C.241E-02	9736.36= 0.232E-02	9750.64= C.222E-02
9764.92= 0.240E-02	9779.20= C.240E-02	9793.48= 0.246E-02	9807.76= 0.256E-02	9822.04= C.243E-02
9836.32= 0.261E-02	9850.60= C.245E-02	9864.87= C.277E-02	9879.16= 0.264E-02	9893.44= C.261E-02
9907.71= 0.256E-02	9922.00= C.279E-02	9936.28= 0.261E-02	9950.56= 0.262E-02	9964.84= C.231E-02
9979.12= 0.296E-02	9993.40= C.231E-02	10007.68= 0.286E-02	10021.96= 0.262E-02	10036.24= C.276E-02
10050.52= 0.277E-02	10064.80= C.253E-02	10079.08= 0.284E-02	10093.36= 0.275E-02	10107.64= C.305E-02
10121.92= 0.264E-02	10136.20= C.259E-02	10150.48= 0.854E-02	10164.76= 0.294E-02	10179.04= C.315E-02
10193.32= 0.281E-02	10207.60= C.311E-02	10221.87= 0.313E-02	10236.16= 0.284E-02	10250.44= C.301E-02
10264.71= 0.311E-02	10279.00= C.315E-02	10293.28= C.305E-02	10307.56= 0.298E-02	10321.84= C.353E-02
10336.12= 0.294E-02	10350.40= C.340E-02	10364.68= 0.332E-02	10378.96= 0.308E-02	10392.24= C.241E-02
10407.52= 0.358E-02	10421.80= C.342E-02	10436.08= 0.325E-02	10450.36= 0.332E-02	10464.64= C.302E-02
10478.92= 0.320E-02	10493.20= C.357E-02	10507.48= 0.336E-02	10521.76= 0.384E-02	10536.04= C.311E-02
10550.32= 0.327E-02	10564.60= C.376E-02	10578.87= 0.383E-02	10593.16= 0.385E-02	10607.44= C.424E-02
10621.71= 0.392E-02	10636.00= C.426E-02	10650.28= 0.379E-02	10664.56= 0.343E-02	10678.84= C.321E-02
10693.12= 0.429E-02	10707.40= C.446E-02	10721.68= 0.479E-02	10735.96= 0.524E-02	10750.24= C.432E-02
10764.52= 0.495E-02	10778.80= C.451E-02	10793.08= 0.483E-02	10807.36= 0.429E-02	10821.64= C.414E-02
10835.92= 0.656E-02	10850.20= C.544E-02	10864.48= C.606E-02	10878.76= 0.476E-02	10893.04= C.641E-02
10907.32= 0.514E-02	10921.60= C.480E-02	10935.87= 0.785E-02	10950.16= 0.522E-02	10964.44= C.811E-02
10978.71= 0.691E-02	10992.00= C.660E-02	11007.28= 0.65[illegible]-02	11021.56= 0.609E-02	11035.84= C.866E-02

ORIGINAL PAGE IS
OF POOR QUALITY

ORIGINAL PAGE IS
OF POOR QUALITY

RECORD NUMBER 1414

WAVELENGTH/RADIANCE	WAVELENGTH/RADIANCE	WAVELENGTH/RADIANCE	WAVELENGTH/RADIANCE	WAVELENGTH/RADIANCE
4195.72= 0.635E-03	4210.00= 0.637E-03	4224.28= 0.648E-03	4238.56= 0.648E-03	4252.84= 0.644E-03
4267.12= 0.647E-03	4281.40= 0.642E-03	4295.68= 0.586E-03	4309.96= 0.628E-03	4324.24= 0.666E-03
4339.52= 0.656E-03	4353.80= 0.637E-03	4367.08= 0.640E-03	4381.36= 0.683E-03	4395.64= 0.700E-03
4409.92= 0.710E-03	4424.20= 0.708E-03	4438.48= 0.730E-03	4452.76= 0.742E-03	4467.04= 0.755E-03
4481.32= 0.780E-03	4495.60= 0.753E-03	4509.87= 0.740E-03	4524.16= 0.766E-03	4538.44= 0.755E-03
4552.71= 0.761E-03	4567.00= 0.780E-03	4581.28= 0.811E-03	4595.56= 0.792E-03	4609.84= 0.773E-03
4624.12= 0.790E-03	4638.40= 0.769E-03	4652.68= 0.767E-03	4666.96= 0.748E-03	4681.24= 0.715E-03
4695.52= 0.784E-03	4709.80= 0.788E-03	4724.08= 0.769E-03	4738.36= 0.801E-03	4752.64= 0.756E-03
4766.92= 0.837E-03	4781.20= 0.814E-03	4795.48= 0.808E-03	4809.76= 0.785E-03	4824.04= 0.733E-03
4838.32= 0.705E-03	4852.60= 0.734E-03	4866.87= 0.779E-03	4881.16= 0.773E-03	4895.44= 0.767E-03
4909.71= 0.791E-03	4924.00= 0.820E-03	4938.28= 0.756E-03	4952.56= 0.797E-03	4966.84= 0.754E-03
4981.12= 0.787E-03	4995.40= 0.791E-03	5009.68= 0.794E-03	5023.96= 0.844E-03	5038.24= 0.687E-03
5052.52= 0.875E-03	5066.80= 0.868E-03	5081.08= 0.920E-03	5095.36= 0.918E-03	5109.64= 0.928E-03
5123.92= 0.956E-03	5138.20= 0.908E-03	5152.48= 0.947E-03	5166.76= 0.103E-02	5181.04= 0.107E-02
5195.32= 0.113E-02	5209.60= 0.117E-02	5223.87= 0.122E-02	5238.16= 0.118E-02	5252.44= 0.125E-02
5266.71= 0.133E-02	5281.00= 0.138E-02	5295.28= 0.138E-02	5309.56= 0.139E-02	5323.84= 0.145E-02
5338.12= 0.146E-02	5352.40= 0.145E-02	5366.68= 0.147E-02	5380.96= 0.146E-02	5395.24= 0.151E-02
5409.52= 0.154E-02	5423.80= 0.154E-02	5438.08= 0.156E-02	5452.36= 0.156E-02	5466.64= 0.160E-02
5480.92= 0.158E-02	5495.20= 0.161E-02	5509.48= 0.162E-02	5523.76= 0.162E-02	5538.04= 0.161E-02
5552.32= 0.157E-02	5566.60= 0.155E-02	5580.87= 0.158E-02	5595.16= 0.156E-02	5609.44= 0.157E-02
5623.71= 0.155E-02	5638.00= 0.154E-02	5652.28= 0.152E-02	5666.56= 0.148E-02	5680.84= 0.146E-02
5695.12= 0.142E-02	5709.40= 0.146E-02	5723.68= 0.141E-02	5737.96= 0.140E-02	5752.24= 0.141E-02
5766.52= 0.136E-02	5780.80= 0.138E-02	5795.08= 0.136E-02	5809.36= 0.138E-02	5823.64= 0.134E-02
5837.92= 0.131E-02	5852.20= 0.130E-02	5866.48= 0.123E-02	5880.76= 0.125E-02	5895.04= 0.137E-02
5909.32= 0.127E-02	5923.60= 0.128E-02	5937.87= 0.125E-02	5952.16= 0.129E-02	5966.44= 0.128E-02
5980.71= 0.123E-02	5995.00= 0.124E-02	6009.28= 0.120E-02	6023.56= 0.125E-02	6037.84= 0.125E-02
6052.12= 0.123E-02	6066.40= 0.122E-02	6080.68= 0.115E-02	6094.96= 0.117E-02	6109.24= 0.111E-02
6123.52= 0.113E-02	6137.80= 0.111E-02	6152.08= 0.109E-02	6166.36= 0.111E-02	6180.64= 0.111E-02
6194.92= 0.111E-02	6209.20= 0.110E-02	6223.48= 0.107E-02	6237.76= 0.109E-02	6252.04= 0.107E-02
6266.32= 0.107E-02	6280.60= 0.106E-02	6294.87= 0.107E-02	6309.16= 0.108E-02	6323.44= 0.107E-02
6337.71= 0.108E-02	6352.00= 0.107E-02	6366.28= 0.106E-02	6380.56= 0.106E-02	6394.84= 0.106E-02
6409.12= 0.103E-02	6423.40= 0.101E-02	6437.68= 0.100E-02	6451.96= 0.996E-03	6466.24= 0.971E-03
6480.52= 0.963E-03	6494.80= 0.940E-03	6509.08= 0.962E-03	6523.36= 0.934E-03	6537.64= 0.950E-03
6551.92= 0.849E-03	6566.20= 0.866E-03	6580.48= 0.900E-03	6594.76= 0.897E-03	6609.04= 0.883E-03
6623.32= 0.899E-03	6637.60= 0.879E-03	6651.87= 0.868E-03	6666.16= 0.852E-03	6680.44= 0.847E-03
6694.71= 0.842E-03	6709.00= 0.832E-03	6723.28= 0.825E-03	6737.56= 0.825E-03	6751.84= 0.828E-03
6766.12= 0.853E-03	6780.40= 0.850E-03	6794.68= 0.850E-03	6808.96= 0.841E-03	6823.24= 0.847E-03
6837.52= 0.879E-03	6851.80= 0.853E-03	6866.08= 0.838E-03	6880.36= 0.881E-03	6894.64= 0.845E-03
6908.92= 0.104E-02	6923.20= 0.113E-02	6937.48= 0.125E-02	6951.76= 0.131E-02	6966.04= 0.128E-02
6980.32= 0.148E-02	6994.60= 0.158E-02	7008.87= 0.169E-02	7023.16= 0.178E-02	7037.44= 0.181E-02
7051.71= 0.193E-02	7066.00= 0.207E-02	7080.28= 0.216E-02	7094.56= 0.222E-02	7108.84= 0.232E-02
7123.12= 0.239E-02	7137.40= 0.249E-02	7151.68= 0.253E-02	7165.96= 0.248E-02	7180.24= 0.248E-02
7194.52= 0.254E-02	7208.80= 0.272E-02	7223.08= 0.277E-02	7237.36= 0.284E-02	7251.64= 0.285E-02
7265.92= 0.297E-02	7280.20= 0.307E-02	7294.48= 0.313E-02	7308.76= 0.324E-02	7323.04= 0.324E-02
7337.32= 0.344E-02	7351.60= 0.352E-02	7365.87= 0.355E-02	7380.16= 0.357E-02	7394.44= 0.365E-02
7408.71= 0.365E-02	7423.00= 0.371E-02	7437.28= 0.376E-02	7451.56= 0.381E-02	7465.84= 0.378E-02
7480.12= 0.375E-02	7494.40= 0.385E-02	7508.68= 0.376E-02	7522.96= 0.383E-02	7537.24= 0.387E-02
7551.52= 0.388E-02	7565.80= 0.386E-02	7580.08= 0.382E-02	7594.36= 0.265E-02	7608.64= 0.226E-02
7622.92= 0.233E-02	7637.20= 0.256E-02	7651.48= 0.254E-02	7665.76= 0.328E-02	7680.04= 0.354E-02
7694.32= 0.367E-02	7708.60= 0.369E-02	7722.87= 0.372E-02	7737.16= 0.376E-02	7751.44= 0.378E-02
7765.71= 0.377E-02	7780.00= 0.381E-02	7794.28= 0.382E-02	7808.56= 0.381E-02	7822.84= 0.382E-02
7837.12= 0.377E-02	7851.40= 0.371E-02	7865.68= 0.364E-02	7879.96= 0.366E-02	7894.24= 0.370E-02
7908.52= 0.377E-02	7922.80= 0.368E-02	7937.08= 0.365E-02	7951.36= 0.366E-02	7965.64= 0.368E-02
7979.92= 0.355E-02	7994.20= 0.361E-02	8008.48= 0.368E-02	8022.76= 0.353E-02	8037.04= 0.355E-02
8051.32= 0.365E-02	8065.60= 0.369E-02	8079.87= 0.363E-02	8094.16= 0.360E-02	8108.44= 0.359E-02
8122.71= 0.346E-02	8137.00= 0.343E-02	8151.28= 0.330E-02	8165.56= 0.332E-02	8179.84= 0.321E-02
8194.12= 0.331E-02	8208.40= 0.327E-02	8222.68= 0.330E-02	8236.96= 0.331E-02	8251.24= 0.337E-02
8265.52= 0.342E-02	8279.80= 0.340E-02	8294.08= 0.337E-02	8308.36= 0.328E-02	8322.64= 0.324E-02
8336.92= 0.342E-02	8351.20= 0.347E-02	8365.48= 0.351E-02	8379.76= 0.352E-02	8394.04= 0.346E-02
8408.32= 0.350E-02	8422.60= 0.351E-02	8436.87= 0.354E-02	8451.16= 0.354E-02	8465.44= 0.353E-02
8479.71= 0.353E-02	8494.00= 0.352E-02	8508.28= 0.343E-02	8522.56= 0.338E-02	8536.84= 0.336E-02
8551.12= 0.333E-02	8565.40= 0.337E-02	8579.68= 0.347E-02	8593.96= 0.351E-02	8608.24= 0.345E-02
8622.52= 0.350E-02	8636.80= 0.346E-02	8651.08= 0.340E-02	8665.36= 0.340E-02	8679.64= 0.337E-02
8693.92= 0.334E-02	8708.20= 0.340E-02	8722.48= 0.347E-02	8736.76= 0.349E-02	8751.04= 0.345E-02
8765.32= 0.344E-02	8779.60= 0.343E-02	8793.87= 0.346E-02	8808.16= 0.346E-02	8822.44= 0.344E-02
8836.71= 0.344E-02	8851.00= 0.337E-02	8865.28= 0.348E-02	8879.56= 0.339E-02	8893.84= 0.345E-02
8908.12= 0.337E-02	8922.40= 0.341E-02	8936.68= 0.324E-02	8950.96= 0.317E-02	8965.24= 0.333E-02
8979.52= 0.301E-02	8993.80= 0.298E-02	9008.08= 0.303E-02	9022.36= 0.303E-02	9036.64= 0.306E-02
9050.92= 0.303E-02	9065.20= 0.321E-02	9079.48= 0.313E-02	9093.76= 0.300E-02	9108.04= 0.302E-02
9122.32= 0.299E-02	9136.60= 0.302E-02	9150.87= 0.304E-02	9165.16= 0.291E-02	9179.44= 0.303E-02
9193.71= 0.293E-02	9208.00= 0.303E-02	9222.28= 0.298E-02	9236.56= 0.299E-02	9250.84= 0.297E-02
9265.12= 0.277E-02	9279.40= 0.269E-02	9293.68= 0.261E-02	9307.96= 0.244E-02	9322.24= 0.285E-02
9336.52= 0.259E-02	9350.80= 0.270E-02	9365.08= 0.204E-02	9379.36= 0.207E-02	9393.64= 0.216E-02
9407.92= 0.211E-02	9422.20= 0.220E-02	9436.48= 0.217E-02	9450.76= 0.225E-02	9465.04= 0.228E-02
9479.32= 0.228E-02	9493.60= 0.233E-02	9507.87= 0.230E-02	9522.16= 0.237E-02	9536.44= 0.231E-02
9550.71= 0.234E-02	9565.00= 0.235E-02	9579.28= 0.236E-02	9593.56= 0.235E-02	9607.84= 0.235E-02
9622.12= 0.279E-02	9636.40= 0.277E-02	9650.68= 0.289E-02	9664.96= 0.287E-02	9679.24= 0.277E-02
9693.52= 0.277E-02	9707.80= 0.286E-02	9722.08= 0.298E-02	9736.36= 0.287E-02	9750.64= 0.311E-02
9764.92= 0.300E-02	9779.20= 0.315E-02	9793.48= 0.317E-02	9807.76= 0.327E-02	9822.04= 0.310E-02
9836.32= 0.299E-02	9850.60= 0.305E-02	9864.87= 0.326E-02	9879.16= 0.312E-02	9893.44= 0.306E-02
9907.71= 0.323E-02	9922.00= 0.312E-02	9936.28= 0.319E-02	9950.56= 0.314E-02	9964.84= 0.315E-02
9979.12= 0.347E-02	9993.40= 0.317E-02	10007.68= 0.318E-02	10021.96= 0.321E-02	10036.24= 0.328E-02
10051.52= 0.323E-02	10064.80= 0.316E-02	10079.08= 0.328E-02	10093.36= 0.311E-02	10107.64= 0.327E-02
10121.92= 0.319E-02	10136.20= 0.336E-02	10150.48= 0.318E-02	10164.76= 0.326E-02	10179.04= 0.345E-02
10193.32= 0.341E-02	10207.60= 0.325E-02	10221.87= 0.345E-02	10236.16= 0.308E-02	10250.44= 0.332E-02
10264.71= 0.335E-02	10279.00= 0.345E-02	10293.28= 0.315E-02	10307.56= 0.325E-02	10321.84= 0.311E-02
10336.12= 0.330E-02	10350.40= 0.332E-02	10364.68= 0.329E-02	10378.96= 0.326E-02	10393.24= 0.332E-02
10407.52= 0.313E-02	10421.80= 0.334E-02	10436.08= 0.343E-02	10450.36= 0.311E-02	10464.64= 0.311E-02
10478.92= 0.309E-02	10493.20= 0.350E-02	10507.48= 0.328E-02	10521.76= 0.362E-02	10536.04= 0.323E-02
10550.32= 0.327E-02	10564.60= 0.317E-02	10578.87= 0.307E-02	10593.16= 0.306E-02	10607.44= 0.321E-02
10621.71= 0.315E-02	10636.00= 0.314E-02	10650.28= 0.303E-02	10664.56= 0.265E-02	10678.84= 0.307E-02
10693.12= 0.326E-02	10707.40= 0.317E-02	10721.68= 0.276E-02	10735.96= 0.374E-02	10750.24= 0.254E-02
10764.52= 0.280E-02	10778.80= 0.265E-02	10793.08= 0.268E-02	10807.36= 0.307E-02	10821.64= 0.283E-02
10835.92= 0.241E-02	10850.20= 0.241E-02	10864.48= 0.309E-02	10878.76= 0.291E-02	10893.04= 0.445E-02
10907.32= 0.272E-02	10921.60= 0.222E-02	10935.87= 0.266E-02	10950.16= 0.871E-03	10964.44= 0.425E-02
10978.71= 0.266E-02	10993.00= 0.318E-02	11007.28= 0.225E-02	11021.56= 0.318E-02	11035.84= 0.155E-02

ORIGINAL PAGE IS
OF POOR QUALITY

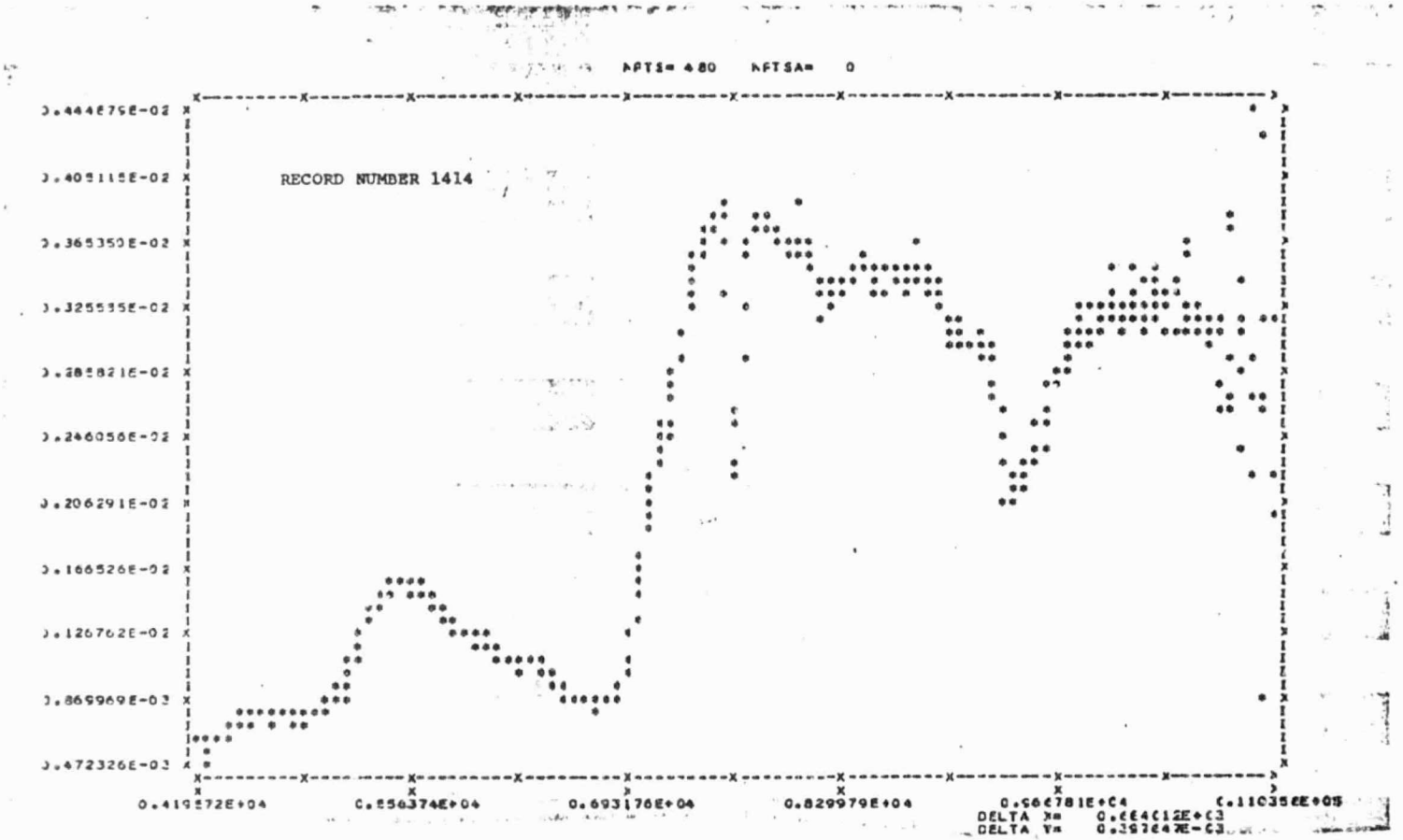

ORIGINAL PAGE IS
OF POOR QUALITY

RECORD NUMBER 1426

WAVELENGTH/RADIANCE		WAVELENGTH/RADIANCE		WAVELENGTH/RADIANCE		WAVELENGTH/RADIANCE		WAVELENGTH/RADIANCE	
4195.72=	0.846E-03	4210.00=	0.836E-03	4224.28=	0.841E-03	4238.56=	0.804E-03	4252.84=	0.784E-03
4267.12=	0.714E-03	4281.40=	0.716E-03	4295.68=	0.785E-03	4309.96=	0.821E-03	4324.24=	0.880E-03
4338.52=	0.899E-03	4352.80=	0.858E-03	4367.08=	0.852E-03	4381.36=	0.879E-03	4395.64=	0.934E-03
4409.92=	0.952E-03	4424.20=	0.944E-03	4438.48=	0.978E-03	4452.76=	0.985E-03	4467.04=	0.103E-02
4481.32=	0.106E-02	4495.60=	0.102E-02	4509.87=	0.101E-02	4524.16=	0.104E-02	4538.44=	0.105E-02
4552.71=	0.134E-02	4567.00=	0.104E-02	4581.28=	0.109E-02	4595.56=	0.106E-02	4609.84=	0.105E-02
4624.12=	0.139E-02	4638.40=	0.105E-02	4652.68=	0.105E-02	4666.96=	0.103E-02	4681.24=	0.103E-02
4695.52=	0.137E-02	4709.80=	0.105E-02	4724.08=	0.106E-02	4738.36=	0.108E-02	4752.64=	0.105E-02
4766.92=	0.109E-02	4781.20=	0.112E-02	4795.48=	0.111E-02	4809.76=	0.109E-02	4824.04=	0.105E-02
4838.32=	0.958E-03	4852.60=	0.101E-02	4866.87=	0.105E-02	4881.16=	0.107E-02	4895.44=	0.105E-02
4909.71=	0.106E-02	4924.00=	0.112E-02	4938.28=	0.111E-02	4952.56=	0.109E-02	4966.84=	0.108E-02
4981.12=	0.106E-02	4995.40=	0.107E-02	5009.68=	0.108E-02	5023.96=	0.111E-02	5038.24=	0.110E-02
5052.52=	0.114E-02	5066.80=	0.117E-02	5081.08=	0.117E-02	5095.36=	0.121E-02	5109.64=	0.122E-02
5123.92=	0.126E-02	5138.20=	0.122E-02	5152.48=	0.119E-02	5166.76=	0.126E-02	5181.04=	0.133E-02
5195.32=	0.142E-02	5209.60=	0.145E-02	5223.87=	0.152E-02	5238.16=	0.150E-02	5252.44=	0.150E-02
5266.71=	0.162E-02	5281.00=	0.169E-02	5295.28=	0.172E-02	5309.56=	0.171E-02	5323.84=	0.170E-02
5338.12=	0.180E-02	5352.40=	0.177E-02	5366.68=	0.183E-02	5380.96=	0.180E-02	5395.24=	0.184E-02
5409.52=	0.189E-02	5423.80=	0.189E-02	5438.08=	0.194E-02	5452.36=	0.191E-02	5466.64=	0.195E-02
5480.92=	0.197E-02	5495.20=	0.199E-02	5509.48=	0.199E-02	5523.76=	0.200E-02	5538.04=	0.202E-02
5552.32=	0.196E-02	5566.60=	0.194E-02	5580.87=	0.193E-02	5595.16=	0.193E-02	5609.44=	0.195E-02
5623.71=	0.194E-02	5638.00=	0.193E-02	5652.28=	0.192E-02	5666.56=	0.190E-02	5680.84=	0.187E-02
5695.12=	0.183E-02	5709.40=	0.185E-02	5723.68=	0.182E-02	5737.96=	0.181E-02	5752.24=	0.180E-02
5766.52=	0.177E-02	5780.80=	0.177E-02	5795.08=	0.177E-02	5809.36=	0.179E-02	5823.64=	0.175E-02
5837.92=	0.172E-02	5852.20=	0.172E-02	5866.48=	0.164E-02	5880.76=	0.160E-02	5895.04=	0.165E-02
5909.32=	0.167E-02	5923.60=	0.167E-02	5937.87=	0.166E-02	5952.16=	0.167E-02	5966.44=	0.164E-02
5980.71=	0.166E-02	5995.00=	0.165E-02	6009.28=	0.165E-02	6023.56=	0.166E-02	6037.84=	0.166E-02
6052.12=	0.166E-02	6066.40=	0.163E-02	6080.68=	0.159E-02	6094.96=	0.160E-02	6109.24=	0.158E-02
6123.52=	0.154E-02	6137.80=	0.153E-02	6152.08=	0.151E-02	6166.36=	0.154E-02	6180.64=	0.153E-02
6194.92=	0.154E-02	6209.20=	0.152E-02	6223.48=	0.149E-02	6237.76=	0.149E-02	6252.04=	0.145E-02
6266.32=	0.151E-02	6280.60=	0.149E-02	6294.87=	0.148E-02	6309.16=	0.150E-02	6323.44=	0.145E-02
6337.71=	0.151E-02	6352.00=	0.150E-02	6366.28=	0.152E-02	6380.56=	0.151E-02	6394.84=	0.147E-02
6409.12=	0.149E-02	6423.40=	0.144E-02	6437.68=	0.146E-02	6451.96=	0.142E-02	6466.24=	0.141E-02
6480.52=	0.142E-02	6494.80=	0.138E-02	6509.08=	0.139E-02	6523.36=	0.139E-02	6537.64=	0.133E-02
6551.92=	0.129E-02	6566.20=	0.127E-02	6580.48=	0.134E-02	6594.76=	0.134E-02	6609.04=	0.132E-02
6623.32=	0.122E-02	6637.60=	0.131E-02	6651.87=	0.127E-02	6666.16=	0.128E-02	6680.44=	0.127E-02
6694.71=	0.130E-02	6709.00=	0.127E-02	6723.28=	0.127E-02	6737.56=	0.123E-02	6751.84=	0.124E-02
6766.12=	0.130E-02	6780.40=	0.127E-02	6794.68=	0.128E-02	6808.96=	0.127E-02	6823.24=	0.128E-02
6837.52=	0.133E-02	6851.80=	0.130E-02	6866.08=	0.125E-02	6880.36=	0.126E-02	6894.64=	0.137E-02
6908.92=	0.145E-02	6923.20=	0.156E-02	6937.48=	0.165E-02	6951.76=	0.176E-02	6966.04=	0.187E-02
6980.32=	0.201E-02	6994.60=	0.210E-02	7008.87=	0.222E-02	7023.16=	0.231E-02	7037.44=	0.242E-02
7051.71=	0.252E-02	7066.00=	0.259E-02	7080.28=	0.269E-02	7094.56=	0.280E-02	7108.84=	0.254E-02
7123.12=	0.300E-02	7137.40=	0.294E-02	7151.68=	0.316E-02	7165.96=	0.304E-02	7180.24=	0.255E-02
7194.52=	0.302E-02	7208.80=	0.321E-02	7223.08=	0.336E-02	7237.36=	0.340E-02	7251.64=	0.346E-02
7265.92=	0.355E-02	7280.20=	0.363E-02	7294.48=	0.370E-02	7308.76=	0.382E-02	7323.04=	0.354E-02
7337.32=	0.411E-02	7351.60=	0.420E-02	7365.87=	0.425E-02	7380.16=	0.427E-02	7394.44=	0.425E-02
7408.71=	0.435E-02	7423.00=	0.437E-02	7437.28=	0.448E-02	7451.56=	0.450E-02	7465.84=	0.447E-02
7480.12=	0.453E-02	7494.40=	0.456E-02	7508.68=	0.451E-02	7522.96=	0.451E-02	7537.24=	0.455E-02
7551.52=	0.459E-02	7565.80=	0.446E-02	7580.08=	0.411E-02	7594.36=	0.350E-02	7608.64=	0.271E-02
7622.92=	0.267E-02	7637.20=	0.287E-02	7651.48=	0.327E-02	7665.76=	0.370E-02	7680.04=	0.410E-02
7694.32=	0.433E-02	7708.60=	0.440E-02	7722.87=	0.441E-02	7737.16=	0.446E-02	7751.44=	0.447E-02
7765.71=	0.445E-02	7780.00=	0.452E-02	7794.28=	0.452E-02	7808.56=	0.452E-02	7822.84=	0.447E-02
7837.12=	0.444E-02	7851.40=	0.450E-02	7865.68=	0.442E-02	7879.96=	0.436E-02	7894.24=	0.437E-02
7908.52=	0.438E-02	7922.80=	0.434E-02	7937.08=	0.426E-02	7951.36=	0.433E-02	7965.64=	0.425E-02
7979.92=	0.424E-02	7994.20=	0.434E-02	8008.48=	0.433E-02	8022.76=	0.418E-02	8037.04=	0.422E-02
8051.32=	0.426E-02	8065.60=	0.428E-02	8079.87=	0.423E-02	8094.16=	0.421E-02	8108.44=	0.421E-02
8122.71=	0.409E-02	8137.00=	0.407E-02	8151.28=	0.350E-02	8165.56=	0.382E-02	8179.84=	0.371E-02
8194.12=	0.374E-02	8208.40=	0.380E-02	8222.68=	0.377E-02	8236.96=	0.383E-02	8251.24=	0.362E-02
8265.52=	0.392E-02	8279.80=	0.363E-02	8294.08=	0.387E-02	8308.36=	0.390E-02	8322.64=	0.352E-02
8336.92=	0.374E-02	8351.20=	0.402E-02	8365.48=	0.403E-02	8379.76=	0.405E-02	8394.04=	0.401E-02
8408.32=	0.432E-02	8422.60=	0.402E-02	8436.87=	0.356E-02	8451.16=	0.405E-02	8465.44=	0.403E-02
8479.71=	0.405E-02	8494.00=	0.413E-02	8508.28=	0.351E-02	8522.56=	0.388E-02	8536.84=	0.386E-02
8551.12=	0.385E-02	8565.40=	0.378E-02	8579.68=	0.394E-02	8593.96=	0.392E-02	8608.24=	0.354E-02
8622.52=	0.393E-02	8636.80=	0.359E-02	8651.08=	0.379E-02	8665.36=	0.386E-02	8679.64=	0.365E-02
8693.92=	0.363E-02	8708.20=	0.383E-02	8722.48=	0.384E-02	8736.76=	0.400E-02	8751.04=	0.357E-02
8765.32=	0.300E-02	8779.60=	0.410E-02	8793.87=	0.377E-02	8808.16=	0.391E-02	8822.44=	0.360E-02
8836.71=	0.385E-02	8851.00=	0.377E-02	8865.28=	0.377E-02	8879.56=	0.375E-02	8893.84=	0.375E-02
8908.12=	0.377E-02	8922.40=	0.378E-02	8936.68=	0.349E-02	8950.96=	0.337E-02	8965.24=	0.325E-02
8979.52=	0.324E-02	8993.80=	0.328E-02	9008.08=	0.313E-02	9022.36=	0.317E-02	9036.64=	0.311E-02
9050.92=	0.321E-02	9065.20=	0.304E-02	9079.48=	0.309E-02	9093.76=	0.325E-02	9108.04=	0.311E-02
9122.32=	0.316E-02	9136.60=	0.313E-02	9150.87=	0.314E-02	9165.16=	0.310E-02	9179.44=	0.306E-02
9193.71=	0.310E-02	9208.00=	0.320E-02	9222.28=	0.313E-02	9236.56=	0.324E-02	9250.84=	0.304E-02
9265.12=	0.259E-02	9279.40=	0.253E-02	9293.68=	0.268E-02	9307.96=	0.254E-02	9322.24=	0.225E-02
9336.52=	0.214E-02	9350.80=	0.158E-02	9365.08=	0.184E-02	9379.36=	0.203E-02	9393.64=	0.158E-02
9407.92=	0.211E-02	9422.20=	0.222E-02	9436.48=	0.215E-02	9450.76=	0.222E-02	9465.04=	0.210E-02
9479.32=	0.216E-02	9493.60=	0.217E-02	9507.87=	0.213E-02	9522.16=	0.233E-02	9536.44=	0.221E-02
9550.71=	0.237E-02	9565.00=	0.247E-02	9579.28=	0.236E-02	9593.56=	0.252E-02	9607.84=	0.245E-02
9622.12=	0.264E-02	9636.40=	0.259E-02	9650.68=	0.291E-02	9664.96=	0.277E-02	9679.24=	0.275E-02
9693.52=	0.300E-02	9707.80=	0.305E-02	9722.08=	0.331E-02	9736.36=	0.314E-02	9750.64=	0.315E-02
9764.92=	0.316E-02	9779.20=	0.315E-02	9793.48=	0.314E-02	9807.76=	0.324E-02	9822.04=	0.325E-02
9836.32=	0.346E-02	9850.60=	0.334E-02	9864.87=	0.347E-02	9879.16=	0.348E-02	9893.44=	0.344E-02
9907.71=	0.344E-02	9922.00=	0.352E-02	9936.28=	0.349E-02	9950.56=	0.356E-02	9964.84=	0.363E-02
9979.12=	0.386E-02	9993.40=	0.378E-02	10007.68=	0.380E-02	10021.96=	0.360E-02	10036.24=	0.375E-02
10050.52=	0.352E-02	10064.80=	0.375E-02	10079.08=	0.384E-02	10093.36=	0.385E-02	10107.64=	0.384E-02
10121.92=	0.387E-02	10136.20=	0.392E-02	10150.48=	0.409E-02	10164.76=	0.394E-02	10179.04=	0.434E-02
10193.32=	0.357E-02	10207.60=	0.426E-02	10221.87=	0.430E-02	10236.16=	0.410E-02	10250.44=	0.413E-02
10264.71=	0.417E-02	10279.00=	0.413E-02	10293.28=	0.418E-02	10307.56=	0.437E-02	10321.84=	0.358E-02
10336.12=	0.426E-02	10350.40=	0.434E-02	10364.68=	0.436E-02	10378.96=	0.442E-02	10393.24=	0.477E-02
10407.52=	0.410E-02	10421.80=	0.415E-02	10436.08=	0.529E-02	10450.36=	0.465E-02	10464.64=	0.487E-02
10478.92=	0.437E-02	10493.20=	0.480E-02	10507.48=	0.425E-02	10521.76=	0.519E-02	10536.04=	0.555E-02
10550.32=	0.531E-02	10564.60=	0.510E-02	10578.87=	0.548E-02	10593.16=	0.548E-02	10607.44=	0.512E-02
10621.71=	0.480E-02	10636.00=	0.531E-02	10650.28=	0.504E-02	10664.56=	0.547E-02	10678.84=	0.541E-02
10693.12=	0.516E-02	10707.40=	0.554E-02	10721.68=	0.647E-02	10735.96=	0.647E-02	10750.24=	0.610E-02
10764.52=	0.555E-02	10778.80=	0.337E-02	10793.08=	0.514E-02	10807.36=	0.506E-02	10821.64=	0.482E-02
10835.92=	0.652E-02	10850.20=	0.562E-02	10864.48=	0.713E-02	10878.76=	0.690E-02	10893.04=	0.730E-02
10907.32=	0.533E-02	10921.60=	0.426E-02	10935.87=	0.626E-02	10950.16=	0.416E-02	10964.44=	0.864E-02
10978.71=	0.637E-02	10993.00=	0.601E-02	11007.28=	0.676E-02	11021.56=	0.636E-02	11035.84=	0.555E-02

ORIGINAL PAGE IS
OF POOR QUALITY

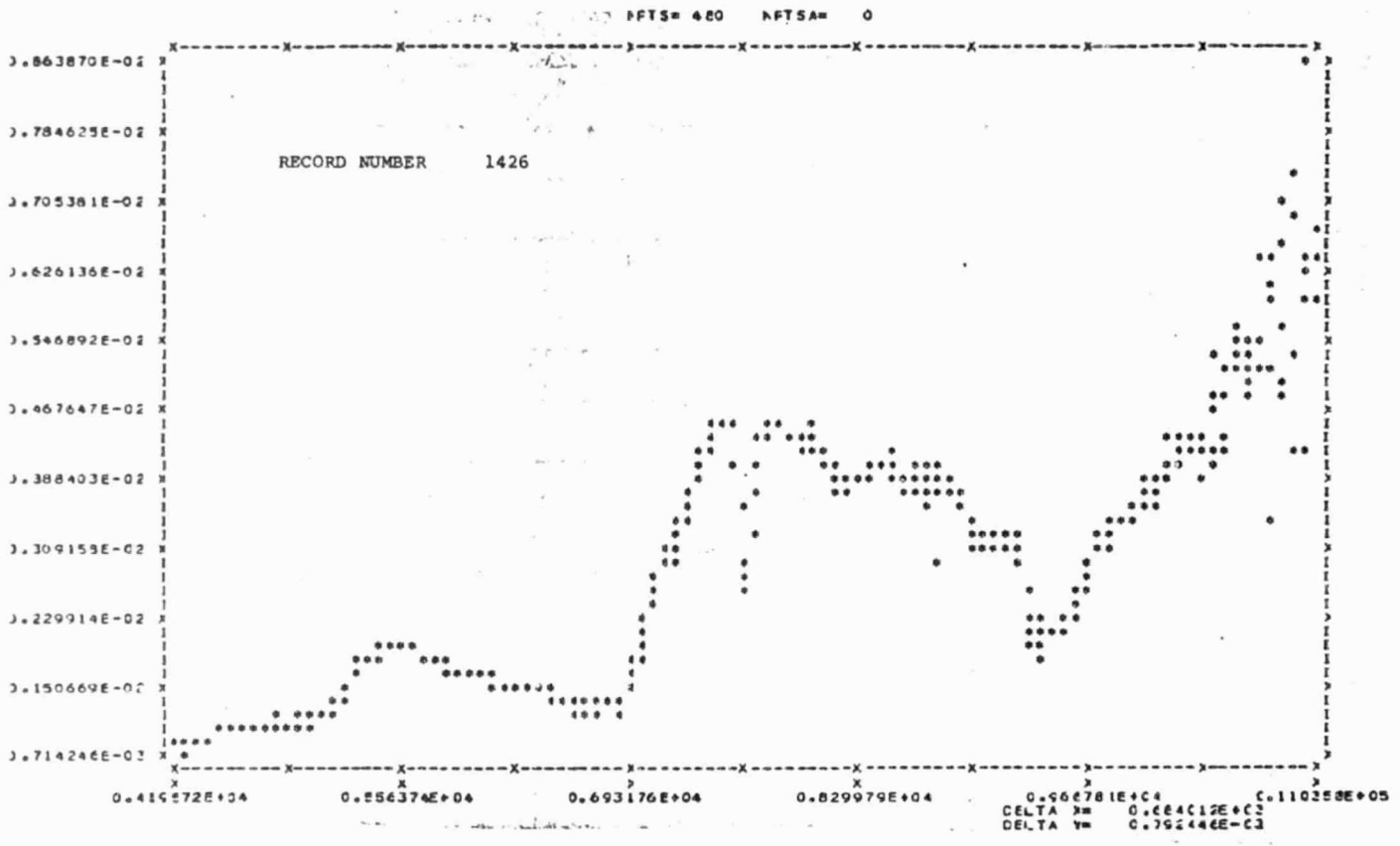

ORIGINAL PAGE IS
OF POOR QUALITY

RECORD NUMBER 1423

WAVELENGTH/RADIANCE	WAVELENGTH/RADIANCE	WAVELENGTH/RADIANCE	WAVELENGTH/RADIANCE	WAVELENGTH/RADIANCE
4195.72= 0.910E-03	4210.00= .845E-03	4224.28= 0.800E-03	4238.56= 0.884E-03	4252.84= 0.855E-03
4267.12= 0.765E-03	4281.40= 0.802E-03	4295.68= 0.860E-03	4309.96= 0.890E-03	4324.24= 0.944E-03
4338.52= 0.944E-03	4352.80= 0.904E-03	4367.08= 0.931E-03	4381.36= 0.963E-03	4395.64= 0.101E-02
4409.92= 0.101E-02	4424.20= 0.997E-03	4438.48= 0.106E-02	4452.76= 0.106E-02	4467.04= 0.114E-02
4481.32= 0.113E-02	4495.60= 0.108E-02	4509.87= 0.107E-02	4524.16= 0.111E-02	4538.44= 0.111E-02
4552.71= 0.108E-02	4567.00= 0.112E-02	4581.28= 0.114E-02	4595.56= 0.114E-02	4609.84= 0.111E-02
4624.12= 0.112E-02	4638.40= 0.109E-02	4652.68= 0.109E-02	4666.96= 0.109E-02	4681.24= 0.110E-02
4695.52= 0.112E-02	4709.80= 0.113E-02	4724.08= 0.110E-02	4738.36= 0.114E-02	4752.64= 0.114E-02
4766.92= 0.114E-02	4781.20= 0.116E-02	4795.48= 0.115E-02	4809.76= 0.114E-02	4824.04= 0.110E-02
4838.32= 0.993E-03	4852.60= 0.109E-02	4866.87= 0.111E-02	4881.16= 0.110E-02	4895.44= 0.109E-02
4909.71= 0.112E-02	4924.00= 0.115E-02	4938.28= 0.115E-02	4952.56= 0.112E-02	4966.84= 0.113E-02
4981.12= 0.111E-02	4995.40= 0.112E-02	5009.68= 0.113E-02	5023.96= 0.118E-02	5038.24= 0.120E-02
5052.52= 0.122E-02	5066.80= 0.123E-02	5081.08= 0.126E-02	5095.36= 0.129E-02	5109.64= 0.125E-02
5123.92= 0.131E-02	5138.20= 0.126E-02	5152.48= 0.128E-02	5166.76= 0.138E-02	5181.04= 0.144E-02
5195.32= 0.153E-02	5209.60= 0.159E-02	5223.87= 0.163E-02	5238.16= 0.161E-02	5252.44= 0.165E-02
5266.71= 0.177E-02	5281.00= 0.184E-02	5295.28= 0.184E-02	5309.56= 0.185E-02	5323.84= 0.192E-02
5338.12= 0.195E-02	5352.40= 0.194E-02	5366.68= 0.196E-02	5380.96= 0.194E-02	5395.24= 0.195E-02
5409.52= 0.201E-02	5423.80= 0.203E-02	5438.08= 0.207E-02	5452.36= 0.204E-02	5466.64= 0.210E-02
5480.92= 0.215E-02	5495.20= 0.211E-02	5509.48= 0.213E-02	5523.76= 0.211E-02	5538.04= 0.213E-02
5552.32= 0.206E-02	5566.60= 0.205E-02	5580.87= 0.206E-02	5595.16= 0.207E-02	5609.44= 0.203E-02
5623.71= 0.205E-02	5638.00= 0.200E-02	5652.28= 0.201E-02	5666.56= 0.197E-02	5680.84= 0.193E-02
5695.12= 0.189E-02	5709.40= 0.192E-02	5723.68= 0.185E-02	5737.96= 0.184E-02	5752.24= 0.184E-02
5766.52= 0.180E-02	5780.80= 0.181E-02	5795.08= 0.179E-02	5809.36= 0.181E-02	5823.64= 0.181E-02
5837.92= 0.174E-02	5852.20= 0.176E-02	5866.48= 0.164E-02	5880.76= 0.163E-02	5895.04= 0.162E-02
5909.32= 0.167E-02	5923.60= 0.165E-02	5937.87= 0.168E-02	5952.16= 0.168E-02	5966.44= 0.167E-02
5980.71= 0.164E-02	5995.00= 0.161E-02	6009.28= 0.162E-02	6023.56= 0.166E-02	6037.84= 0.168E-02
6052.12= 0.165E-02	6066.40= 0.162E-02	6080.68= 0.157E-02	6094.96= 0.159E-02	6109.24= 0.154E-02
6123.52= 0.154E-02	6137.80= 0.150E-02	6152.08= 0.148E-02	6166.36= 0.153E-02	6180.64= 0.152E-02
6194.92= 0.152E-02	6209.20= 0.149E-02	6223.48= 0.146E-02	6237.76= 0.147E-02	6252.04= 0.146E-02
6266.32= 0.147E-02	6280.60= 0.146E-02	6294.87= 0.146E-02	6309.16= 0.147E-02	6323.44= 0.145E-02
6337.71= 0.147E-02	6352.00= 0.145E-02	6366.28= 0.145E-02	6380.56= 0.146E-02	6394.84= 0.146E-02
6409.12= 0.141E-02	6423.40= 0.139E-02	6437.68= 0.139E-02	6451.96= 0.137E-02	6466.24= 0.138E-02
6480.52= 0.132E-02	6494.80= 0.131E-02	6509.08= 0.134E-02	6523.36= 0.131E-02	6537.64= 0.134E-02
6551.92= 0.129E-02	6566.20= 0.128E-02	6580.48= 0.127E-02	6594.76= 0.126E-02	6609.04= 0.125E-02
6623.32= 0.127E-02	6637.60= 0.124E-02	6651.87= 0.121E-02	6666.16= 0.121E-02	6680.44= 0.119E-02
6694.71= 0.122E-02	6709.00= 0.120E-02	6723.28= 0.119E-02	6737.56= 0.118E-02	6751.84= 0.119E-02
6766.12= 0.123E-02	6780.40= 0.124E-02	6794.68= 0.123E-02	6808.96= 0.122E-02	6823.24= 0.122E-02
6837.52= 0.127E-02	6851.80= 0.122E-02	6866.08= 0.120E-02	6880.36= 0.125E-02	6894.64= 0.125E-02
6908.92= 0.148E-02	6923.20= 0.159E-02	6937.48= 0.172E-02	6951.76= 0.184E-02	6966.04= 0.192E-02
6980.32= 0.205E-02	6994.60= 0.215E-02	7008.87= 0.231E-02	7023.16= 0.245E-02	7037.44= 0.258E-02
7051.71= 0.274E-02	7066.00= 0.283E-02	7080.28= 0.295E-02	7094.56= 0.307E-02	7108.84= 0.318E-02
7123.12= 0.328E-02	7137.40= 0.337E-02	7151.68= 0.342E-02	7165.96= 0.336E-02	7180.24= 0.345E-02
7194.52= 0.343E-02	7208.80= 0.371E-02	7223.08= 0.377E-02	7237.36= 0.383E-02	7251.64= 0.354E-02
7265.92= 0.401E-02	7280.20= 0.412E-02	7294.48= 0.423E-02	7308.76= 0.426E-02	7323.04= 0.452E-02
7337.32= 0.466E-02	7351.60= 0.480E-02	7365.87= 0.482E-02	7380.16= 0.493E-02	7394.44= 0.495E-02
7408.71= 0.490E-02	7423.00= 0.504E-02	7437.28= 0.513E-02	7451.56= 0.514E-02	7465.84= 0.513E-02
7480.12= 0.521E-02	7494.40= 0.527E-02	7508.68= 0.523E-02	7522.96= 0.524E-02	7537.24= 0.527E-02
7551.52= 0.524E-02	7565.80= 0.503E-02	7580.08= 0.456E-02	7594.36= 0.368E-02	7608.64= 0.326E-02
7622.92= 0.318E-02	7637.20= 0.351E-02	7651.48= 0.402E-02	7665.76= 0.454E-02	7680.04= 0.468E-02
7694.32= 0.503E-02	7708.60= 0.505E-02	7722.87= 0.511E-02	7737.16= 0.511E-02	7751.44= 0.514E-02
7765.71= 0.515E-02	7780.00= 0.525E-02	7794.28= 0.524E-02	7808.56= 0.526E-02	7822.84= 0.516E-02
7837.12= 0.514E-02	7851.40= 0.515E-02	7865.68= 0.508E-02	7879.96= 0.503E-02	7894.24= 0.503E-02
7908.52= 0.502E-02	7922.80= 0.501E-02	7937.08= 0.458E-02	7951.36= 0.501E-02	7965.64= 0.458E-02
7979.92= 0.497E-02	7994.20= 0.503E-02	8008.48= 0.503E-02	8022.76= 0.481E-02	8037.04= 0.482E-02
8051.32= 0.457E-02	8065.60= 0.503E-02	8079.87= 0.489E-02	8094.16= 0.486E-02	8108.44= 0.486E-02
8122.71= 0.474E-02	8137.00= 0.461E-02	8151.28= 0.444E-02	8165.56= 0.440E-02	8179.84= 0.431E-02
8194.12= 0.439E-02	8208.40= 0.441E-02	8222.68= 0.441E-02	8236.96= 0.435E-02	8251.24= 0.446E-02
8265.52= 0.453E-02	8279.80= 0.454E-02	8294.08= 0.446E-02	8308.36= 0.452E-02	8322.64= 0.451E-02
8336.92= 0.459E-02	8351.20= 0.467E-02	8365.48= 0.466E-02	8379.76= 0.465E-02	8394.04= 0.465E-02
8408.32= 0.467E-02	8422.60= 0.474E-02	8436.87= 0.470E-02	8451.16= 0.470E-02	8465.44= 0.465E-02
8479.71= 0.464E-02	8494.00= 0.469E-02	8508.28= 0.452E-02	8522.56= 0.446E-02	8536.84= 0.446E-02
8551.12= 0.439E-02	8565.40= 0.450E-02	8579.68= 0.457E-02	8593.96= 0.463E-02	8608.24= 0.459E-02
8622.52= 0.453E-02	8636.80= 0.451E-02	8651.08= 0.439E-02	8665.36= 0.438E-02	8679.64= 0.438E-02
8693.92= 0.442E-02	8708.20= 0.446E-02	8722.48= 0.447E-02	8736.76= 0.450E-02	8751.04= 0.456E-02
8765.32= 0.376E-02	8779.60= 0.470E-02	8793.87= 0.450E-02	8808.16= 0.445E-02	8822.44= 0.445E-02
8836.71= 0.440E-02	8851.00= 0.431E-02	8865.28= 0.437E-02	8879.56= 0.429E-02	8893.84= 0.433E-02
8908.12= 0.426E-02	8922.40= 0.432E-02	8936.68= 0.407E-02	8950.96= 0.406E-02	8965.24= 0.352E-02
8979.52= 0.272E-02	8993.80= 0.377E-02	9008.08= 0.360E-02	9022.36= 0.367E-02	9036.64= 0.370E-02
9050.92= 0.371E-02	9065.20= 0.376E-02	9079.48= 0.363E-02	9093.76= 0.370E-02	9108.04= 0.356E-02
9122.32= 0.355E-02	9136.60= 0.365E-02	9150.87= 0.353E-02	9165.16= 0.360E-02	9179.44= 0.356E-02
9193.71= 0.358E-02	9208.00= 0.370E-02	9222.28= 0.357E-02	9236.56= 0.369E-02	9250.84= 0.351E-02
9265.12= 0.332E-02	9279.40= 0.322E-02	9293.68= 0.312E-02	9307.96= 0.280E-02	9322.24= 0.252E-02
9336.52= 0.228E-02	9350.80= 0.228E-02	9365.08= 0.207E-02	9379.36= 0.231E-02	9393.64= 0.227E-02
9407.92= 0.232E-02	9422.20= 0.248E-02	9436.48= 0.250E-02	9450.76= 0.232E-02	9465.04= 0.237E-02
9479.32= 0.241E-02	9493.60= 0.241E-02	9507.87= 0.239E-02	9522.16= 0.256E-02	9536.44= 0.248E-02
9550.71= 0.263E-02	9565.00= 0.241E-02	9579.28= 0.259E-02	9593.56= 0.256E-02	9607.84= 0.244E-02
9622.12= 0.265E-02	9636.40= 0.267E-02	9650.68= 0.302E-02	9664.96= 0.316E-02	9679.24= 0.316E-02
9693.52= 0.328E-02	9707.80= 0.328E-02	9722.08= 0.330E-02	9736.36= 0.309E-02	9750.64= 0.326E-02
9764.92= 0.351E-02	9779.20= 0.339E-02	9793.48= 0.348E-02	9807.76= 0.343E-02	9822.04= 0.347E-02
9836.32= 0.364E-02	9850.60= 0.357E-02	9864.87= 0.374E-02	9879.16= 0.359E-02	9893.44= 0.361E-02
9907.71= 0.361E-02	9922.00= 0.372E-02	9936.28= 0.377E-02	9950.56= 0.362E-02	9964.84= 0.368E-02
9979.12= 0.401E-02	9993.40= 0.370E-02	10007.68= 0.376E-02	10021.96= 0.388E-02	10036.24= 0.402E-02
10050.52= 0.371E-02	10064.80= 0.383E-02	10079.08= 0.404E-02	10093.36= 0.373E-02	10107.64= 0.401E-02
10121.92= 0.394E-02	10136.20= 0.394E-02	10150.48= 0.374E-02	10164.76= 0.395E-02	10179.04= 0.423E-02
10193.32= 0.393E-02	10207.60= 0.406E-02	10221.87= 0.417E-02	10236.16= 0.378E-02	10250.44= 0.419E-02
10264.71= 0.435E-02	10279.00= 0.398E-02	10293.28= 0.383E-02	10307.56= 0.419E-02	10321.84= 0.383E-02
10336.12= 0.376E-02	10350.40= 0.448E-02	10364.68= 0.421E-02	10378.96= 0.424E-02	10393.24= 0.448E-02
10407.52= 0.429E-02	10421.80= 0.415E-02	10436.08= 0.427E-02	10450.36= 0.424E-02	10464.64= 0.424E-02
10478.92= 0.392E-02	10493.20= 0.469E-02	10507.48= 0.421E-02	10521.76= 0.506E-02	10536.04= 0.485E-02
10550.32= 0.459E-02	10564.60= 0.485E-02	10578.87= 0.456E-02	10593.16= 0.533E-02	10607.44= 0.533E-02
10621.71= 0.537E-02	10636.00= 0.565E-02	10650.28= 0.525E-02	10664.56= 0.529E-02	10678.84= 0.478E-02
10693.12= 0.468E-02	10707.40= 0.612E-02	10721.68= 0.533E-02	10735.96= 0.668E-02	10750.24= 0.574E-02
10764.52= 0.681E-02	10778.80= 0.573E-02	10793.08= 0.690E-02	10807.36= 0.667E-02	10821.64= 0.574E-02
10835.92= 0.741E-02	10850.20= 0.633E-02	10864.48= 0.740E-02	10878.76= 0.651E-02	10893.04= 0.713E-02
10907.32= 0.695E-02	10921.60= 0.657E-02	10935.87= 0.101E-01	10950.16= 0.638E-02	10964.44= 0.104E-01
10978.71= 0.876E-02	10993.00= 0.885E-02	11007.28= 0.106E-01	11021.56= 0.755E-02	11035.84= 0.913E-02

ORIGINAL PAGE IS
OF POOR QUALITY

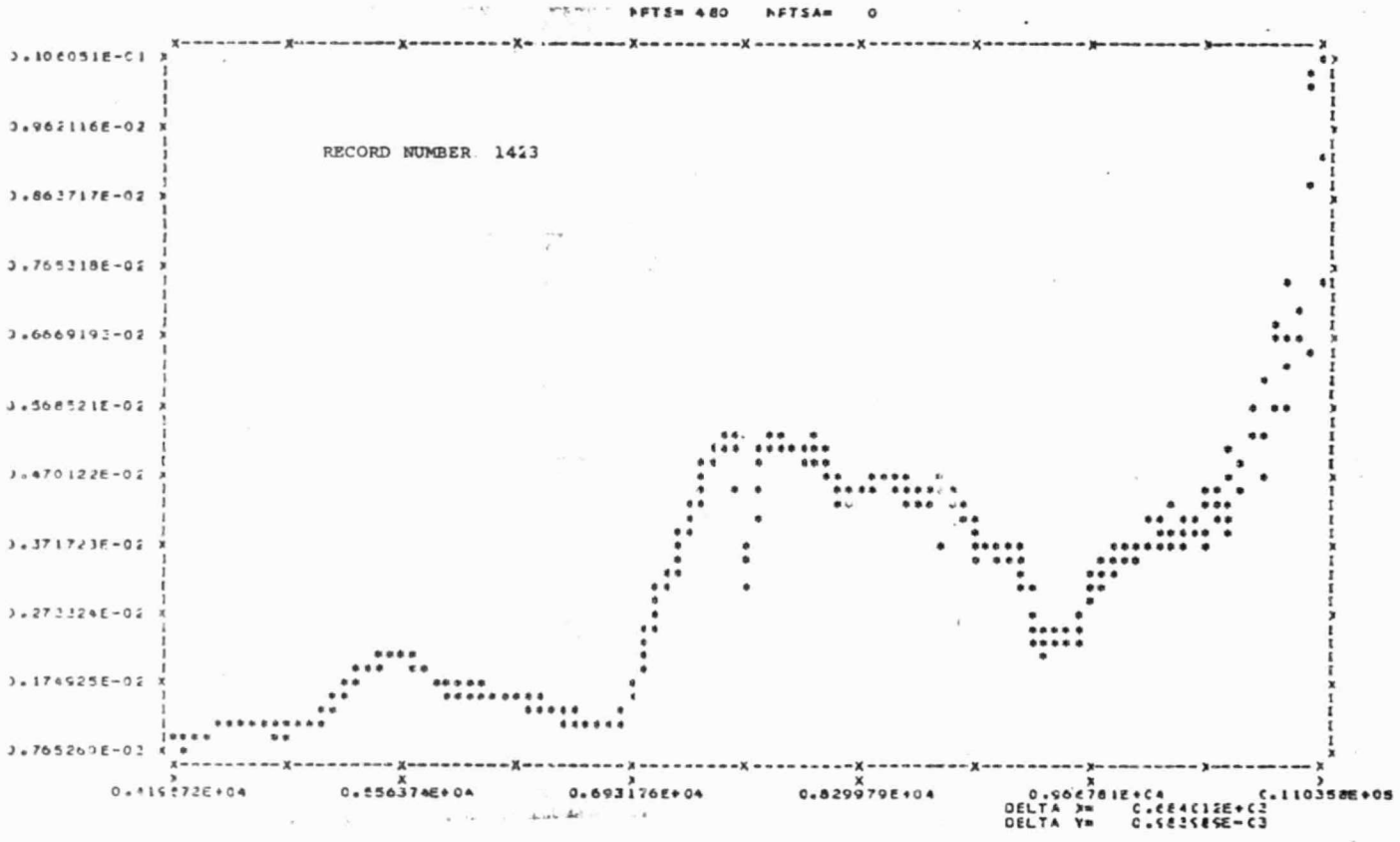

ORIGINAL PAGE IS
OF POOR QUALITY

** CHEBYSHEV COEFFICIENTS OF SPECTRA FROM JOTTER BASIN

ORIGINAL PAGE IS
OF POOR QUALITY

RECORD	1414	1423	1425
COEFFICIENTS			
1=	6.515E-3	6.534E-3	5.368E-3
2=	4.075E-3	4.118E-3	3.705E-3
3=	2.620E-3	2.667E-3	2.143E-3
4=	2.435E-3	2.321E-3	2.035E-3
5=	-2.056E-4	-1.547E-4	-1.109E-4
6=	-5.652E-4	-5.163E-4	-4.697E-4
7=	-3.644E-4	-3.493E-4	-2.784E-4
8=	-3.776E-4	-3.598E-4	-3.078E-4
9=	2.004E-4	1.872E-4	1.667E-4
10=	1.790E-4	1.606E-4	1.596E-4
11=	-5.358E-5	-6.050E-5	-5.807E-5
12=	-8.615E-5	-8.063E-5	-8.835E-5
13=	-1.558E-4	-1.412E-4	-1.455E-5
14=	-4.249E-5	-3.012E-5	-3.261E-5
15=	6.611E-5	7.582E-5	7.749E-5
16=	1.115E-4	1.335E-4	1.253E-4
17=	6.785E-5	9.600E-5	8.654E-5
18=	-1.736E-5	-1.966E-6	-4.491E-7
19=	-2.870E-5	-1.806E-5	-1.893E-5
20=	-1.209E-4	-1.039E-4	-9.978E-5
21=	-3.944E-5	-4.004E-5	-5.254E-5
22=	2.281E-5	2.131E-5	1.567E-5
23=	3.465E-5	3.085E-5	3.141E-5
24=	2.946E-5	3.363E-5	3.387E-5
25=	-1.749E-5	-2.009E-5	-1.759E-5
26=	1.243E-5	3.990E-6	7.186E-6
27=	1.258E-5	4.645E-6	1.815E-5
28=	1.554E-6	1.623E-6	-7.973E-7
29=	2.967E-6	2.117E-6	1.028E-5
30=	1.897E-5	1.793E-5	1.622E-5

RECORD	1458	1461	1474
COEFFICIENTS			
1=	7.041E-3	6.753E-3	6.979E-3
2=	5.155E-3	4.240E-3	4.955E-3
3=	4.117E-3	3.254E-3	3.939E-3
4=	3.287E-3	2.633E-3	3.130E-3
5=	4.346E-4	2.915E-4	3.522E-4
6=	-2.718E-4	-2.788E-4	-2.861E-4
7=	-3.622E-4	-2.933E-4	-3.437E-4
8=	-5.180E-4	-3.847E-4	-4.699E-4
9=	4.403E-5	4.640E-5	6.045E-5
10=	7.456E-5	6.128E-5	8.879E-5
11=	-6.704E-5	-8.865E-5	-8.946E-5
12=	-5.783E-5	-7.716E-5	-5.805E-5
13=	-1.234E-4	-1.329E-4	-1.261E-4
14=	-3.742E-5	-2.234E-5	-2.143E-5
15=	6.784E-5	7.652E-5	9.001E-5
16=	1.289E-4	1.224E-4	1.422E-4
17=	1.112E-4	8.383E-5	1.123E-4
18=	1.059E-5	-2.297E-6	4.188E-6
19=	1.404E-6	-1.207E-5	-7.523E-5
20=	-1.189E-4	-9.225E-5	-1.096E-4
21=	-7.554E-5	-5.224E-5	-7.611E-5
22=	-1.825E-5	5.483E-6	-2.062E-5
23=	1.004E-5	1.469E-5	2.208E-6
24=	3.214E-5	3.368E-5	2.020E-5
25=	-9.753E-6	-2.675E-5	-2.175E-5
26=	1.254E-5	1.258E-6	1.384E-7
27=	1.917E-5	6.015E-6	1.445E-5
28=	1.636E-6	-3.447E-6	5.855E-6
29=	1.436E-6	-5.170E-6	-2.989E-6
30=	2.654E-5	1.319E-5	2.372E-5